An-Najah National University

Faculty of Graduate Studies

Design of Active Power Filter with Active and Reactive Power Injection Capability, Using Multilevel Inverter and Photovoltaic Arrays

By

Naeil Hantouli

Supervisor

Dr. Kamel Saleh

This Thesis is Submitted in Partial Fulfillment of the Requirements for the Degree of Master of Electrical Power Engineering, Faculty of Graduate Studies, An-Najah National University, Nablus-Palestine.

2018

Design of Active Power Filter with Active and Reactive Power Injection Capability, Using Multilevel Inverter and Photovoltaic Arrays

By

Naeil Hantouli

This Thesis was Defended Successfully on 20/ 5/ 2018 and approved by:

Defense Committee Members		**Signature**
1. Dr. Kamel Saleh	**/ Supervisor**	....
2. Dr. Basem Alsayed	**/ External Examiner**	....
3. Prof. Marwan Mahmmoud	**/ Internal Examiner**	....

Dedicated

To

My Parents and My Family Members

Acknowledgements

I would like to explain my significant appreciation and obligation to my supervisor Dr. Kamel Saleh, from whom I learnt scholastic aptitudes as well as life skills, for his consistent inspiration, bolster, expert guidance, continuous supervision and valuable recommendation for the accommodation of my progress report of thesis work.

I offer my earnest thanks to Dr. Kamel Saleh, for priceless recommendations and steady consolation all through theresearch work.

I would also like to acknowledge the entire staff of Electrical Engineering department for founding a workingambience and for deductive discussions.

At last, I am constantly committed to all my family members, particularly my parents and fiancé for their perpetual support and love.

الإقرار

أنا الموقع أدناه مقدم الرسالة التي تحمل العنوان:

Design of Active Power Filter with Active and Reactive Power Injection Capability, Using Multilevel Inverter and Photovoltaic Arrays

أقر بأن ما اشتملت عليه هذه الرسالة هو نتاج جهدي الخاص، باستثناء ما تمت الإشارة إليه حيث ورد، وأن هذه الرسالة ككل أو أي جزء منها لم يقدم من قبل لنيل أي درجة او لقب علمي او بحثي لدى أي مؤسسة تعليمية أو بحثية أخرى.

Declaration

The work provided in this thesis, unless otherwise referenced, is the researcher's own work, and has not been submitted elsewhere for any other degrees or certifications.

Student's Name: **أسم الطالب:**

Signature: **التوقيع:**

Date: **التاريخ:**

Table of Contents

List of Tables

List of Figures

List of Abbreviations

PF	Power Filter
APF	Active Power Filter
UPQC	Unified Power Quality Conditioner
SHAPF	Shunt Active Power Filter
SAPF	Series Active Power Filter
HAPF	Hybrid Active Power Filter
THD	Total Harmonic Distortion
SOC	State of Charge
PCC	Point of Common Coupling
MPPT	Maximum Power Point Tracker

Design of Active Power Filter with Active and Reactive Power Injection Capability, Using Multilevel Inverter and Photovoltaic Arrays

By

Naeil Hantouli

Supervisor

Dr. Kamel Saleh

Abstract

The Hybrid Active Power filter (HAPF) consists of shunt active power filter connected with series active power filter at a common linking point. Itworked perfectly with total benefits of shunt APF and series APF. In other words, it can mitigate both the current and voltage harmonics. Subsequently, the HAPF can mitigate nearly all kinds of power purity troubles seen by distribution network.

The shunt active power filter is controlled based on the “generalized theory of the instantaneous reactive power in three-phase circuits (p-q theory)", to compensate the load harmonics. The series active power filter is controlled based on the dual instantaneous reactive power theory to compensate the load harmonics.

(HAPF) used 27-level asymmetrical inverters. Each phase of these inverters is composed of three ‘H’ bridges, supplied by three independent photovoltaic arrays Scaled in the power of three, delivering 12.5 kVA to each phase, 10kVA for shunt active filter and 2.5 kVA for series active filter, using multilevelinverters with more than 20 levels can deliver current

waveforms with negligibletotal harmonic distortion. So they can implemented in active filter application without the need of filters.

The outputs of inverters connected directly through a transmission line. In addition to the capability of harmonic elimination of both current and voltage drawn from the source, the combined system can produce real and reactive power to feed the loads during prolonged voltage outagesor source shortage.

A battery pack used as dc link, which is charged from photovoltaic array connected to the battery through a maximum power point tracker and charge controller.The injection of real and reactive power depends on the state of charge (SOC) of batteries, the system frequency, type of the load, and power factor at the common linking point.

The proposed Unified (HAPF) strategy is simulated in MATLAB SIMULINK and the results are shown.From simulation results, the system can mitigate all voltage and current harmonics and reduce the total harmonic distortion from 22% to 1%. In the other hand, it support the electrical network by injecting real power when it’s needed and maintain the stability of the electrical network.

By using voltage reference generation control we will overcome the voltage matching problems, reduce the total harmonic distortion (THD) to minimum and eliminate the need of transformers.

Chapter One
Literature Review

1.1 Introduction

Electricity known as the top effective and public kind of energy and the lifetime is vigorously uses the electricity in its applications. The prosperity cannot be envisioned without the existence of electrical supply. In the meantime, the power quality of distribution network is additionally imperative for proficient functioning of user applications and equipment.

The term power quality turned out to be the most outstanding in power research problems, also the electricity company and its clients are interested in it.

The quality of power delivered to the customers relies on the voltage and frequency ranges of the power. In the event that there is any deviation in the voltage and frequency of the electric power conveyed from that of the standard values then the quality of power conveyed is influenced.

These times the power electronics based nonlinear loads are expanded significantly in the distribution networks.

These nonlinear loads make harmonics or current distortion issues on the supply side of the distribution system [1].

The harmonics induce malfunctions of sensitive equipment's; over voltage by resonance and harmonic voltage drop over the network impedance, and these essentially deteriorate the power quality in the distribution system.

Traditionally, passive filters are utilized to eliminate harmonics and enhance power quality of the distribution system. In any case, it neglects to work in view of certain restriction like fixed compensation, resonance problem and massive in nature. In order to overcome the previously mentioned constraints, another arrangement of compensators based on power electronics technology has been presented in the market [2]. One of the critical arrangement of such compensators is called active power filters.

Many filter topologies found in the old papers and research such- series, shunt, and hybrid APF. In this research, the utilization of Hybrid APF for the optimization of the quality of electricity and injection of real and reactive power is examined and analyzed.

As of late, the need of clean energy makes more interest towards renewable energy resources, for example, solar, wind, geothermal, tidal etc.

Light energy is directly converted into DC power by a photovoltaic array. These DC power from a photovoltaic array is transformed into more advantageous AC power through inverter system.

Multilevel inverters can deliver current waveforms with negligible total harmonic distortion. Moreover, they can work utilizing both amplitude modulation and PWM procedures.

One of the multistage technologies that permit delivering many levels of voltage with a little number of transistors is the one based on “H” bridges scaled in the force of three [3]-[4]. This topology utilizes generally few power devices, and every one of the “H” bridges designed to operate at so low switching frequency, which provides the potential of operating in high power capacity at low semiconductors speed with very low-switching frequency losses, that makes them extremely appropriate for power quality improvement applications or machine drive [5].

The final objective of this line of research is to demonstrate the advantages of using a 27-level hybrid active power filter as power quality conditioner and real-reactive power generation source.

1.2 Literature Review

1.2.1 Filter History

Because of the progression of science and technology, industrial structure changing, and recently the creation of smart grids, electrical companies and end users have a higher interest for improved power quality and reliability [6]. Nonetheless, with the expansion and expanded utilization of power electronics devices and electrical machines loading it is becoming noticeably harder to accomplish this objective [7]-[15]. In mid 1940s, passive power filters (PPF) were advanced to remove current harmonics and improve the power factor [16]. In 1976, active power filters (APF) were created to eliminate harmonics. HAPFs always most effective in the mitigation of harmonics than one part of APFs from practically and economical perspective [17] [18]. To achieve the best performance, the unified power quality conditioner (UPQC), has been advanced with a very high cost [19]. During 1976-2005, HAPFs are primarily applied to conventional industry, such as steel furnace, ASD, etc. Most research works concentrate on fundamental and single function, just the compensation of harmonics. After 2005, a lot of researchers concentrates on the expansion of application, perfect design, and dynamic power factor correction. Some literatures [20]-[23] have talked about the feasibility of HAPF in railway, wind farm, and photovoltaic generator.

As the cost and operating losses of power electronic switches are high, this limit the performance of HAPF, many papers have proposed ideal design method in parameter selection [24], control technique [25][26], and structures. Many survey papers make inclusive summary of HAPF. In 2000, "Active power filters: A review" divided the research work released in five parts: power rating and respond speed, configuration and connection, compensated system parameters, control techniques, reference signal estimating technique [27]. In 2005, "Hybrid filters for power quality improvement" condensed the most HAPF structures based on many combination of AF and PF. The determination criteria are also list in points of interest [28]. In 2005, "Active harmonic filters" explain the performance of three HAPF in detail: the hybrid of active shunt and passive series, the hybrid of active series and passive shunt, transformer less LC-HAPF [29].

In 2009,the active power filter implemented as static VAR compensator with power injection capability using 27-level inverter, this paper used anew topology of multilevel inverter which allows us to generate [7], [9] many more levels of voltage with fewer power semiconductors.

In 2011, “Photovoltaic Array Based Multilevel Inverter for Power Conditioning” This paper shown that the photovoltaic based multilevel inverter configured shunt APF compensates the current harmonics, unbalancing in load and also injects real power whenever it is demanded in the distribution system but with weak and inapplicable method.

In 2012, a good paper split ten HAPFs in two parts: shunt filter and series filter. Five basic control algorithm are also discussed in this research, as Fourier transform, Synchronous reference frame, Instantaneous reactive power theory, High-pass filter method, Low-pass filter method, and Adaptive linear neurons control [30]. In 2013, "Review of Hybrid Active Power Filter Topologies and Controllers" split all HAPFs based on topology, converter configuration, supply system, passive filter type and listed a new control methods in harmonic extracting and controller topologies [31].

In 2016, the research discussed the active power filter (APF) for harmonic mitigation at the common linking point to improve the power quality.

The historical periods of the improvement of HAPF capability can be divided into three strategies: starting stage, creating stage and grown stage.

The primary research work of the functionality of HAPF in each historical period is displayed in Figure below.

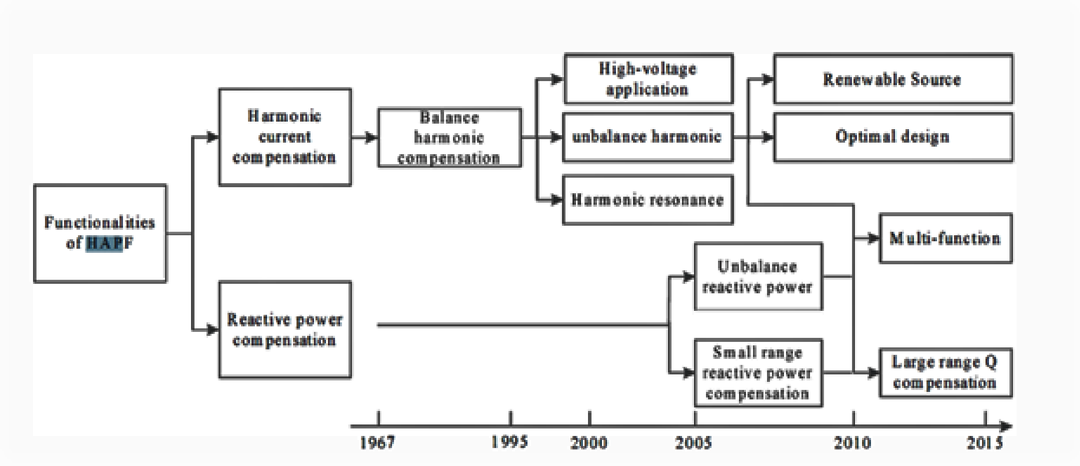

1.2.2 Hybrid Active Power Filter (HAPF) Functions

1.2.2.1 Current Harmonic Compensation in HAPF

Harmonic elimination is the most simple and earliest function of HAPF. 1976- 1995 is the starting stage. Through this period, researchers start to implement HAPF to damping balance current harmonic. In this stage, HAPFs were thought to be only suitable in low-and medium-voltage system and benefit in damping harmonic resonance [32].

In 1996-2005, the function of harmonic compensation came into creating period. Three main directions, like high-voltage application, damping harmonic resonance, and unbalance harmonic compensation, have been suggested.

In 2005-now, it can be called grown period. Most papers concentrates on three sides: renewable source, multi-function, and optimum design. Many published research work on the harmonic compensating of HAPF converge on some new application, such as high speed railway [27], photovoltaic generator [28] and wind farm [29].

1.2.2.2 Reactive Power Compensation in HAPF

Reactive power can be compensated using Var generators (reactive power generators). The technology developments of this function are far behind the function of harmonic compensation. The historical period of development in this function can be mainly divided in three strategies.

Before 2005, some researchers think this technique would only be suitable for low-power application and they tried to found alternative methods [35].

During 2005-2009, the alternative of reactive power compensation in active filter was first presented in [36]. The implementations of HAPF have harmonic current, small domain of dynamic and unbalance reactive power, which are more suitable for medium- and low-voltage application.

2009-now, many research work about this multiple function of HAPF in different applications have been reported [38]. To expand the range of reactive power compensation, the combination of shunt HAPF and other controllable reactive power compensating circuit are proposed in [39].

1.2.2.3 Active Power Compensation

In 2007, a beneficial paper talked about the solving of power quality drawbacks and suggest a method for interfacing the renewable energy sources with the distribution network, the active filter depended on two level-three phase four-leg converter.[40]

In 2009, a very good research used the photovoltaic array as active power source to fed the load during prolonged voltage outages.[41]

In 2011, “Photovoltaic Array Based Multilevel Inverter for Power Conditioning” Used a combination of photovoltaic modules to inject real power whenever it is demanded in the distribution system.[42]

1.2.3 History of Multilevel Converters.

1.2.3.1 History of Cascaded H-bridge Multi-level Converter

A serially connected H-bridge with separate multi DC sources is called as cascaded H-bridge multi-level converter. This type of configuration has equal DC voltage sources at each converter leg.

Li Li (2000) proposed a series active power filter using multi-level converter for selective harmonic mitigation with PWM algorithm. The phase shift harmonic extinction method was used as optimization mechanism by obtaining the perfect starting point. [45]

Corzine Keith et al (2004) introduced a new kind of multi-level converter which was created by two cascading three phase three level converter utilizing the load point, but needs just one DC voltage source. This new seven level inverter divides the power diversion converters into a higher voltage lower frequency converter and a lower voltage higher frequency converter. This type of inverters found applications in naval ship propulsion systems which rely on high power quality, survivable drives. New control methods are described involving both joint and separate control of the individual three level inverter. Two types of controlling methods were developed for this inverter. The first one relies on controlling both three level converters and the other utilizes separate controllers. Both the controls include capacitor voltage balancing so that a DC source was needed for one three level inverter [46].

Mariethoz et al (2005) developed a cascaded multilevel inverter which focuses on asymmetrical topologies where the cell input voltages are different values. These hybrid topologies are advantageous for several applications. In this inverter the need of DC-DC converter to supply the cells creates simultaneous commutation problem, which increases the switching losses for some operating points, reduces the design choice to configurations of lower resolution. A three phase six switch voltage source inverter and single phase H-bridge are connected in series to obtain a cascaded multilevel inverter with attractive properties in terms of inverters cost and losses [47].

Sahali et al (2006) presented a comparative study between optimum reduction of total harmonic distortion (THD) and harmonic mitigation with voltage reference signal strategies for multi-level converter. This was devoted to the comparative evaluation of the two modulation strategies developed for multilevel inverter control, the harmonic elimination technique with voltage control and the optimal minimization of the total harmonic distortion method, which are very important and efficient strategies of eliminating selected harmonics from spectrum of the output voltage or minimizing its total harmonic distortion in order to improve its quality. [48]

EbrahimBabaei (2008) proposed a cascaded multi-level converter technique with minimal number of semiconductor switches. This new multilevel inverter topology have more voltage levels with less power electronic switches. The proposed topology composed from series connected sub multi-level converters. The above method outcomes in decreasing in the number of semiconductors, losses, needed space and converter cost. [49]

Agelidis et al (2008a,b) reported a five level symmetrically defined multilevel Selective Harmonic Elimination Pulse Width Modulation (SHEPWM) strategy. This technique has equal number of switching transitions when compared against the well-known multicarrier phase shifted sinusoidal PWM technique. It was assumed that the four triangular carriers of the sinusoidal pulse width modulation method have nine levels per unit frequency resulting in seventeen switching transitions for every quarter period. The proposed multilevel SHEPWM method controls sixteen harmonics and the fundamental. It is noted that the proposed Multilevel SHEPWM offers significantly higher inverter bandwidth in the standard range of the modulation index. [50]

Chih Chiang Hua et al (2009) proposed a current control technique with predictive control method for multilevel inverter. In this method, the inductor current is sensed by the current control method of variable sampling point. It is reported the switching noise caused by the turn on or turn off power devices are avoided by this control method. The measured value of the inductor current was used to estimate the inverter output voltage at the next switching period with a simple linear extrapolation by forcing the output current to follow the current reference. Compared to the conventional predictive current controllers, the features of the proposed control are as follows: only the inductor current measurement was required and it was able to achieve a cost effective and less complex circuit, whereas the output voltage and current measurements are required for a conventional controller. [51]

Sung Geun Song et al (2009) proposed an isolated cascaded multilevel inverter employing low frequency three phase transformers and a single DC input power source. In this topology, four H-bridge modules are connected to the same DC input source in parallel and each secondary of the four transformers are connected in series. The proposed circuit configuration can reduce number of transformers compared with traditional three phase multilevel inverter using single phase transformers. An optimal switching pattern identified with the fundamental frequency of the output voltage and controls the switching phase angle. By the proposed circuit configuration, a number of transformers can be reduced, compared with traditional three phase multilevel inverter using single phase transformers. [52]

Zheng Du et al (2009) presented a new multilevel inverter which was developed without the inductors called cascaded H-bridge multilevel boost inverter. This research developed for the applications of Electrical and Hybrid Electrical Vehicles (HEV). At present, the HEV power inverter system utilizes a DC-DC step up converter to increase the voltage of the battery for a typical three phase inverter system. The disadvantages of the current HEV traction drive inverters are the density of power is low, not cheap and not efficient. These problems occur due to the necessity of bulky inductor in the system. Because all H-bridge needs a DC power supply, the proposed design uses a standard three leg inverter and an H-bridge. The H-bridge connected in series with every inverter leg which utilizes a condenser as the DC reactive power source. [53]

GierriWaltrich et al (2010) designed a modular three phase multilevel inverter especially suited for electrical drive applications. This topology works based on the solar cells joint in cascade utilizing two inverter legs connected in series. To perform a suited voltage operation and very small harmonic deformation, the H-bridge modules are normally linked in cascade on their AC part. To make this inverter as cost effective, power cells are used with identical a characteristic which leads to modular structure of the system. [54]

Joachim Holtz et al (2010) demonstrated the different inverter topologies which are suited for very high power applications. The higher machine voltages are obtained from these topologies than the three levels DCMLI topology. The power capabilities of pulse width modulated inverters are increased for the development of medium voltage drives. Parallel connection and series connection of power semiconductor devices permits to increase the output current and output voltage respectively. In both the cases, additional means are required for balancing the current or voltage stress of the devices. The technical and economic constraint involved with multilevel inverter topologies improves the performance of voltage drives. The parallel connection of two three level inverter doubles the maximum output power by doubling the maximum output current. [55]

Patricio Cortes et al (2010) presented a model predictive current control algorithm that was suitable for multilevel inverter. Its application to a three phase cascaded H-bridge inverter for optimization was proposed in order to this algorithm reduces the amount of calculations needed for the selection of the optimal voltage vectors, by choosing a subset of the available voltage vectors by which the operation of three phase cascaded H-bridge inverter is optimized. Although the proposed control method was valid for any number of levels, by using this method, five level and nine level cascaded H-bridge multilevel inverters were presented in this paper. The proposed control method can be easily extended to include any additional requirements. [56]

Young Min Parky et al (2010) designed a cascaded H-bridge multi-level inverter utilizing semiconductor switches building blocks and high execution of control to optimize current control and increase fault tolerance capability. Since the individual inverter modules operate more independently, the expansion and modularization characteristics of the cascaded H-bridge multilevel inverters are improved. It was also shown that the performance of current control can be improved with voltage delay compensation and the fault tolerance performance can be increased by using unbalance three phase control. [57]

1.2.3.2 Hybrid H-bridge Multilevel Inverter

A serially connected H-bridge with separate DC sources are called as hybrid H-bridge multilevel inverter. Each succeeding voltage source has the voltage values in the order of 1Vdc, 2Vdc and 4Vdc.

Manjrekar and Lipo (1998) reported various topologies and modulation strategies for utility and drive applications. This paper was devoted to the investigation of a 500 HP induction machine drive based on a seven level 4.5 KV hybrid inverter. Different design criteria, spectral structure and other practical matters such as capacitor voltage balancing are researched. Manjrekar et al (2000) devoted to the investigation of a hybrid multilevel power conversion system for medium voltage high power applications. By trends in power semiconductor technology, the authors selected different power devices based on their switching frequency and voltage sustaining capability and created a new hybrid topology. The new power inverter topologies permit modular realization of multilevel inverter using a hybrid approach involving Integrated Gate Commutated Thyristors (IGCT) and Insulated Gate Bipolar Transistors (IGBT) operating together. With this modular H-bridge topology, realization of multilevel inverter using a hybrid approach involving IGCTs and IGBTs is possible, which are useful in required high power applications. [58]

Miguel Lopez et al (2003) proposed an active power filter implemented with multiples single phase full bridge voltage source inverters connected in series. It was aimed to compensate current harmonic components in medium and high voltage power distribution systems [59].

Haiwen Liu et al (2008) presented a hybrid cascaded multilevel inverter with PWM method. It consists of a three leg inverter and single H bridge connected in series with every inverter leg. the single DC power source can be used to fed a standard three leg inverter with three complete H-bridge fed by capacitors. Multi-level carrier with PWM algorithm was implemented to maintain a five level phase voltage. [60].

Zambra et al (2010) reviewed a comparison of three topologies of multilevel inverter applied to drive an induction motor of 500 HP/4.16 KV rating. In this paper, Neutral point clamped inverter; symmetrical cascaded multilevel inverter and hybrid asymmetrical cascaded multilevel inverter are compared for the performance indexes such as total harmonic distortion, first term distortion factor, second term distortion factor, common mode voltage, semiconductor power loss distribution and heat sink volume [61].

Domingo Ruiz-Caballero et al (2010) proposed novel symmetric hybrid multilevel topologies that are introduced for both single phase and three phase medium voltage high power systems. The topologies are based on a low switch count three level pulse width modulation switching cell connected to a low frequency switched bridge, thus, high modularity was achieved. Compared with an H-bridge cascaded multilevel inverter, the number of overall insulated DC sources was reduced in the proposed inverter, Furthermore, by reducing the number of insulated DC supplies; the number of cables connecting the input transformer terminals to the rectifying bridges is minimized. With same numbers of semiconductors in cascaded H-bridge inverter and three insulated DC sources, the three phase topology are generated five level output.[62]

Jing Zhao et al (2010) proposed a novel pulse width modulation control method. The PWM control method was called higher and a lower carrier cell which is an alternative phase opposition PWM for the hybrid clamped multilevel inverter and developed based on the improvement of carrier phase disposition PWM. The particular carrier waveforms of switching semiconductors are divide into numerous carrier cells depending on the carrier period. The sub stitutional phase reverse PWM can be calculated by increasing carrier cells. This can reduce switching losses and improve the output harmonic distortion in low order harmonics. [63]

1.2.3.3 New Hybrid H-Bridge Multilevel Inverter

The multi-level inverter utilizing cascaded H-bridge with multi DC sources forming a needed voltage from separated sources of DC voltages. Each succeeding voltage source has the voltage values in the order of 1Vdc, 3Vdc and 9Vdc called new hybrid H-bridge multilevel inverter.

Ayob and Chee (2005) proposed a new hybrid multilevel inverter topology with harmonics profile improvement. As per the literature, a largest output levels and the lowest total harmonics distortion percentage can be achieved by the hybrid MLI with DC sources in trinary configuration. However, the output contains low order harmonics topology, due to the impossibility of modulating all adjacent voltage levels among all adjacent levels of output waveform [64].

Jianye Rao et al (2008) devoted to the investigation of a new hybrid multilevel inverter system typically suitable for high performance high power applications. In this paper the motors are achieved by an H-bridge inverter and the three level diode clamped inverter are connected together. But only the main inverter concerned with DC voltage source. The conditioning inverter was supplied by the floating ultra-capacitors to store the braking energy of motors, which will be reused. The eligibility of the system will be increased. Compared with the traditional H-bridge inverter, this new scheme can reduce the DC sources while maintaining the same voltage output. When the motor was at steady state, the improvement in power factor can be achieved by supplying the motor from the conditioning inverter [65].

Jianye Rao et al (2009) the proposed hybrid cascaded multi-level and SVM controls implemented for sensor less drive of induction motor. In the proposed drive system, the main inverter and the conditioning inverter are connected together to drive motor, but only the main inverter was supplied by DC voltage source. The conditioning inverter just uses suspended super capacitors as its power source. The main and conditioning inverters can be either H-bridge inverter or three level DCMLI inverter. Thus, great energy efficiency improvement is carried out when compared with conventional H-bridge inverter [66].

Ki Seon Kim et al (2009) presented an innovative hybrid casual PWM algorithm based on a TMS320LF2407 Digital Signal Processor (DSP), The DSP generates the random numbers, and the Pseudo Random Binary Sequence (PRBS) bits with a lead lag random bit and the three phase reference signals [67].

1.2.4 Maximum Power Point Tracking MPPT

MPPT controller is needed to operate the photovoltaic array at extreme power point and improve the productivity of the photovoltaic system by ensuring that the photovoltaic module continuously supplies maximum power regardless of changes in weather conditions. So, as the tracking control of the maximum power point is a complicated problem, to overcome these problems and ensure the high efficiency of the PV system, different solar regulators based on many MPPT strategies have been developed, such as Fractional Short-Circuit Current (FSCC), Fractional Open-Circuit Voltage (FOCV), Fuzzy Logic, Neural Network, Perturbation and Observation (P&O), and Incremental Conductance algorithms. These algorithms have some drawbacks such as high cost, difficulty, complexity and instability. All previously mentioned MPPT methods have the same goal which is maximizing the PV array output power by tracking the maximum power on every operating condition. This research proposes a novel technique, easy-to-implement MPPT strategy based on the enhanced P&O algorithm that improves performance of the solar system. Thus, this technique combines low cost, high stability, great accuracy and fast response time.

1.2.5 Battery Chargers

A lot of industrial applications like Utility Switchgear, Gas Turbines, Oil Platforms, Process Control, etc., comprise the operation of critical DC loads. Dropping any of these critical loads may result in ultimate and costly circumstances. Thus, these applications need the use of batteries as a backup power source in case of a power outage. Hence, a need was created for equipment utilized to maintain the charge in the batteries. Battery charger / DC power supply technologies have been advanced over the years to increase the efficiency, reliability and minimize the cost of the equipment. These several technologies serve the same aim of supporting the DC loads and preserve a full charge in the battery of a DC system. Each technology, however, has its benefits and drawbacks.

From the battery perspective, the major factors that influence the life span of a battery are the characteristics of the DC power that is provided by the charger; such as, DC voltage level, AC ripple, overcharging, undercharging and frequency. The characteristics of a Battery Charger's DC output power are at most regarding to the design intelligence and quality. Various Battery Charger technologies could supply DC signals that are very close in characteristics if they were implemented correctly. However, one technology's design criteria could be more difficult than another in order to fulfill the same output characteristics. But if all design and safety sides were taken into account, many technologies can provide similar performance.

1.3 Thesis Motivation.

1.3.1 Problems of Power Quality

The efficiency of power is influenced when there is any deflection in the current, voltage or system frequency. The mutual issues that influence the sensibility of the equipment are-

- Transient states
- Frequency deviations
- Network noise and harmonics

- Surges
- Current outages
- Network Faults
- Wrong earth influence

The fundamental influence created by these issues is the generation of and harmonics. The existence of noise and harmonics break down the purity of power and will harm the client’s equipment’s. These network harmonics will increase the temperature of transmission lines, insulation damage in electrical network, minimizes the working age of electrical machines, decrease the efficiency by increasing system damages etc.

1.3.2 Problem Solving of Power Quality

The better valuable resolution to enhance the power purity is the utilization of filters for harmonics reduction. The main principle of utilizing a filter is presented in Fig. 1.1, The APF is a Voltage Source Inverter (VSI) or Current Source Inverter (CSI) that injects the reference voltage or current according to the electrical network status, where the generated signal injected to mitigate the harmonics in electrical source due to the existence of nonlinear loads.

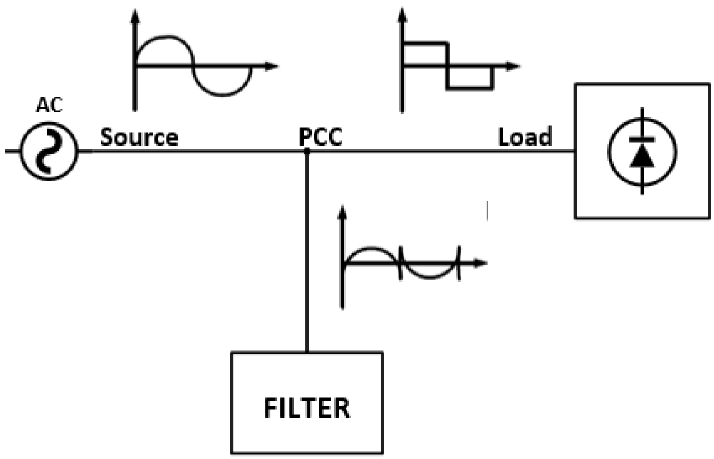

Fig.1.1: Principle of filter working**.**

In the research field a various filter kinds like- passive, active, hybrid. The passive power filters are utilized to mitigate a certain order harmonics but with a problem of parallel resonance. The other way is utilize of Active Power Filter (APF). There are many kinds of APF such as shunt APF, series APF. The shunt APF is expensive and is not utilized for big systems. The series APF acts like a harmonic isolator and utilized to minimize the negative-sequence voltage. A filter kind which composed from series APF and shunt APF named as Hybrid Active Power Filter (HAPF).

1.3.3 Benefits of Hybrid APF

(HAPF) is a collection of shunt APF and series APF filters. Through the different existence kinds, series and shunt power filters types is preferred as it has the benefits of both series and shunt active power filters. The features of the both filters are increased, preventing the troubles of utilize one of them alone. The series APF composed with shunt connected APF is mostly utilized because of the above benefits. So, the operation of series APF composed with shunt connected APF is implemented and tested in this research to solve the distribution network problems.

1.4 Research Objectives

This thesis addresses the Active Power Filter with Active Power Injection Capability, Using a Multi-Level Inverter and Photovoltaic Array. The control works through the wide load range, and the batteries feed the loads during prolonged voltage outages or source shortage.

The specific objectives are to:

- Propose and implement hybrid active power filter to achieve a fully harmonic and power factor compensation for wide contaminating load range.
- Use 27-level asymmetrical inverters in series and shunt active power filter to increase the capability of the hybrid active power filter in harmonic compensation and power injection.
- Implement and test a precise control techniques to track the load and source current and voltage to generate the needed pulses to the multilevel inverters gate to eliminate the harmonics, make unity power factor and monitor the injection of active power.
- Utilize the photovoltaic arrays as real and reactive power source, and chooses the number of arrays needed to maintain stability of the system during 24 hour working.

- Design the charge controller and the maximum power point tracker required to charge the batteries needed to store the power from photovoltaic arrays.

- Compute the size of battery packs to fed 12.5 kVA load during night hours.

- Inject a real and reactive power to the system when it's needed, where the injection depends on the state of charge (SOC) of batteries, the frequency of the system, real and reactive power of the load, and power factor at the point of common coupling (PCC).

1.5 Organization of Research

The research presented in this thesis focuses mainly on new Hybrid Active Power Filter (HAPF) using 27-level inverters fed by photovoltaic dc source.

The all research is sorted into seven chapters with introduction and every chapter is briefed below.

Chapters 2 review the kinds of filters. It includes all types of filter algorithms that are utilized for the enhancement of the quality of power. It discusses in specifics every filter kind over their advantages and disadvantages.

Chapter 3 it presented and discussed the control algorithm of the series and shunt APF. It shows how the APF generate the needed signals to optimize the purity of power. The mathematical models of the series and shunt APF are extracted and the control algorithm for all HAPF parts has been analyzed. The design of controller depended on Dual Instantaneous Power Theory (d-q) for shunt and Reactive Instantaneous Power (p-q) theory for series APF.

Finally, the results using MATLAB SIMULINK prove the correct design and work of the control algorithm.

Chapter 4this chapter is focused on the study of multilevel converters. First of all, an overview of the most typical converter topologies has been presented. Then we discussed and tested by simulation the cascaded H-bridge 27 level inverter used in our system, and finally an overview of the modulation techniques that are used in cascaded H-Bridge converters.

Chapter5 discussed the working principle of photovoltaic cells and its connections to form arrays. The modeling of photovoltaic cells and the influence of solar irradiance and ambient temperature on it and proposed the photovoltaic arrays with MPPT, P & O method and DC-DC step-up converter including its modes of operation and waveforms. The results for boost converter with maximum power point tracker have been tested using MATLAB SIMULINK program.

Chapter 6 presented the complete system results. It contained the MATLAB SIMULINK results proposed Hybrid Active Power Filter(HAPF).

Chapter 7includes the recommendation, some practical considerations, and future study with thesis references.

Chapter Two
Filters Classifications

2.1 Introduction.

The distribution networks is influenced by different issues like transients, voltage sag/swell, noise, which prompts the creation of harmonics and impact the quality of power conveyed to customers. The harmonics components appearing voltage or current waveforms, which present losses in the active power transferred. In this manner the reaction at harmonics must be limited from influencing the working of the system. To accomplish this, filter is utilized at the common linking point at the load connection point. This filter mitigate the harmonics and enhances the efficiency of the grid. In this chapter all kinds of filters clarified and discussed in details.

2.2 Filter Classifications.

The kind of filters mentioned in the literature is divided into three main kinds. The first one is Passive Filter and the others are Active Filter and Hybrid filter. Every kind has its types and properties. The ranking of the filters shown in Fig. 2.1.

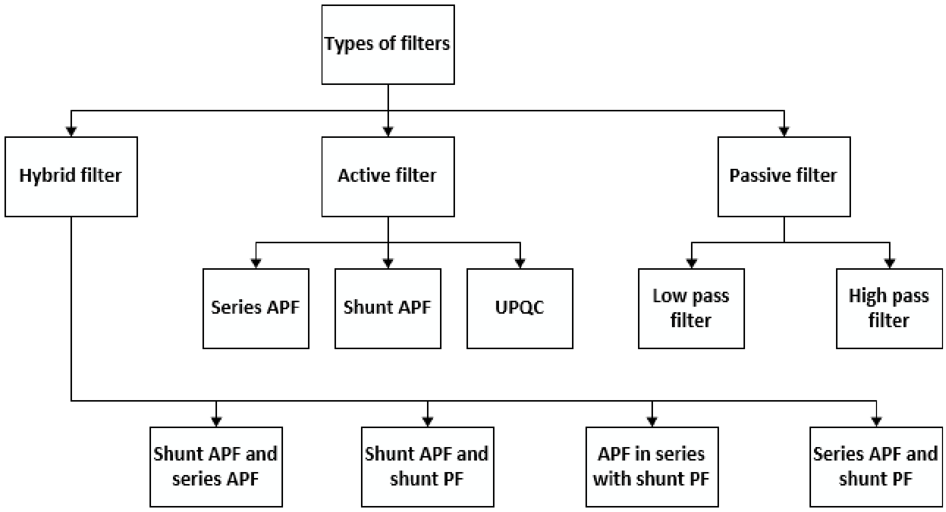

Fig.2.1: Classification of filters

2.2.1 Passive Power Filters.

These filters composed from passive parts such as- inductor, capacitor and resistor. They are vastly utilized because of ease of use and very low cost. In addition, the passive filters also inject reactive power apart from compensating the harmonics. These types of filter extremely dependent on the system impedance. Passive filters are also categorized into two kinds- low pass and high pass filter.

2.2.1.1 Low Pass Filter.

The LPF is a calibrating LC circuit that is set to make a pass for some harmonic current. It utilized for power factor improvement because it is a good source of reactive power. In practical field, LPF especially utilized to compensate 5th and 7th order harmonics. Fig. 2.2. shows the circuit scheme for LPF.

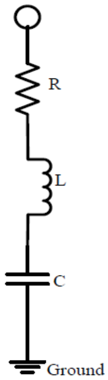

Fig.2.2: Low pass filter

2.2.1.2 High Pass Filter.

The HPF are also consist from passive parts such as capacitor and inductor but behave as small impedance for harmonic current above a certain limited frequency. This kind of filter mitigates all the harmonics above the setting frequency point. There are various filter kinds such as first-order, second-order and third-order etc., depend on the amount of passive filters used in it.

The two-order filter is mostly utilized in practice. Fig. 2.3 illustrates the HPF circuit.

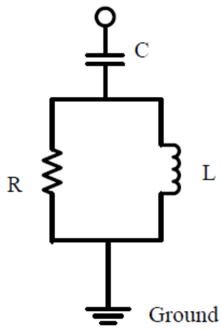

Fig.2.3: High pass filter.

The passive filters have a lot of drawbacks, such as-

- The filter merits has big dependence on the impedance of the system increasing the chance of problems in the working of passive filter on account of harmonic current circulation producing from power electronic nonlinear loads.
- The variation of the nonlinear load will disturb the filter, so retune it is necessary when the load varied.
- Small compensating range that is utilized to mitigate each specific orders or some high harmonic terms.
- The issue of circuit resonance can be produced which reasons non stable working and functioning.
- On account of these drawbacks the passive power filters could not give an efficient re solution to promote the purity of the power network. Therefore, the APF are utilized to get rid of the above mentioned disadvantages.

2.2.2 Active Power Filters (APF).

To get rid of the disadvantage of passive power filters, dynamic mitigation named as Active Power Filter (APF) is utilized newly. The APF is a Voltage Source Inverter (VSI) that injects the reference voltage or current according to the electrical network status. It was presented in 1970's. After that a big progress in power electronics algorithms [43], Concurrently with the theory of instantaneous reactive and active power(p-q theory)that was presented in 1983, APF is an new solution using very fast switching semiconductors, high efficiency and rapid digital transformation switches with normal price. Rely on the circuit arrangement and implementation, APF‟s are split into 3 types and everyone is clarified in carefully below.

2.2.2.1 Shunt APF.

The voltage source inverter (VSI) founded Shunt APF is like as static compensator. It is linked in parallel at the linking point. It generates the necessary current which is Comparative and adverse of the harmonic current. It works as a current source compensating harmonics and it is appropriate for all kinds of nonlinear load. In addition it optimizes the power factor of the load. The line circuit of the distribution network with shunt connected APF is proved in Fig. 2.4. The cost of these kinds of filters is comparatively high, so they are not chooses for large power networks.

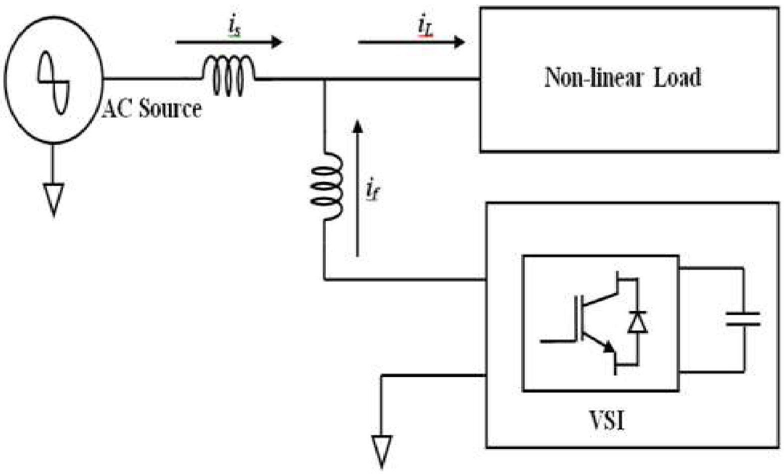

Fig.2.4: Line circuit of shunt APF

2.2.2.2 Series APF

From its name and using transformers, this type of filters are connected in series with distribution network line. The above mentioned filter generates the reference voltage in series with the grid voltage. Therefore, it behaves as a dynamic voltage source which can be varied to mitigate the voltage sag/swell. In the voltage sensitive applications these kinds of filters have mostly used and implemented.

The line circuit of the distribution network composed with series connected APF is seen in Fig. 2.5. The above filter is not utilized in practice, because they have to deal with high current values which raise the filter volume. Therefore, the system losses increased.

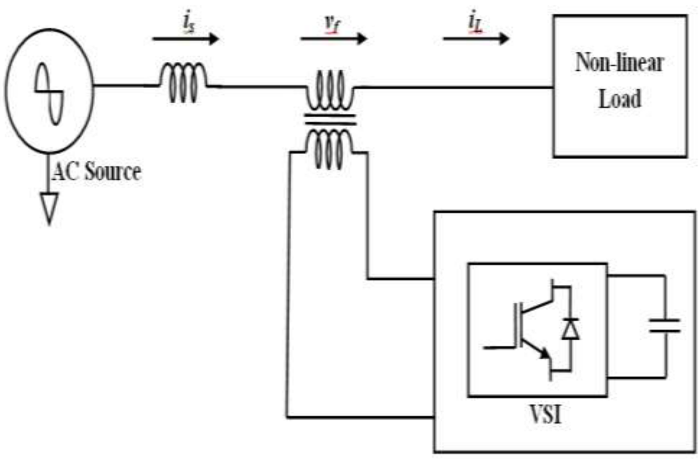

Fig.2.5: Line circuit of series APF.

2.2.2.3 Unified Power Quality Conditioner (UPQC).

The (UPQC) is a summation of series and shunt APF. It supports the benefit of two series APF and shunt APF. In other words, it mitigates the voltage and current harmonics of the grid signal. Thus, this type of filters can mitigate at most all kinds of power problems that the distribution network exposed to them [44]. The line circuit of distribution network with UPQC is clear in Fig. 2.6.

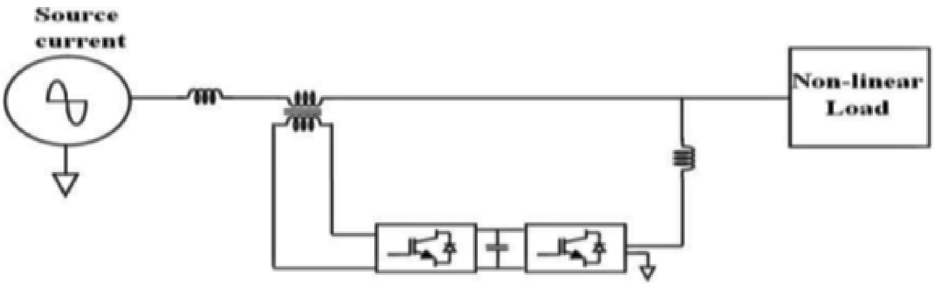

Fig.2.6: Line circuit with UPQC

2.2.3 Hybrid APF.

The APF are the perfect solution for power quality enhancement taking in to account the higher converter ratings. To get rid of from the above disadvantage, hybrid APF have been analyzed and implemented. The hybrid APF has the benefits of all active and passive filters. A lot of hybrid APF depending on the circuit building and configuration. Which include:

- Shunt APF with Series APF
- Shunt APF with Shunt Passive Filter
- APF in series with Shunt Passive Filter
- Series APF with Shunt Passive Filter

2.2.3.1 Series APF and Shunt APF.

These kind of filters configurations have the benefit of series connected APF. Such as mitigation of grid voltage harmonic also what shunt linked APF have like eliminating current harmonic. The line circuit is cleared in Figure. 2.7. The above filter locate it is implementation in Flexible AC Transmission Systems (FACTS). These filters integration is more applicable in eliminating all voltage and current harmonic. Therefore, the research topology is utilized for the enhancement of electric power purity.

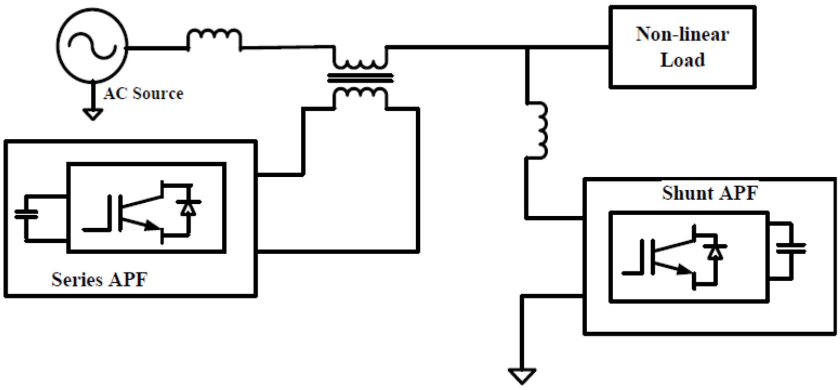

Fig.2.7 Series APF and shunt APF combination

2.2.3.2 Shunt APF and Shunt Passive Filter

The size and electrical ratings of APF components relies on the magnitude of frequencies need to compensate. Therefore, to mitigate low order frequencies, we need APF with less power, low size and small cost. Also we need a big size, high power and high cost APF to compensate high order harmonics. So for low order harmonics, the shunt connected APF used to mitigate them, while for high frequency harmonics, the shunt connected passive filter used to compensate them. A line diagram for the above filter algorithm is seen in Figure. 2.8.

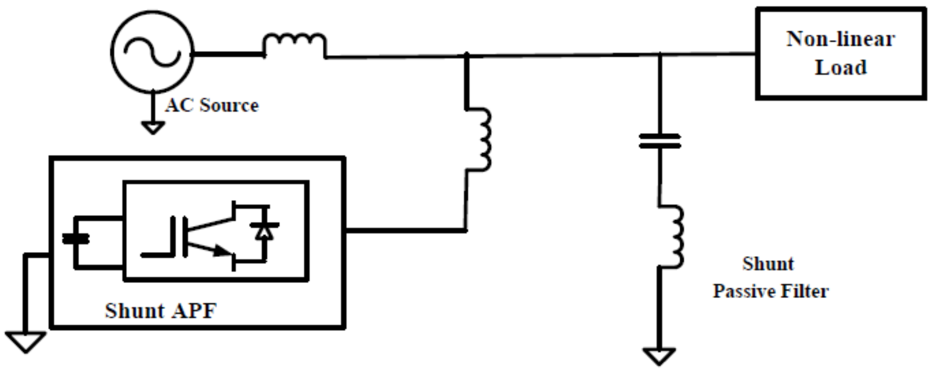

Fig.2.8: Shunt passive filter combined with SAPF.

The major drawback of this kind of filter combination, it is not appropriate for compensating non stable electrical loads. Because the passive filter will set to mitigate a specific and known high order frequencies, so we need to retune it when the load changed.

2.2.3.3 Shunt Passive Filter in Series with Shunt APF

For these kinds of filters combinations, the shunt APF is connected to the distribution network through Shunt linked Passive Filter. The line circuit diagram of the above mentioned filter is seen in Figure. 2.9. The benefit of the below combination is the using of passive filter to minimize the working pressure on the APF semiconductors. The above filter utilized in quite high voltage domain.

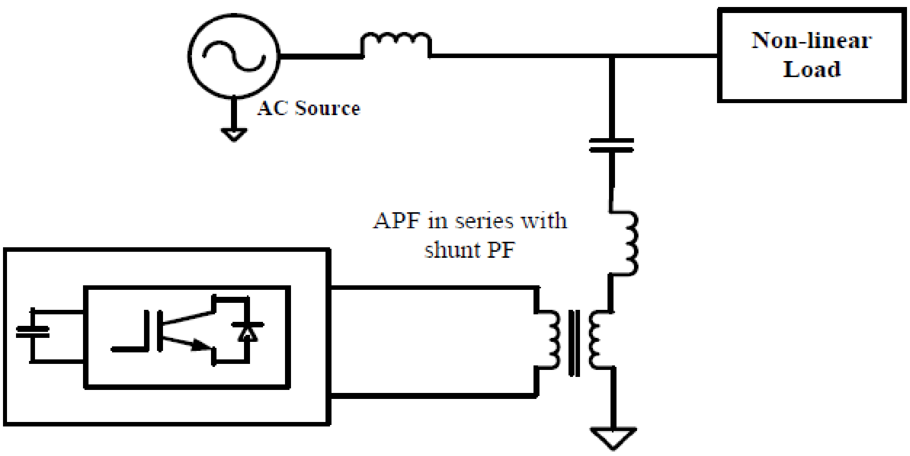

Fig.2.9: Shunt passive filter in series with APF

2.2.3.4 Shunt Connected Passive Filter with Series APF

The above filter arrangement is proved in Fig. 2.10.

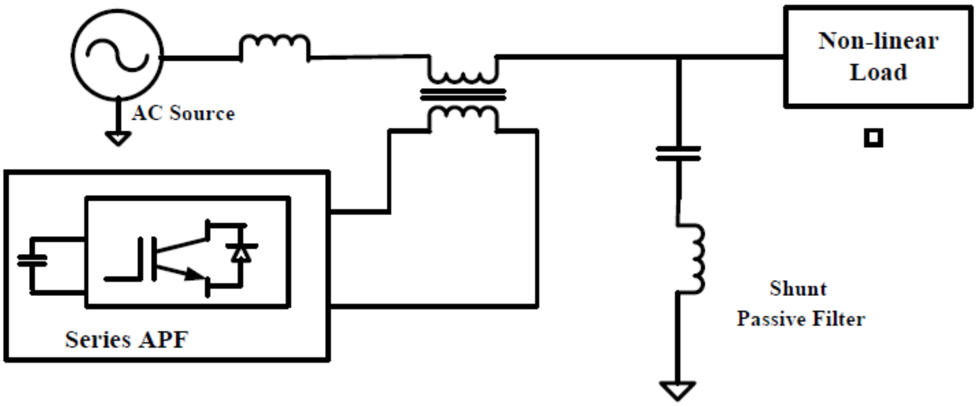

Fig.2.10: Shunt linked passive filter with series APF

In this configuration the series APF acts like small impedance (nearly equals zero) for low order harmonic terms while the shunt APF acts like small impedance for high order harmonics components and eliminate almost all high order frequencies.

2.3 Chapter Summary

The above section present various filter algorithms which are utilized for the enhancement of electric power efficiency. It demonstrates in comprehensive every filter combination included all advantages and disadvantages. It is obvious from the above explanations that the passive filters are less cost types with non-efficient working. Utilizing APF's will delete all the demerits of passive filter taking into account hard control algorithm and complex implementation and design. Therefore, a hybrid APF is utilized to optimize the task needed from the filters.

Chapter Three
Shunt and Series Active Filters

3.1 Overview

The main duty of filters is to eliminate the harmonic and optimize the power in distribution network. The required filters connected must be designed and implemented correctly to get the correct functioning as needed. Along with the various obtainable filter combinations, the hybrid APF which composed from series APF and shunt APF is utilized and implemented in this thesis. The control algorithm of the shunt APF is implemented in order to optimize the current generated from the APF to mitigate the harmonics in the current drained from the source, get a unity power factor at the point of common coupling (PCC) and also inject real power to the system from photovoltaic arrays sources. Whereas the control algorithm of the series connected APF is implemented in order to optimize the voltage injected by the APF to eliminate the harmonics in the voltage drained from the source. The filter design and the control algorithm of the hybrid APF is demonstrated from all perspectives in this section.

3.2 Design of Shunt APF

A shunt APF utilized for the power quality enhancement is recognized as a Current Source Inverter (CSI) [8]. The CSI formed by a three-phase CSI or three single-phase CSI‟s gives the same operation task. A three-phase CSI had been implemented and tested in this work.

The CSI is linked in shunt with the source impedance at the common linking point(PCC). The line circuit of shunt APF is illustrated in Fig.3.1.

Noted that the shunt filter connected directly to (PCC) by using a transmission line without any kind of passive filters.

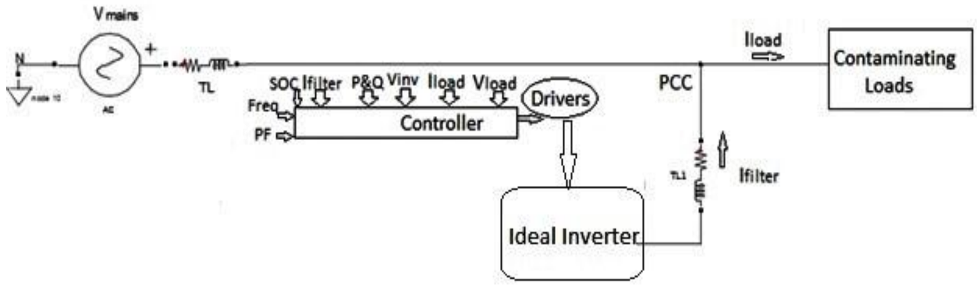

Fig.3.1: Line circuit of shunt APF.

3.3 Design of Series APF

A series APF utilized for the power quality enhancement is defined as a Voltage Source Inverter (VSI). The VSI formed by a three single-phase VSI or three-phase VSI gives the same operation task. A VSI is linked in serial with the distribution network using step up linking transformer. The line circuit of series APF is illustrated in Fig. 3.2.

The parameters of this filter have been chosen taking into account the transformer rated values.

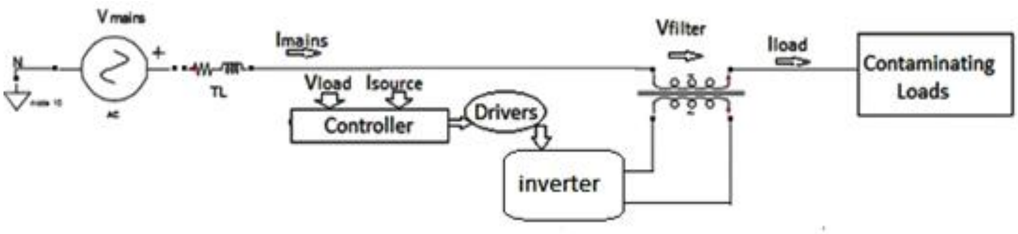

Fig.3.2: Line circuit of series APF**.**

3.4 Harmonic Current Extraction Methods.

The active power filtering goal is to mitigate the harmonics currents generated by the contaminating grid loads, to get pure voltage and current electrical source. At the beginning of filtering working, the reference current must be extract from the grid information. The filtering quality mainly depending on the extracting method of reference signal. A lot of extraction ways were presented in literary and publications. They can be divided into two families: the first family uses the Fast Fourier Transform (FFT) in the frequency field to extract the current harmonics [44, 45]. The major drawbacks of this algorithm are the instability results during transient state, the complexity in working and calculations, and utilizing a big memory in practical applications [45]. In addition to a delay in the extraction of harmonics which can be at least one period.

The second family is based on the time domain calculations in the extraction of harmonics. Some of its methods are based on the instantaneous active and reactive power theory. Also some methods depended on the finding of direct and indirect current terms. In these days, the neural networks and the adaptive linear neural networks have been utilized to extract the voltage and current components and use them to generate the reference needed signals.

Using of time domain methods will reduce the transient period and minimize the calculation and the memory need in practical applications.[45].

3.4.1 Instantaneous Active and Reactive Power Theory (PQ-Theory).

This method offers acceptable precision and easy of functioning. The major drawbacks it is not applicable unbalanced grid voltage case [44]. In this case, A Self Tuning Filter (STF) can be used after the measurement of the grid voltages to extract the fundamental balanced three phase voltage components of the distorted unbalanced one.

Normally the APFs have been implemented using the instantaneous active and reactive power (p-q) theory, the first method presented by Akagi et al in 1983 [46, 47]. Firstly, it was modeled for non-neutral three-phase networks, after that the Watanabe and Aredes proposed a model for three-phase four wires distribution networks [47].The algorithm utilizes the transformation of distorted currents from three phase frame abc into bi-phase stationary frame αβ.

The main principle of this theory is that the harmonic currents raised by contaminating loads in the electrical network can be mitigated using controlled nonlinear load. The p-q algorithm is depending on a set of instantaneous powers defined in the time domain.

The three-phase supply voltages (va, vb, vc) and currents (ia, ib, ic) are transformed utilizing the Clarke (or α-β) transformation into a different coordinate system getting instantaneous active and reactive power terms. This transformation may be observed as a projection of the three-phase terms onto a stationary two-axis reference frame. The Clarke transformation for the voltage variables is presented by [3.1]:

$$\begin{pmatrix} v\alpha \\ v\beta \\ v0 \end{pmatrix} = sqrt(\frac{2}{3}) \begin{pmatrix} 1 & -\frac{1}{2} & -\frac{1}{2} \\ 0 & \frac{sqrt(3)}{2} & -\frac{sqrt(3)}{2} \\ \frac{1}{sqrt(2)} & \frac{1}{sqrt(2)} & \frac{1}{sqrt(2)} \end{pmatrix} \begin{pmatrix} va \\ vb \\ vc \end{pmatrix} \tag{3.1}$$

In the same way, we can extract the equation for contaminating load currents as seen below.

$$\begin{pmatrix} i\alpha \\ i\beta \\ i0 \end{pmatrix} = sqrt(\frac{2}{3}) \begin{pmatrix} 1 & -\frac{1}{2} & -\frac{1}{2} \\ 0 & \frac{sqrt(3)}{2} & -\frac{sqrt(3)}{2} \\ \frac{1}{sqrt(2)} & \frac{1}{sqrt(2)} & \frac{1}{sqrt(2)} \end{pmatrix} \begin{pmatrix} ia \\ ib \\ ic \end{pmatrix} \tag{3.2}$$

The instantaneous active power p(t) is known as

$$p(t) = v_a i_a + v_b i_b + v_c i_c \tag{3.3}$$

The above equation can be given in the stationary frame by:

$$p(t) = v_\alpha i_\alpha + v_\beta i_\beta \tag{3.4}$$

$$p_0(t) = v_0 i_0 \tag{3.5}$$

Where, p(t) is the instantaneous active power, p_0(t) is the instantaneous homo-polar sequence power. In the same way, the instantaneous reactive power can be given by:

$$\boldsymbol{q(t) = -\frac{1}{sqrt(3)}[(v_a - v_b)i_c + (v_b - v_c)i_a + (v_c - v_a)i_b = v_\alpha i_\beta - v\beta i_\alpha} \quad (3.6)$$

It is essential to note that the instantaneous reactive power q(t) benefit much than the simple reactive power. The instantaneous reactive power algorithm taking into consideration all the current and voltage harmonics, while the normal reactive power take only the fundamentals of current and voltage [50].

From eqns.3.5 and 3.6 the instantaneous active and reactive power can be presented in matrix form by:

$$\begin{pmatrix} \boldsymbol{p} \\ \boldsymbol{q} \end{pmatrix} = \begin{pmatrix} \boldsymbol{v\alpha v\beta} \\ \boldsymbol{-v\beta v\alpha} \end{pmatrix} \begin{pmatrix} \boldsymbol{i\alpha} \\ \boldsymbol{i\beta} \end{pmatrix} \quad (3.7)$$

Generally, each the active and reactive instantaneous power terms includes a direct term and an alternating term. The direct term of every one represents the power of the fundamentals of current and voltage. The alternating component is the power of the harmonics of currents and voltages.

So as to split the harmonics from the fundamentals of the load currents, it is adequate to extract the direct component of the instantaneous power from the alternating component. A Low Pass Filter (LPF) with feed-forward influence can be utilized to achieve this duty. Figure 3.3 shows the principle of this extraction filter.

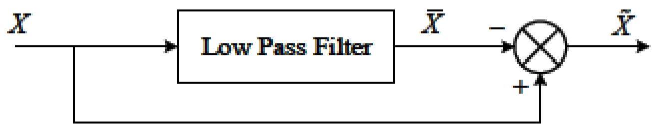

Fig.3.3: Diagram of the low pass filter with feed-forward**.**

After the segregation of the direct and alternating terms of instantaneous power, the harmonic components of the load currents can be given utilizing the inverse of equation (3.6) which gives:

$$\begin{pmatrix} i\alpha \\ i\beta \end{pmatrix} = \frac{1}{(v^2{s\alpha}+v^2{s\beta})} \begin{pmatrix} vs\alpha & -vs\beta \\ vs\beta vs\alpha & \end{pmatrix} \begin{pmatrix} p^{\sim} \\ q^{\sim} \end{pmatrix} \tag{3.8}$$

Where, the ˜ symbol indicates to the alternating component and the ¯ symbol indicate to the direct term of every active and reactive power. The APF reference current can be presented by:

$$\begin{pmatrix} i_{fa} \\ i_{fb} \\ i_{fc} \end{pmatrix} = sqrt\left(\frac{2}{3}\right) \begin{pmatrix} 1 & 0 \\ -\frac{1}{2} & \frac{sqrt(3)}{2} \\ -\frac{1}{2} & -\frac{sqrt(3)}{2} \end{pmatrix} \begin{pmatrix} i^{\sim}\alpha \\ i^{\sim}\beta \end{pmatrix} \tag{3.9}$$

Figure 3.4 presents the principle of the active and reactive instantaneous power. This method offers the advantage of the possibility of harmonic mitigation and/or reactive power mitigation. If reactive power mitigation used, it is equate to send the reactive power q(t) immediately to the reference current calculation block without the utilizing of any extraction filter.

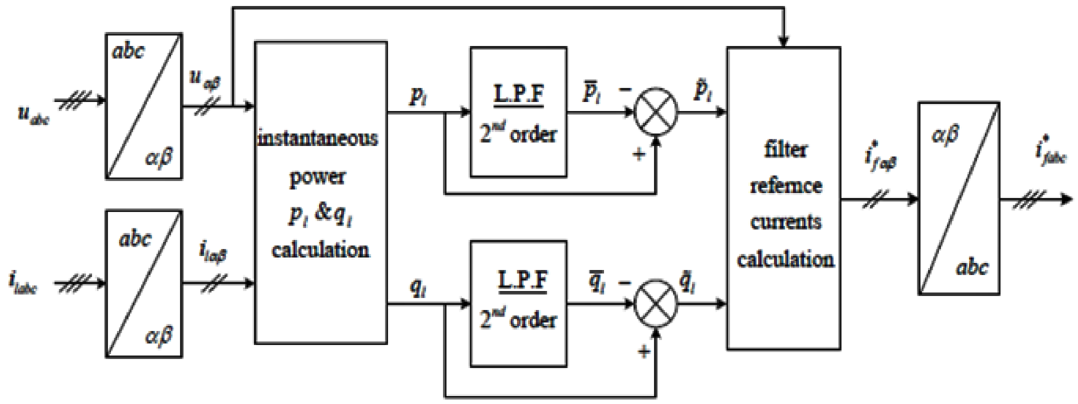

Fig.3.4: Principle of instantaneous active and reactive power theory.

3.4.2 Synchronous Reference d-q Method.

In Synchronous Reference d-q algorithm, the load currents are converted from three phase frame reference (abc) into synchronous reference [51]. (dq) in order to extract the harmonic contents from the fundamentals . It gives better behavior even in the case where the three phase voltage is not symmetrical.

The d-q transformation and Operation utilizing a control algorithm which is depend on d-q axis control theory.

This d-q axis control system enables the power controller to follow the variations in reference values like AC voltage, DC link voltage, real and reactive powers through the line. By using a d-q axis controller it is possible to output a relatively fast response and to minimize the interaction between real and reactive power flow.

In this control method, the transformation of a three phase system to d-q and d-q to 3-phase quantities is done according to Park's transformation, through which real and reactive power can be controlled separately, while also regulating the local bus voltage. Then in d-q control system real power is influenced by the phase angle. Whereas reactive power is dependent on the voltage magnitude.

Reference frame theory based d-q model of Shunt active filter is presented in this section. However, expressing instantaneous voltages and currents in three phase circuits mathematically, it is enough to express their quantities as the instantaneous space vectors. Vector explanation of instantaneous three phase quantities a, b and c which are displaced by an angle 2π/3 from each other is shown in Fig. 3.5

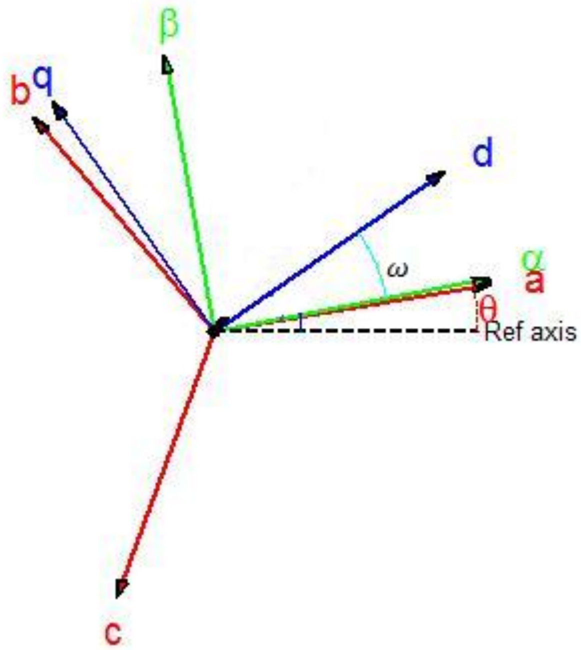

Fig 3.5: α β to d-q transformation.

Where ω is the angular velocity of the d-q reference frame (Fig. 3.5).

The current components in the d- q reference frame can be similarly obtained using the α-β to d-q transformation matrix. The unit vector required for this transformation is generated using the stepped down grid voltages.

The instantaneous current and voltage space vectors are expressed in terms of instantaneous voltages and currents as.

$$v = [vavbvc]T \tag{3.10}$$

$$i = [iaibic]T \tag{3.11}$$

The Instantaneous currents and voltages on the ABC coordinates can be converted into the quadrature α, β coordinates by Clark Transformation as follows:

$$\begin{pmatrix} v\alpha \\ v\beta \\ v0 \end{pmatrix} = T1 \begin{pmatrix} va \\ vb \\ vc \end{pmatrix} \tag{3.12}$$

$$\begin{pmatrix} i\alpha \\ i\beta \\ i0 \end{pmatrix} = T1 \begin{pmatrix} ia \\ ib \\ ic \end{pmatrix} \tag{3.13}$$

Where:

$$\mathbf{T1}=\sqrt[2]{\frac{2}{3}} * \begin{pmatrix} \mathbf{1} & -\frac{1}{2} & -\frac{1}{2} \\ \mathbf{0} & \frac{\sqrt[2]{3}}{2} & -\frac{\sqrt[2]{3}}{2} \\ \frac{1}{\sqrt[2]{2}} & \frac{1}{\sqrt[2]{2}} & \frac{1}{\sqrt[2]{2}} \end{pmatrix} \tag{3.14}$$

Since in a balanced three-phase three-wire system neutral current is zero, the zero sequence current does not exist. Hence the voltages and currents in the α-β reference frame can be expressed as shown in equation 3.15&3.16.

$$\begin{pmatrix} v\alpha \\ v\beta \end{pmatrix} = \sqrt[2]{\frac{2}{3}} * \begin{pmatrix} 1 & -\frac{1}{2} & -\frac{1}{2} \\ 0 & -\frac{\sqrt[2]{3}}{2} & \frac{\sqrt[2]{3}}{2} \end{pmatrix} \begin{pmatrix} va \\ vb \\ vc \end{pmatrix} \tag{3.15}$$

$$\begin{pmatrix} vd \\ vq \end{pmatrix} = T2 \begin{pmatrix} v\alpha \\ v\beta \end{pmatrix} \tag{3.16}$$

Where

$$T2=\begin{pmatrix} cos(\omega) & -sin(\omega) \\ sin(\omega) & cos(\omega) \end{pmatrix} \tag{3.17}$$

Fig.3.6 presents the algorithm of the synchronous reference frame (d-q) extraction method.

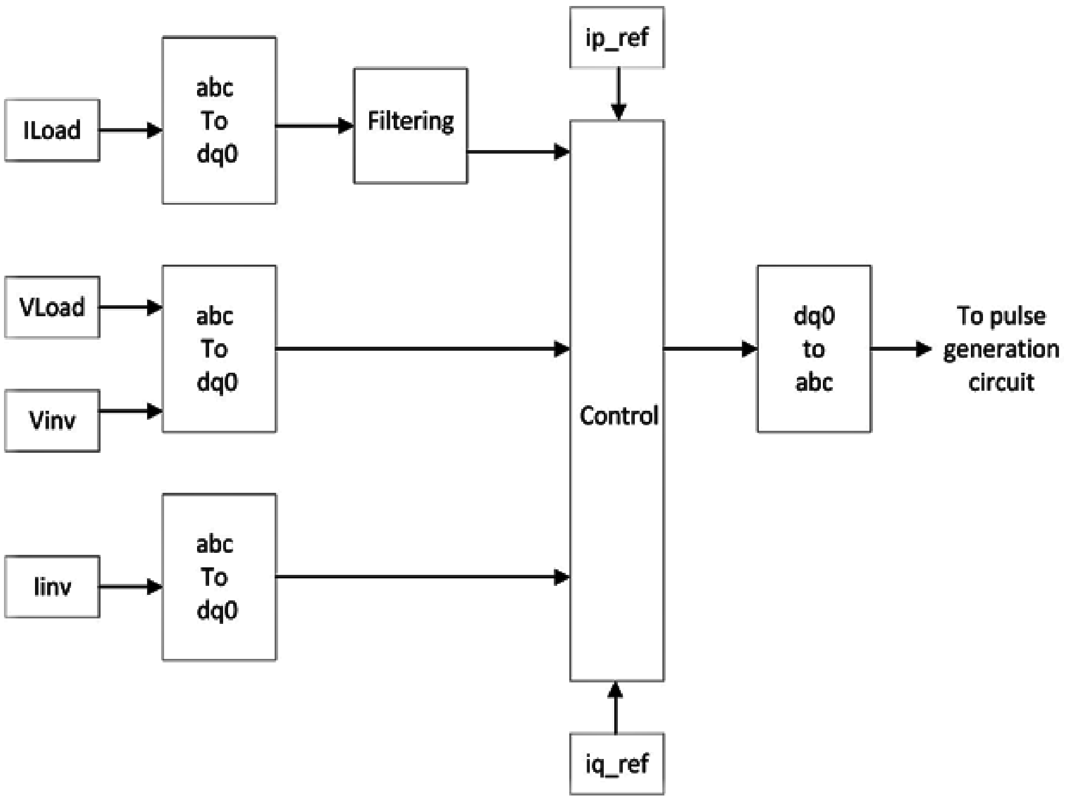

Fig.3.6: Synchronous reference frame extraction method for SHAPF.

3.4.3 RMS Value Based Algorithm

For a three-phase three wire electrical power system, the load currents (i_{la}, i_{lb}, i_{lc}) are measured and transformed into stationary reference system. According to this method the high order harmonics, both in the phase and the magnitude of the load's current vector, are eliminated from the load currents. Then Eqn.3.18 is used to calculate the magnitude of the reference current vector [48].

$$|\boldsymbol{I_{ref}}| = \boldsymbol{sqrt}(\boldsymbol{i_\alpha}^{\mathbf{2}} + \boldsymbol{i_\beta}^{\mathbf{2}}) \tag{3.19}$$

3.4.4 Active and Reactive Currents Method.

In this method, instead of using the Clark transform to calculate instantaneous active and reactive power, it calculates directly the active and reactive parts of the load current. The currents are determined under the constraint that they must transport the same power absorbed by the load [49].

The reactive instantaneous current in the system is a component that doesn't contribute in the active energy transfer. But, it increases the current amplitude and the losses. This current can be determined using the Lagrange method.

If we suppose that the load current i_{ln} with n=a, b, c is composed of active i_{lna} and reactive i_{lnr} parts as:

$$\boldsymbol{i_{ln}} = \boldsymbol{i_{lna}} + \boldsymbol{i_{lnr}} \tag{3.20}$$

The principle of this method is to determine the active current in the load current with the constraint that the reactive current doesn't produce any instantaneous active power. The task is then to minimize the function L given by:

$$L(i_{la}, i_{lb}, i_{lc}) = i_{la}{}^2 + i_{lb}{}^2 + i_{lc}{}^2 \tag{3.21}$$

With the constraint that:

$$p = v_a i_{la} + v_b i_{lb} + v_c i_{lc} \tag{3.22}$$

The problem can be solved using Lagrange method which leads to:

$$\begin{pmatrix} 2 & 0 & 0 \\ 0 & 2 & 0 \\ 0 & 0 & 2 \end{pmatrix} \begin{pmatrix} i_{la} \\ i_{lb} \\ i_{lc} \end{pmatrix} = -⅄ \begin{pmatrix} va \\ vb \\ vc \end{pmatrix} \tag{3.23}$$

In this equation, ⅄ is given by:

$$⅄ = -\frac{2p}{v_a{}^2 + v_b{}^2 + v_c{}^2} \tag{3.24}$$

From Eqns. 3.23 and 3.24 the currents can be given by:

$$\begin{pmatrix} i_{laa} \\ i_{lba} \\ i_{lca} \end{pmatrix} = \frac{p}{v_a{}^2 + v_b{}^2 + v_c{}^2} \begin{pmatrix} va \\ vb \\ vc \end{pmatrix} \tag{3.25}$$

The active currents obtained by Eqn. 3.25and the original load currents produce the same instantaneous active power. This means that the load currents are equal to the active currents from the power point of view.

The difference is that the active currents don't produce any reactive power and they have less root mean squared value than the original currents.

As in the PQ theory, the active instantaneous power has two components in addition to the zero components. The first direct represents the fundamentals of current and voltage and the second alternative represents the harmonics.

$$\boldsymbol{p} = \boldsymbol{p}^{-} + \boldsymbol{p}^{\sim} + \boldsymbol{p}_{\mathbf{0}} \qquad (3.26)$$

If we use the direct component of the power, the active fundamental currents will be achieved.

$$\begin{pmatrix} \boldsymbol{i_{laaf}} \\ \boldsymbol{i_{lbaf}} \\ \boldsymbol{i_{lcaf}} \end{pmatrix} = \frac{\boldsymbol{p}^{-}}{\boldsymbol{v_a}^2+\boldsymbol{v_b}^2+\boldsymbol{v_c}^2} \begin{pmatrix} \boldsymbol{va} \\ \boldsymbol{vb} \\ \boldsymbol{vc} \end{pmatrix} \qquad (3.27)$$

A low pass filter of the second order can be used to extract the direct component of the power.

3.5 Modeling of Shunt Active Power Filter.

Nonlinear load is considered. The source voltages (v_{sa}, v_{sb},v_{sc})and the inverter output voltages (v_{fa}, v_{fb}, v_{fc}), Fig. 3.7 shows the circuit diagram of phase A.

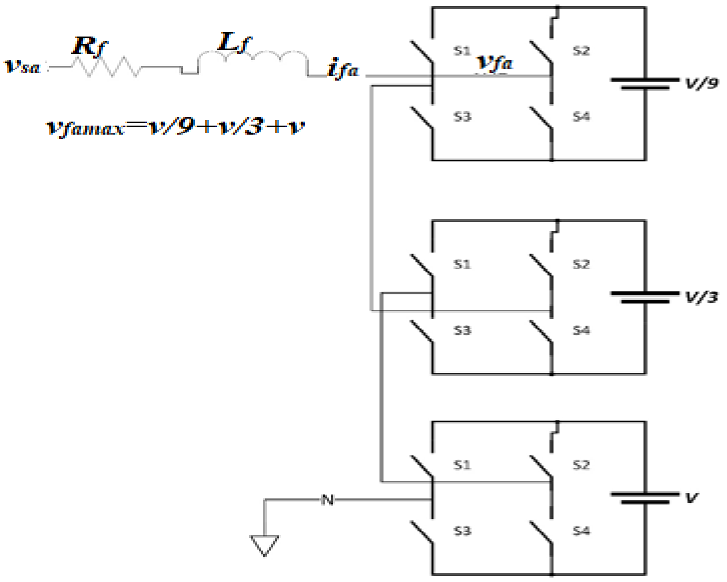

Fig.3.7: Circuit diagram of phase A.

The inverter output is connected through the inductor L_f and resistor R_f to the source side. The source voltage can be expressed as follows:

$$v_{sa} = i_{fa}R_f + L_f\frac{di_{fa}}{dt} + v_{fa} \tag{3.28}$$

$$v_{sb} = i_{fb}R_f + L_f\frac{di_{fb}}{dt} + v_{fb} \tag{3.29}$$

$$v_{sc} = i_{fc}R_c + L_f\frac{di_{fc}}{dt} + v_{fc} \tag{3.30}$$

The equations 3. (28, 29, 30) are transformed in terms of the d-q variables using the reference frame transformation follow:

$$L_f\frac{di_d}{dt} = -i_dR_f + (V_{sad} - V_{fad}) - \omega L_f i_q \tag{3.31}$$

$$L_f\frac{di_q}{dt} = -i_qR_f + (V_{saq} - V_{faq}) - \omega L_f i_d \tag{3.32}$$

$$L_f\frac{di_d}{dt} = -idR_f + vd \tag{3.33}$$

$$L_f\frac{di_q}{dt} = -iqR_f + vq \tag{3.34}$$

Where:

$$v_d = (V_{sad} - V_{fad}) - \omega L_f iq \quad (3.35)$$

$$v_q = (V_{saq} - V_{faq}) + \omega L_f i_d \quad (3.36)$$

From the above equations the current controllers are derived as shown in Figs. 3.8.

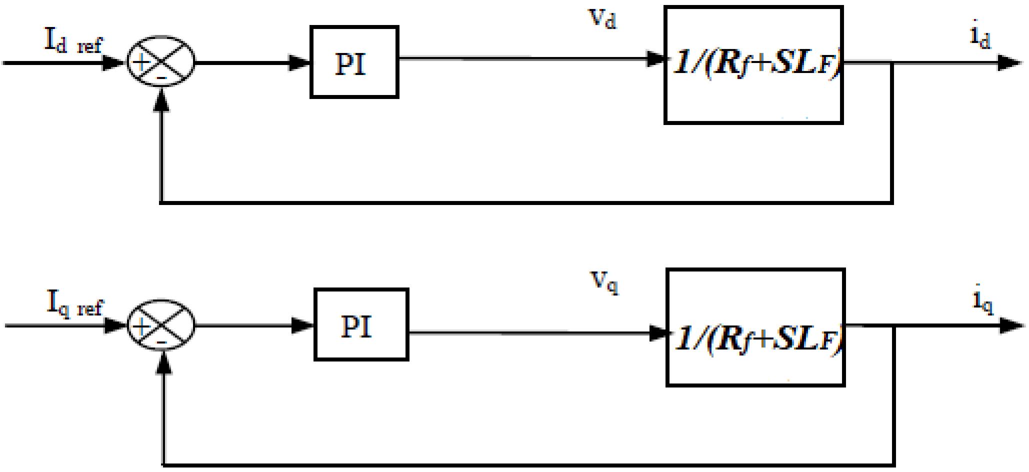

Fig.3.8: Circuit diagram of current controllers

The output voltage of active power filter denoted as in Fig.3.2 is generated to compensate the reactive power was covered from the source, and a certain amount of real power depending on the state of charge of batteries(SOC) and the frequency of the system. To maintain this algorithm the voltages V_{fa}, V_{fb} and V_{fc} are controlled by changing the switching pulses.

3.6 Modeling of Series APF

The designing of the series APF is required for filter controlling.

In our work, the model of the series active power filter which is nothing but a three-phase VSI is executed in 2-ϕ stationary reference frame (α-β). Therefore, the three phase quantities, voltage and current vectors, are converted into α-β coordinates by utilizing Clarke's Transformation.

In a 3-ϕ three-wire system the voltage vector is demonstrated as-

$$v = [vavbvc]T \tag{3.37}$$

The current vector in three-phase domain can be write as-

$$i = [iaibic]T \tag{3.38}$$

Now these voltage and current vectors are converted into two-phase system utilizing the transformation matrix.

Thus, the instantaneous value of real power in the 0-α-β frame can be found as-

$$P_{3\phi}(t) = v_\alpha i_\alpha + v_\beta i_\beta + v_0 i_0 \tag{3.39}$$

Here in equation (3.39) v0, i0 symbolize the zero sequence voltage and zero sequence current similarly. Their product gives the zero sequence power denoted as p0.

Therefore, the equation (3.40) can be given as-

$$P_{3\phi}(t) = p + p_0 \tag{3.40}$$

Here P symbolizes the instantaneous real power and is given as-

$$P = v_\alpha i_\alpha + v_\beta i_\beta \tag{3.41}$$

The power can be demonstrate in Victoria form utilizing dot product. Therefore the active power when represented in vector format can be given as follows

$$P = i^T_{\alpha\beta} v_{\alpha\beta} \tag{3.42}$$

Here the $i^T_{\alpha\beta}$ transposed current vector in α-β axis and $v_{\alpha\beta}$ is the voltage vector in α-β axis and are illustrated by equations (3.43) and (3.44) likely

$$i_{\alpha\beta} = [i_\alpha i_\beta]T \tag{3.43}$$

$$v_{\alpha\beta} = [v_\alpha v_\beta]T \tag{3.44}$$

In a three-phase three-wire system, the zero sequence power will be zero and hence the term p0 in equation (3.39) can be ignored. The instantaneous imaginary power can be calculated by the equation (3.45) as-

$$q = v_\alpha i_\beta - i_\alpha v_\beta \tag{3.45}$$

The above equation can be written in vector form as-

$$P = i^T_{\alpha\beta\perp} v_{\alpha\beta} \tag{3.46}$$

Where $i^T_{\alpha\beta\perp}$ is the transposed current vector perpendicular to $i_{\alpha\beta}$ and is giving by formula (3.47) as-

$$i_{\alpha\beta\perp} = [i_\beta - i_\alpha]^T \tag{3.47}$$

When the instantaneous real and reactive power in equations (3.42) and (3.46) are expressed in matrix form then the matrix formula is-

$$\begin{pmatrix} p \\ q \end{pmatrix} = \begin{pmatrix} iT\alpha\beta \\ i^T{}_{\alpha\beta_\perp} \end{pmatrix} v\alpha\beta \tag{3.48}$$

The voltage vector can be decomposed in its orthogonal projection on the current vector axis as illustrated in Fig. 3.9.

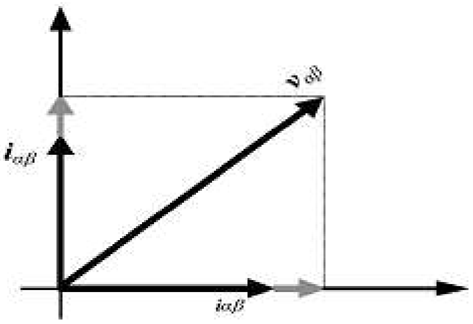

Fig.3.9: Voltage vector decomposition

By using the current vectors and the real and imaginary instantaneous power, the voltage vector can be written as-

$$v\alpha\beta = (p/\, i^2\alpha\beta)\, i\alpha\beta + (q/\, i^2\alpha\beta)\, i\alpha\beta\perp \tag{3.49}$$

In case of three-phase four-wire system, there will be an extra term in the above equation corresponding to the zero sequence current components.

3.7 Control of Active Power Filter

The researchers are always at the point of the research to ameliorate the control methods of the SAPF to achieve better results either from the point of view of better perturbation extraction methods, the amelioration of the dynamic regimes, decreasing the value of the THD,…etc, or the development of new control methods to ameliorate the performance of the APF with the different non-linear loads. There are principally two methods for the compensation of the harmonic currents dependent on the measured current:

3.7.1 Direct Control Method.

In this method the load currents are measured and the harmonic currents are extracted from the load currents [21]. Figure 3.10 shows the diagram of the direct control method. Using this method, the SAPF injects the harmonic currents without any information about the grid currents. All the errors in the system like the parameters uncertainty, the measurement or control errors will appear in the grid current as unfiltered harmonic contents. The main advantage of this method is the system stability. However, this method needs an expanded control algorithm with large number of sensors [60].

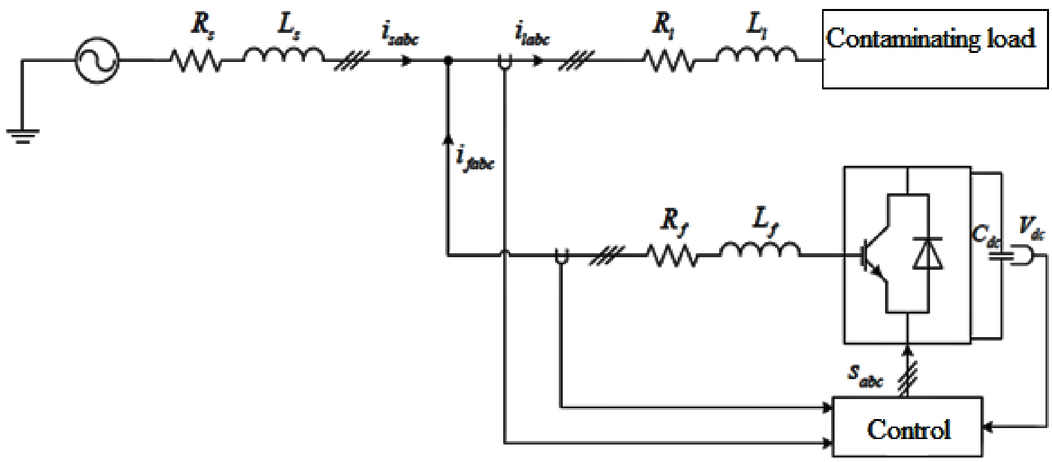

Fig.3.10: Direct control method diagram.

Figure 3.11 presents the global diagram of the direct control method of shunt active power filter. Applying the Laplace transform on the equation of the APF voltages we can find:

$$V_f(S) = V_S(S) + SL_f I_f(S) + R_f I_f(S) \tag{3.50}$$

Where we can describe the filter current by:

$$I_f(S) = \frac{(V_f(S) - V_S(S))}{L_f S + R_f} \tag{3.51}$$

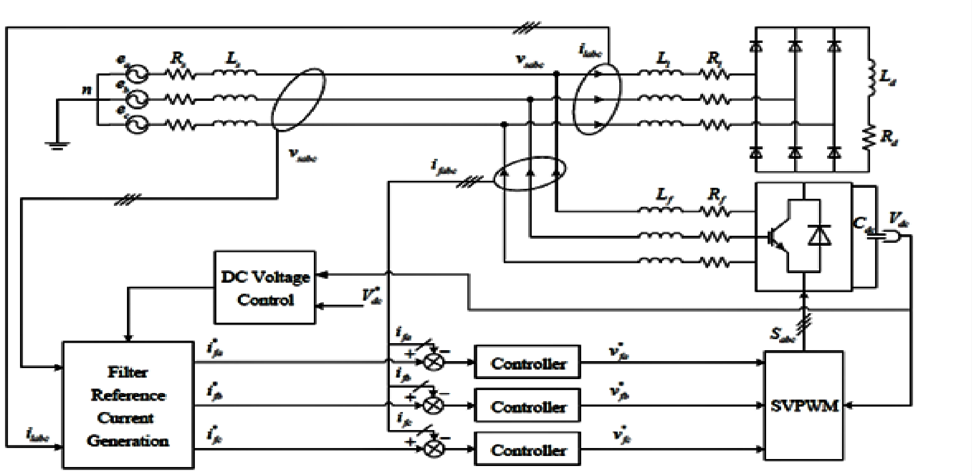

Fig.3.11: Direct control of shunt active power filter.

The voltage V_f given by eqn.3.50 is composed of two different frequency parts. The first is the grid voltage –at the PCC- which is a measurable quantity. The second part is the voltage across the coupling filter L_f when the reference current passes through it [6]. This component is compensated by the current controllers. Figure 3.12 shows the structure of the control loop with the voltage source inverter [61].

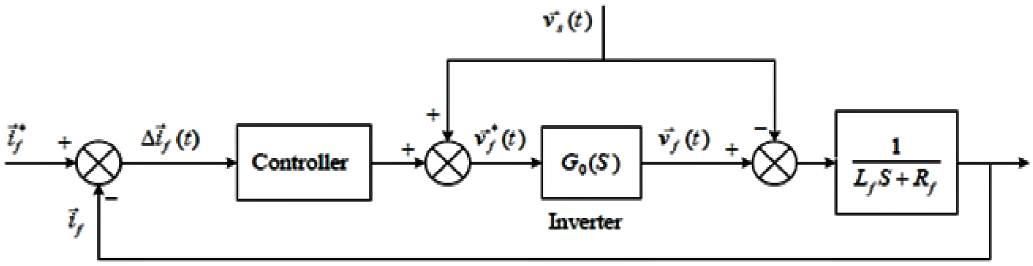

Fig.3.12: Structure of current control loop.

In order that the output voltage of the VSI is equal to its reference, a good choice of the transfer function which represents the inverter is to be 1 [4, 6].

3.7.1.1 Control in the Three Phase Reference

The PI controller is the most classical controller used in the current regulation due to its simplicity. The simplified diagram of the current regulation using PI controller is shown in figure 3.13. Transfer function in closed loop for this diagram is given by:

$$H_{CL} = \frac{k_{pi}S + k_{ii}}{L_f S^2 + (R_f + k_{pi})S + k_{ii}} \tag{3.52}$$

It can be written in the next form:

$$H_{CL} = \frac{(2\zeta\omega_c - \frac{R_f}{L_f})S + \omega_c}{S^2 + 2\zeta\omega_c S + \omega_c{}^2} \tag{3.53}$$

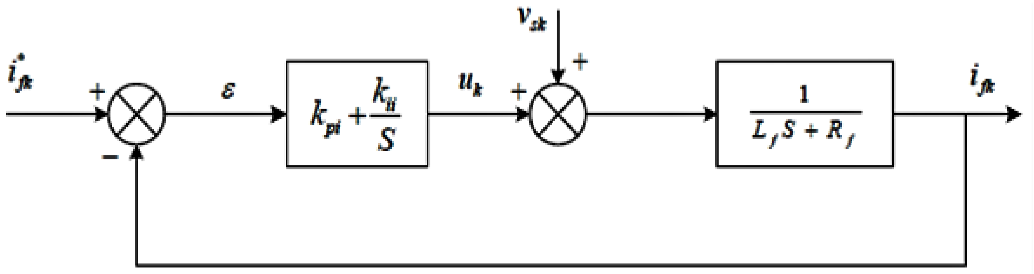

Fig.3.13: Diagram of PI current controller loop.

The value of the damping factor is chosen to be 0.707 for a good dynamic response. In order to reject the harmonics due to the switching, the cut off frequency of the system must be away from the PWM switching frequency [61]. The constants of the controller are given by:

$$k_{pi} = 2\zeta\omega_c L_f - R_f \tag{3.54}$$

$$k_{ii} = L_f \omega_c{}^2 \tag{3.55}$$

$$\omega_c = 2\pi f_c \tag{3.56}$$

The output of the regulator is added to the voltage of the PCC to cancel the effect of this voltage on the static behavior of the filter [6].

3.7.1.2 Control of the Currents id and iq

The currents on the axes d and q are coupled. To simplify the control of these two components, it is enough to separate them, by introducing new terms in the first and the second equation of the system 3. [1, 2, and 3] we define:

$$v_d = L_f \frac{di_{fd}}{dt} + R_f i_{fd} \tag{3.57}$$

$$v_q = L_f \frac{di_{fq}}{dt} + R_f i_{fq} \tag{3.58}$$

It becomes then:

$$v_{fd} *= v_d + v_{sd} + L_f \omega i_{fq} \tag{3.59}$$

$$v_{fq} *= v_q + v_{sq} - L_f \omega i_{fq} \tag{3.60}$$

Applying the Laplace transform on the first and the second system, we find:

$$G_{dq}(S) = \frac{I_{fd}(S)}{V_d(S)} = \frac{I_{fq}(S)}{V_q(S)} = \frac{1}{R_f + L_f S} \tag{3.61}$$

Figure 3.15 shows the diagram of the closed loop current control in the synchronous frame.

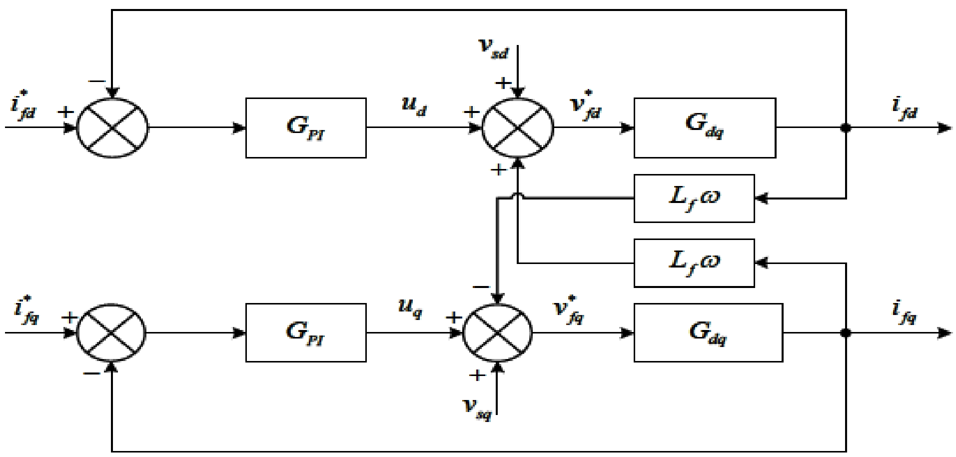

Fig.3.14: Block diagram of the current controllers in synchronous reference.

3.7.1.3 Control of Shunt Active Power Filter.

In this thesis, the synchronous reference frame (d-q) extraction method is used in shunt active power filter for sending the status of load currents and voltages to inverter gates then take a feedback from inverter current and voltage output to Guarantee a precise compensation of load currents. Figure 3.16 shows the block diagram of control algorithm of shunt active power filter using synchronous reference frame (d-q) method.

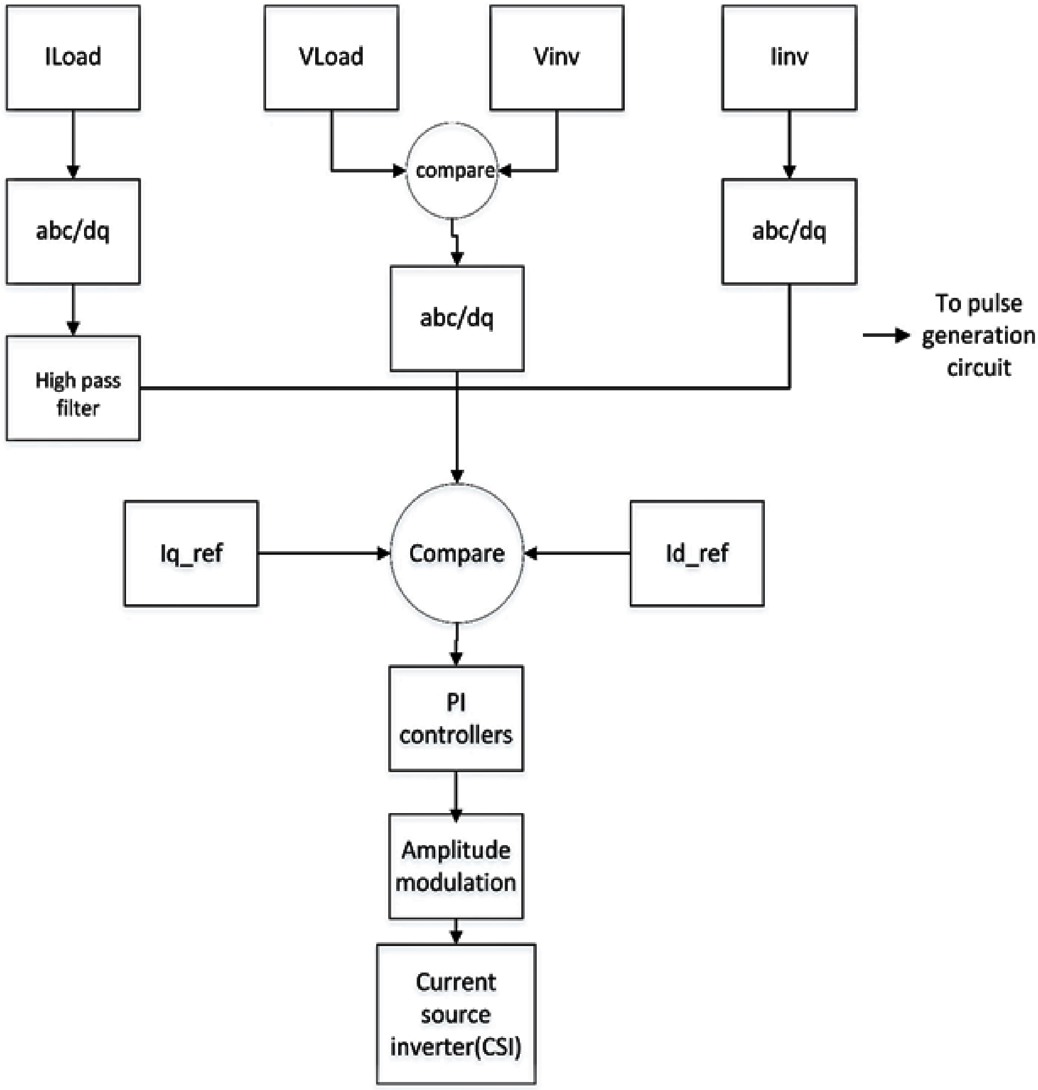

Fig.3.15: Block diagram of control strategy of shunt active power filter using (d-q) method.

Fig.3.16 shows the MATLAB SIMULINK for shunt APF controller

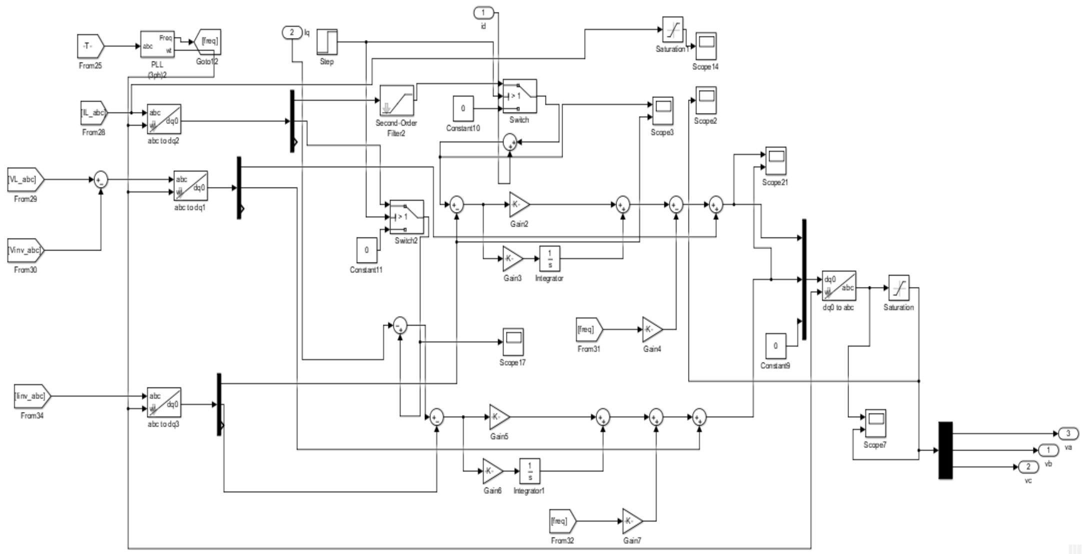

Fig.3.16: MATLAB SIMULINK for Shunt APF controller.

3.7.2 Indirect Control Method

This method based on the measurement of the source currents, and then to impose the sinusoidal form on these currents. The control algorithm is less complicated and needs fewer sensors than the direct control. Figure 3.17 shows the diagram of the indirect control method of the SAPF.

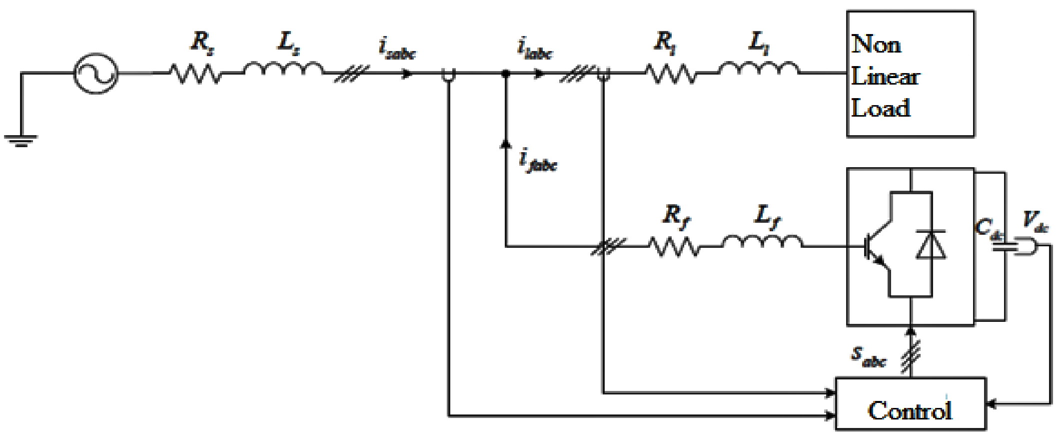

Fig.3.17: Indirect control method diagram.

In indirect control method of the active power filter, we interest in the control of the grid currents without looking at the filter currents. Sinusoidal current reference for the grid is generated using appropriate methods. These currents are then compared with the measured grid currents. The error is fed to a hysteresis current controller which generates the pulses to control the switches of the Series APF.

3.7.2.1 Grid Current Reference Generation.

The generation of the grid reference currents is similar to that used for the generation of filter current reference. In literature one can find different methods for the identification of the grid currents.

From these methods we can find the method based on the PQ theory, the method based on the d-q theory [21], and the method based on the DC voltage controller [64, and 65]. In the next section, we are going to discuss these different methods in the generation of the grid current reference.

3.7.2.2 Indirect Control Based on DC Voltage Controller.

In this method the peak value of the reference grid current Ispeak* is determined by the DC voltage regulator. In order to generate the reference currents of the grid, the peak value of the grid current is multiplied simply by the unit vectors of voltage at the PCC. The reference currents are then given by:

$$i_{sd} *= I_{speak} * \ sin(\Theta) \tag{3.62}$$

$$i_{sd} *= I_{speak} * \ sin(\Theta - \frac{2\pi}{3}) \tag{3.63}$$

$$i_{sd} *= I_{speak} * \ sin\left(\Theta + \frac{2\pi}{3}\right) \tag{3.64}$$

Where the angle θ is the angular position generated using a PLL circuit.

3.7.2.3 Design of PI Controller for the Indirect Control Method.

In this section, we are going to construct the PI controller which is charged to produce the peak value of the grid current. The input of this controller will be the error between the stored energy in the capacitor and its reference value. Its output represents the reference power of the three-phase system at the PCC defined by Eqn. 3.65.the reference power of the filter pf* represents the difference between the grid reference power and the load power, supposing that the filter is able to produce its reference power in each period. This power represents the transmitted power from the source to the filter, neglecting the losses of the filter and the coupling inductance. The integral of the filter power gives the energy stored in the condenser [65]. Figure 3.18 shows the diagram of the voltage regulation.

$$p_S *= \frac{\frac{3V_{speak}\, i_{speak}}{2}}{} \tag{3.65}$$

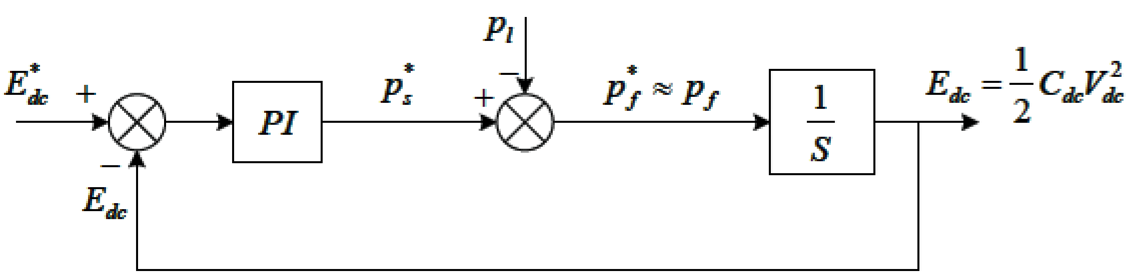

Fig.3.18: Diagram of DC voltage closed loop control.

3.7.2.4 Control of Series APF

The series APF have been controlled in order that the voltage generated by it should mitigate the source voltage harmonics existing in electrical network. The inverter output voltage of APF must be controlled to get needed task in perfect algorithm.

To achieve this task, a voltage reference signal must be generated and then analyzed to generate the needed pulses for inverter gates. And then the APF will inject the needed voltage in series with grid voltage. The flow chart seen in Fig.3.19 shows the control algorithm for series APF.

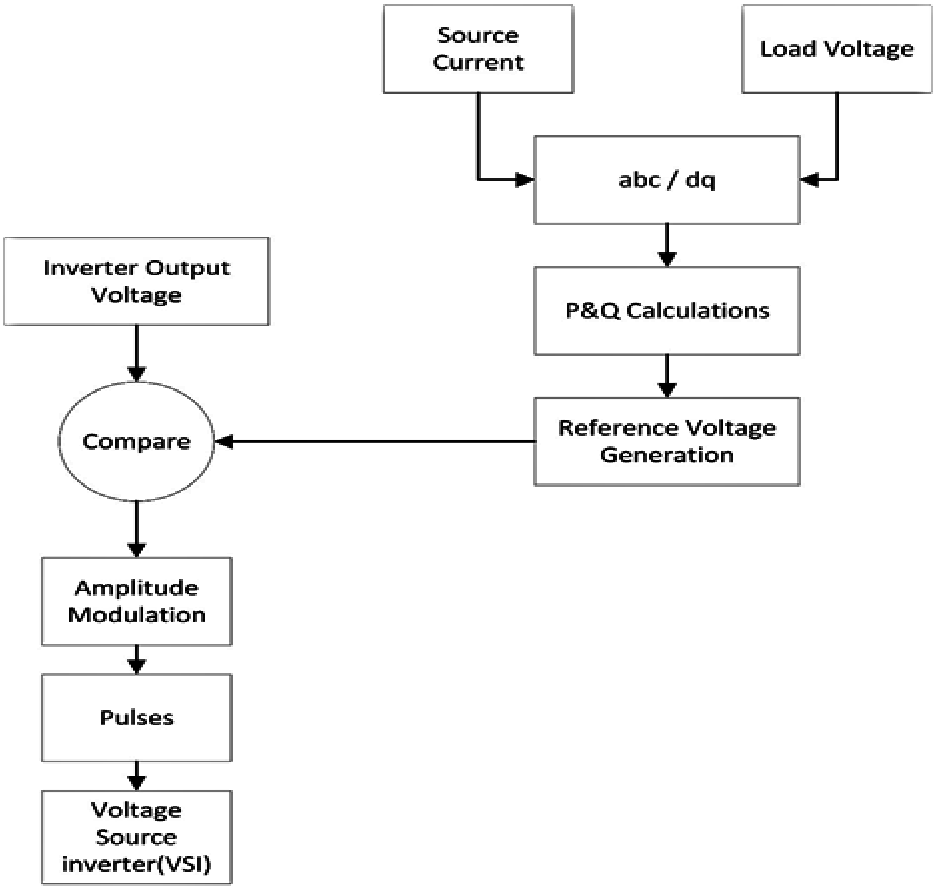

Fig.3.19: Control of series APF

The mitigation algorithm to filtering the harmonics is implemented depend on "Dual Instantaneous Reactive Power Theory". Generally, the distribution network wants to provide a pure and balanced voltage and current waveforms. To do this task, the load current at the common linking point must be co-linear with the electrical company voltage. This situation is achieved if the load is a linear, balanced and resistive.

Fig.3.20 shows the MATLAB SIMULINK for series APF controller.

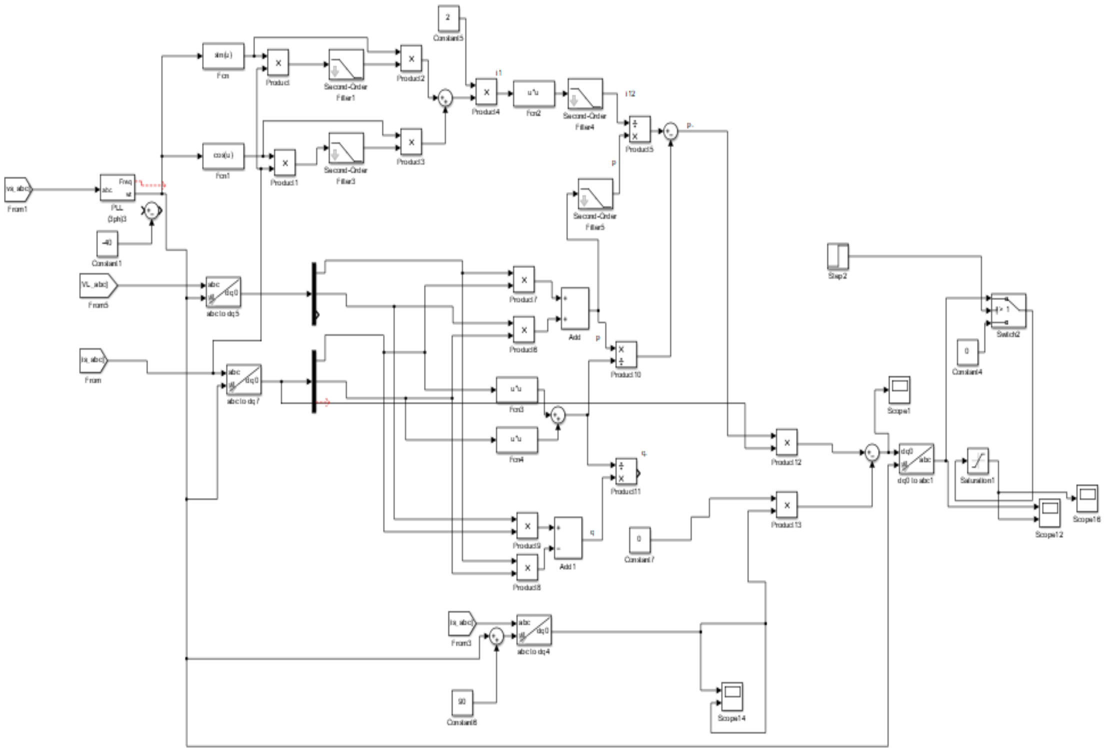

Fig.3.20: MATLAB SIMULINK for Series APF controller.

3.7.2.4.1 Reference Vector Generation for Series APF Control.

The series connected active power filter (APF) controlled by generating a reference vector then compared it with the actual voltage vector [1]. The reference voltage vector is produced by the following control block illustrated in Figure. 3.21. The fundamental current term calculation is illustrated in Figure. 3.22. The fundamental component calculation necessarily the grid voltage angle to calculate its value. The grid voltage angle important for this calculation is calculated by utilizing a Phased Lock Loop (PLL).

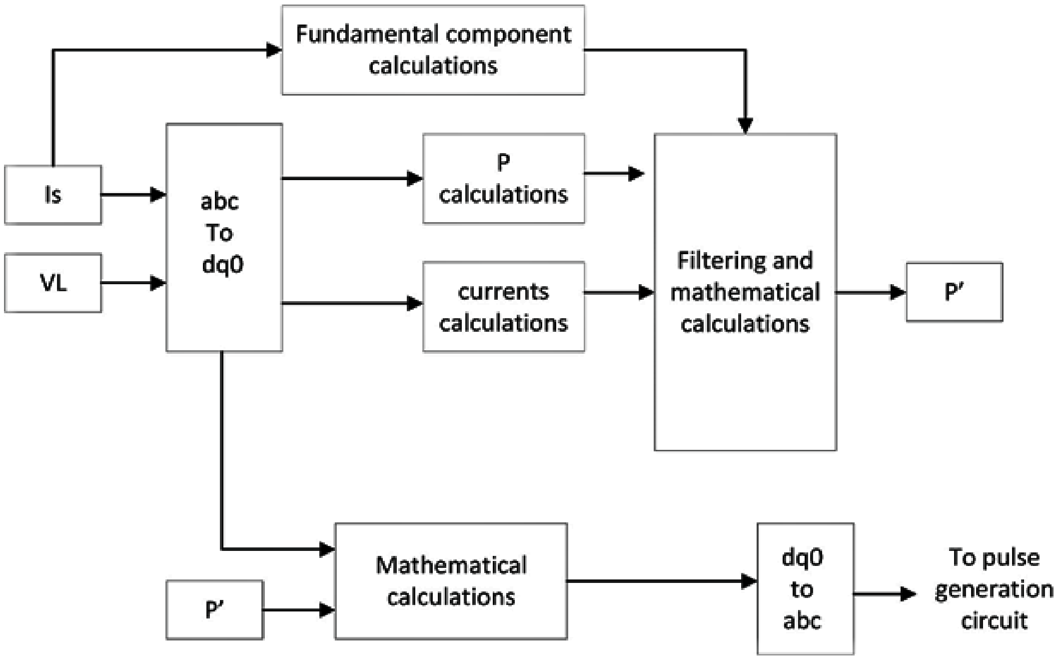

Fig.3.21: Control block to generate reference vector.

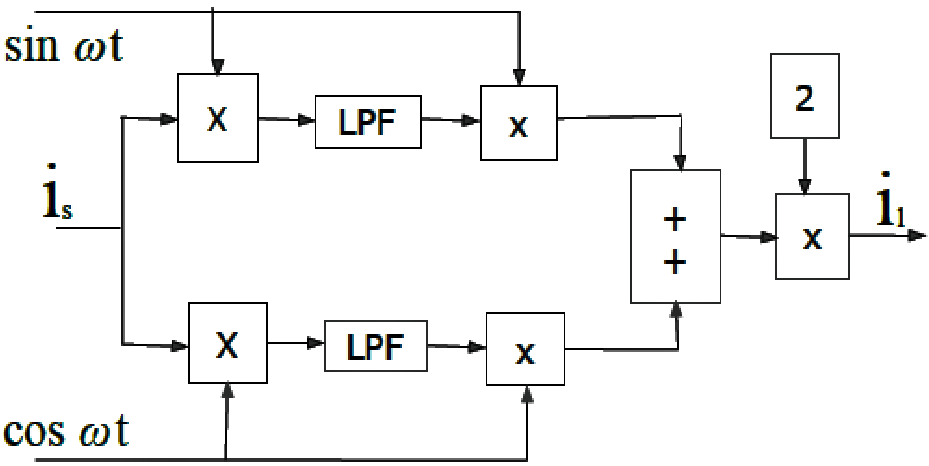

Fig. 3.22: Fundamental term calculation

A (LPF) is implemented in the fundamental component calculation block to mitigate the harmonics and obtain the fundamental component from source current. A comparison is did between the actual and reference values of the output voltage of APF. The difference is the input of a PI controller. The gain of the PI must be tuned in a way to get a zero error between the reference values and actual values. If the all above mentioned tasks achieved correctly, the APF will mitigate the harmonics perfectly.

3.8 Control of Active Power Injection for Shunt APF.

The control of the active power (P) injected to the point of common coupling (PCC) depends on the SOC of all battery packs and the system frequency to ensure the stability of the electrical network.

The flowchart diagram of control algorithm is shown in Fig. 3.23.

The control system will measure the state of charge (SOC) of all batteries and the network frequency then output a signal to multilevel inverter controller contains the optimum value of real power need to inject.

If the SOC of any battery<= 0.28, this state called empty or fault battery state, then the system will charge the batteries at a maximum rate to push the state of charge(SOC) from empty region to charging region.

And If the state of charge (SOC) of all batteries>0.35, and the frequency of the system is normal 50.5> freq.>49.5,this state called normal state and the system will charge the batteries at a rate that guarantee fully charged batteries at the end of sunset. During charging process the excessive power from PV arrays will injected to the electrical distribution network directly by setting the real power reference current (i_d) according to the excessive power from charging process.

When the state of charge(SOC) is >0.5 and the frequency of the system is <49.5,this state called unstable network state. The system will stop charging batteries and inject all power comes from PV arrays, also discharges the batteries at rated discharging current, by setting the real power reference current (i_d) according to the maximum power available.

If frequency of the system is >50.5, or no real power load at distribution network then this state called non real power load state, the system will stop power injection and charges the batteries only, by setting the real power reference current (i_d) to zero.

These SOC limits have been arbitrarily selected and are restrained by the physical limitations of the battery packs.

The charging of the battery through the solar array (when normal network state) is independent on the operation of the multilevel inverter system and gives energy to the batteries whenever the sun is radiating.

The maximum power point tracker (MPPT), will always delivers the optimum amount of energy from the solar panel, and the multilevel system will only take power from the PV arrays and batteries according to the above mentioned states.

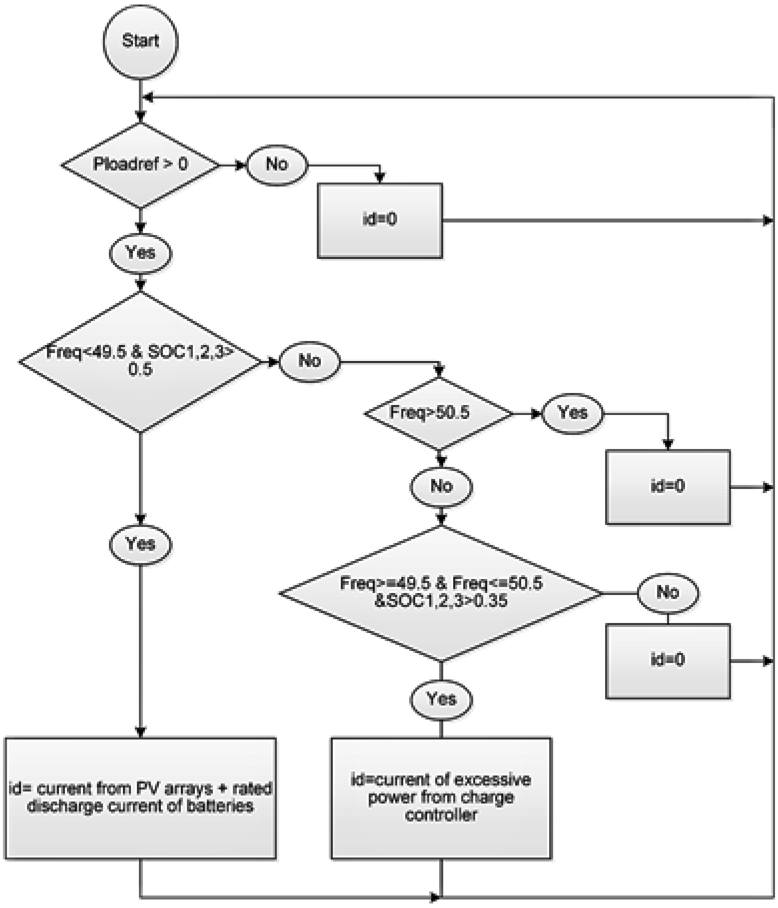

Fig.3.23: Flowchart diagram of real power control algorithm.

3.9 Control of Reactive Power Injection for Shunt APF.

The injection of reactive power (Q)is only necessary when the load drains reactive power from the source.

In the case of empty batteries, the system will disconnect the batteries from the dc link and continue reactive power compensation by inserting of capacitor banks at the dc link of each “H” bridge inverter.

So the reactive power injection did not depend on the state of charge (SOC) of batteries, this will increase the reliability of the hybrid active filter to support the reactive power load even if no power generated from photovoltaic arrays. The flowchart diagram of control algorithm is shown in Fig. 3.24.

When there is no load connected to the source the reactive power current reference (iq-ref) set to zero and no reactive power injected to the point of common coupling (PCC).

And if reactive loads are connected to the distribution network, the system will automatically generates iq-ref required for all reactive power loads connected, and the source will see a unity power factor independent on the type of contaminating load.

The speed of compensation of reactive power depending on the power factor of the electrical network, so if the power factor (PF) < 0.85 (lagging), the system compensate at maximum available reactive power, else the system will inject the excessive results power from charging process.

According to the above explanation, the system works like asynchronous machine, where the reactive power is controlled through the excitation coil. In this case, it is controlled through iq-ref.

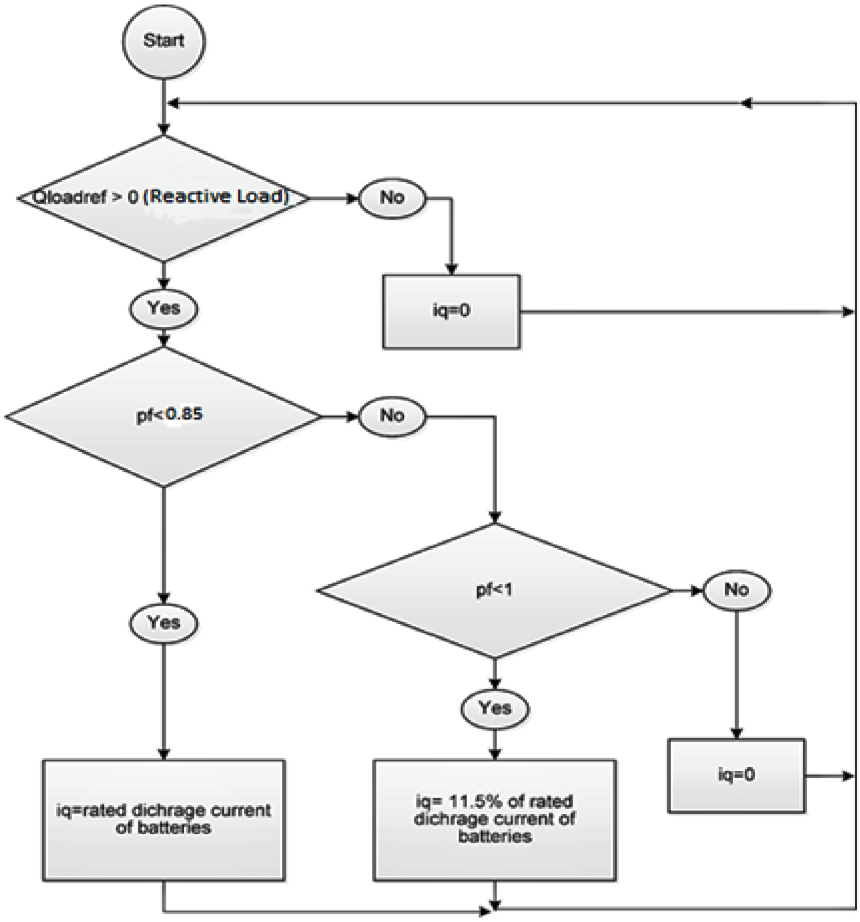

Fig.3.24: Flowchart diagram of reactive power control algorithm.

3.10 Simulation Results for Series and Shunt APF Control Algorithms.

3.10.1 Introduction.

The proposed control strategies for series and shunt APF are simulated with a non-linear balanced three phase load and the performance of the system is discussed.

The load harmonics are filtered by forcing the current and the voltage from the mains (Isource, Vsource) to be sinusoidal.

Also the results including the testing of active and reactive power injection control where P and Q are independently controlled. The reference for P depends on the state of charge (SOC) of the batteries pack and the frequency of the system. On the other hand, Q can be controlled by keeping a unity power factor (for example) at the converter connection point.

Fig.3.25 Shows the MATLAB SIMULINK for series and shunt APF control algorithms using ideal inverter.

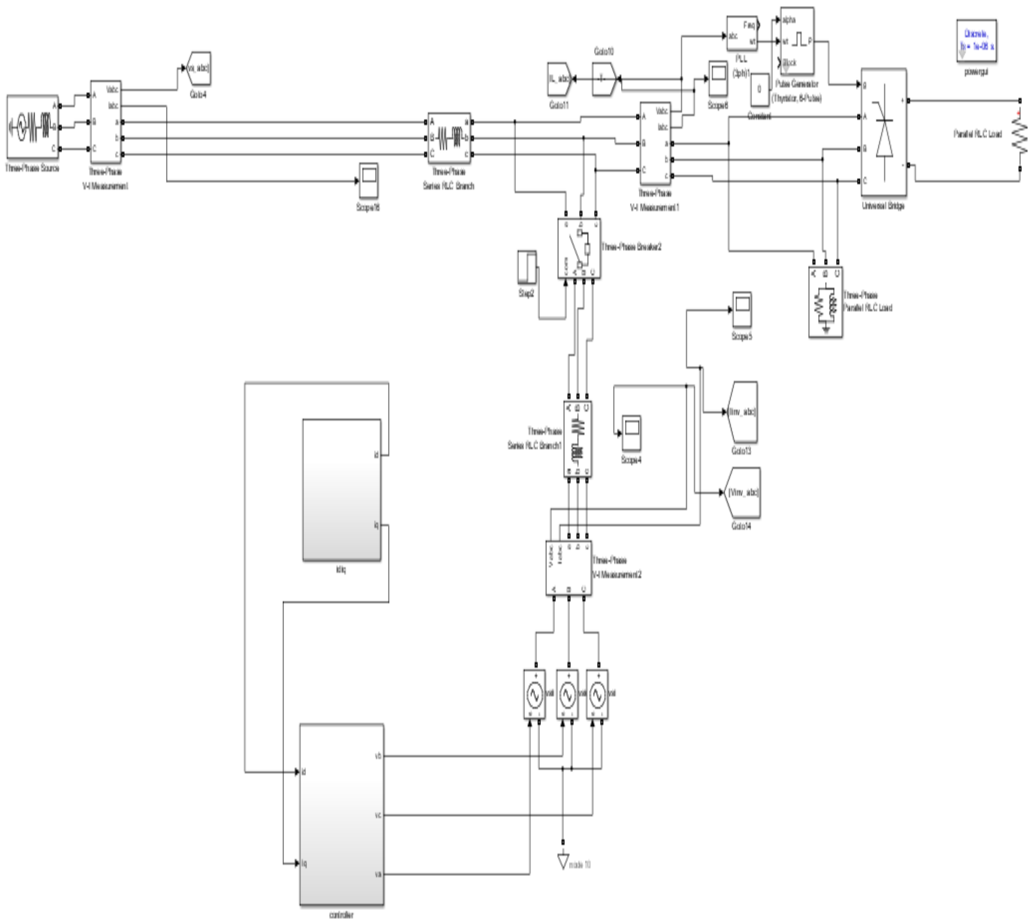

Fig.3.25: MATLAB SIMULINK for series and shunt APF control algorithms using ideal inverter.

3.10.2 Simulation Results for Shunt APF Control System.

To study the correct performance of the shunt APF control system, the load current, source current and the reference signal to converter gate must be seen and discussed.

The three phase load current waveform is shown in Fig. 3.26. Where Fig. 3.26 (a) shows the status of load current when the system start harmonic mitigation and reactive power compensation (at t=0.3S.Fig.3.26 (b) shows the status of load current when the system start active power injection (at t=0.55S).

Fig.3.27 shows the reference signal generated from controller for filtering and active-reactive power injection. Fig.3.27 (a) demonstrate the changing in reference signal when the system start active power injection (at t=0.55S).

The three phase source current waveform is shown Fig.3.28, where Fig.3.28 (a) demonstrate

The correct functioning of harmonic mitigation (at t=0.3S), and it’s clear from Fig.3.28 (b) the active power injection capability of the system (at t=0.55S).the variation of total harmonic distortion (THD) of source current is clear in Fig.3.28(c)

Fig.3.29 proves that the reactive power compensation task is working correctly, and the power factor improved to reach 0.99 as shown in Fig.3.29 (a) and Fig.3.29 (b).

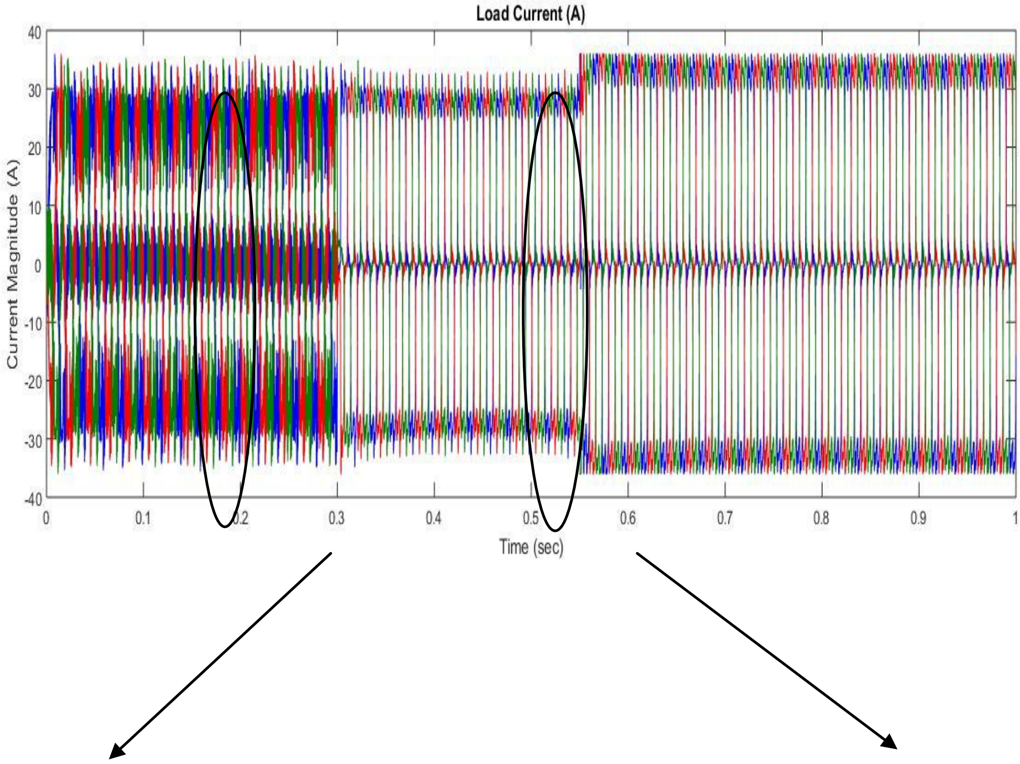

Fig.3.26: Three phase load current waveform**.**

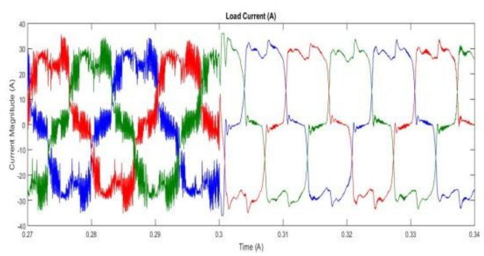

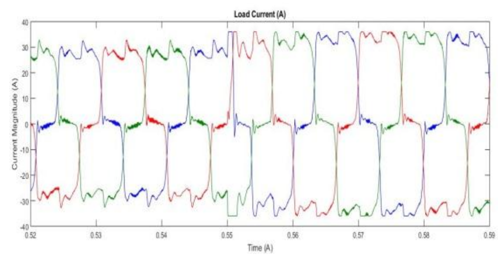

Fig.3.26 (a) **:** Zoom for load current

Fig.3.26 (b): Zoom for load current

From the above waveforms it is clear that there many harmonics presented in the system due to the existence of contaminating loads in distribution network.

The control algorithm tracks these harmonics and generates a reference signal to mitigate the current harmonic and reduce the total harmonic distortion to be nearly zero.

On the other hand the control system observe the power factor changing and inject reactive power to maintain a unity power factor.

The monitoring of load current is necessary under the working of control system to minimize the interruption time of load current when the shunt active power filter inter the network.

As seen in Fig.3.28 (a) and (b) There is no interruption of load current, so the shunt active power filter(SAPF) behaves like a Double Conversion On-Line uninterruptible power supply (UPS),which have 1ms interruption time.

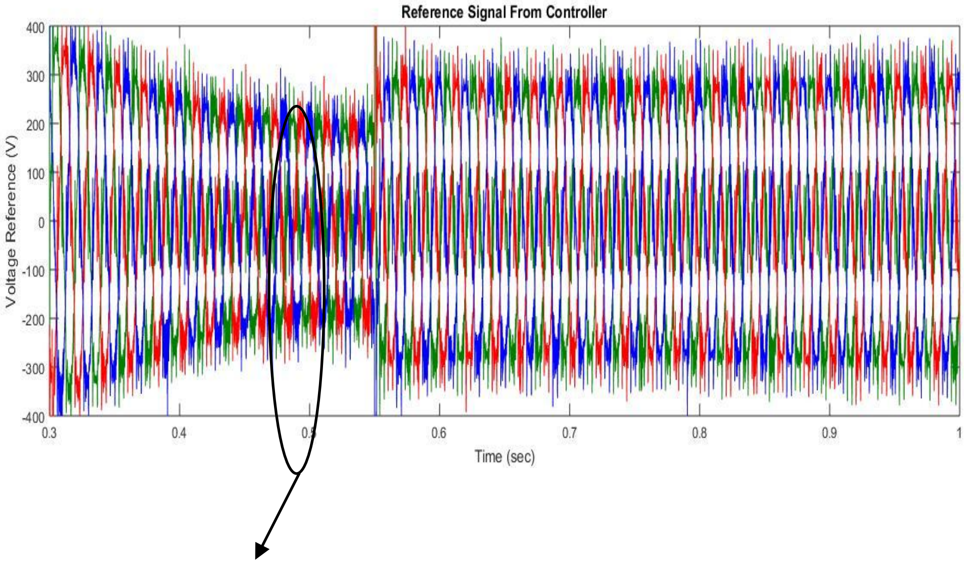

Fig.3.27: Reference signal generated from controller

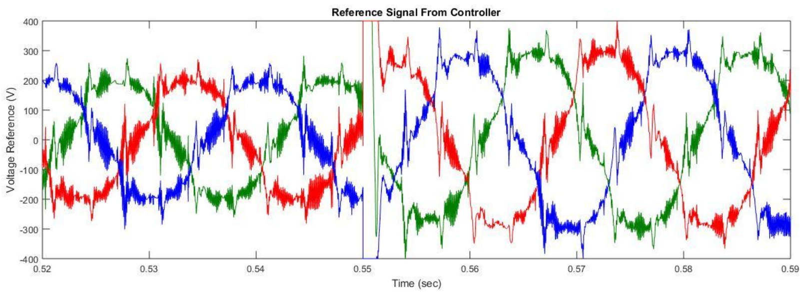

Fig.3.27 (a): Zoom for reference signal generated from controller.

This signal contains active power value and harmonics.

Fig.3.27 shows the reference signal generated from the control system, it contains the filtering signal and active-reactive power signal.

The filtering signal and reactive power signal presented between the times 0.3 to 0.55 S,

Then the active power signal inter the system at time 0.55S as clearly shown in Fig.3.27 (a)This signal fed the multilevel inverter gates and achieved filtering of source current and power injection tasks required from shunt active power filter (SAPF).

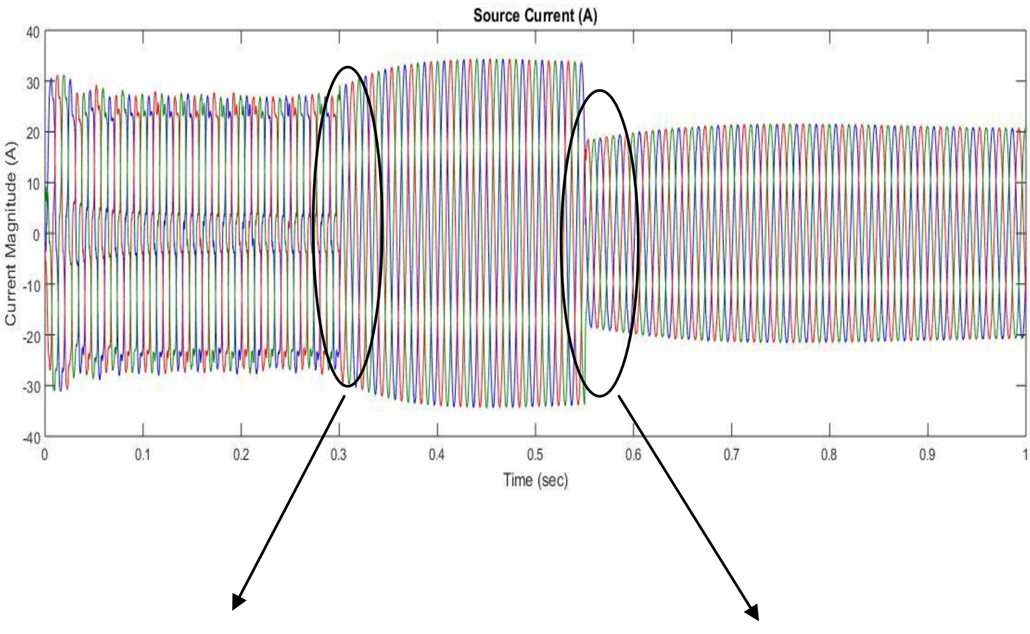

Fig.3.28: Three phase source current waveform

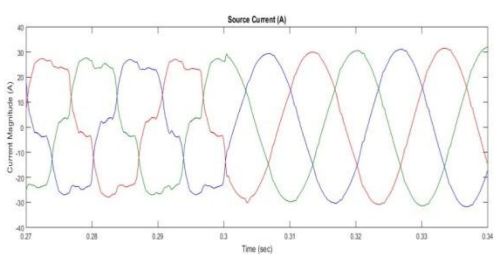

Fig.3.28 (a): Zoom for source current

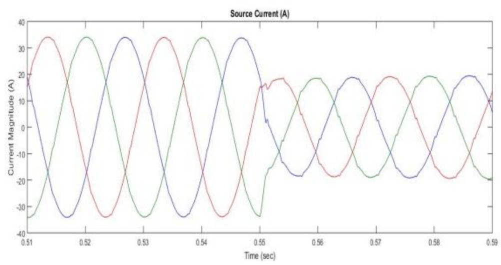

Fig.3.28 (b): Zoom for source current

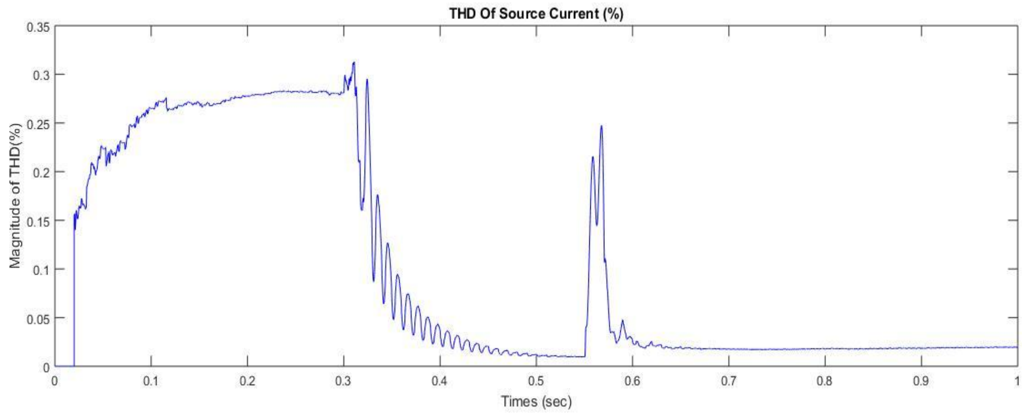

Fig.3.28 (c): Total harmonic distortion for source current.

Fig.3.28 (d) shows the spectrum of source current signal, and proves the correct working of control technique and filter.

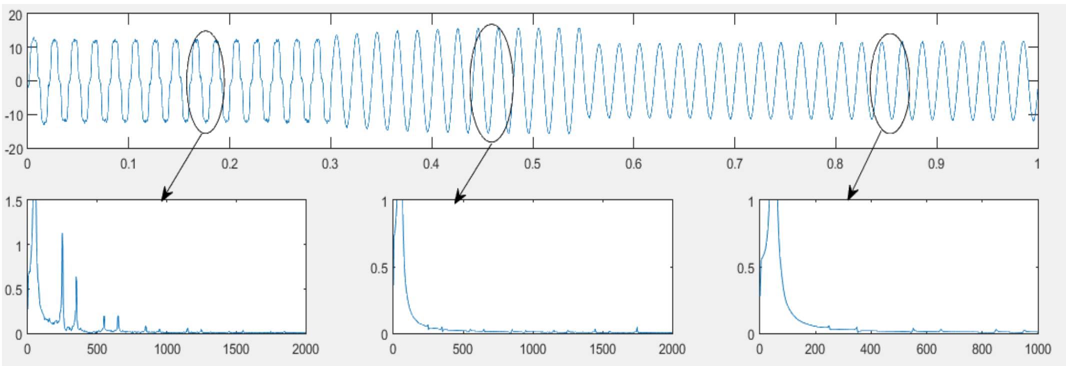

Fig.3.28 (d): Spectrum of source current signal.

As shown in Fig.3.28 (a) at t=0.3 S the shunt active power filter (SAPF) start working to mitigate the harmonic and the source current became pure sinusoidal by reducing the total harmonic distortion (THD) from 27% to 1.2% as proved in Fig.3.28 (c).

The active power injection task start at t=0.55 S with 13 A current contribution as seen in Fig.3.28 (b),so the required current from the source is 17 A to feed 30 A load.

Fig.3.29 shows the capability of shunt active power filter (SAPF) for keeping a unity power factor at the point of common coupling (PCC).

It’s clear from Fig.3.29 (b) and 3.29 (c) that the power factor improved from 0.78 to 0.99.

By injecting the required reactive power to the distribution network and tracking the reactive power of the load to generate the needed reference vector signal.

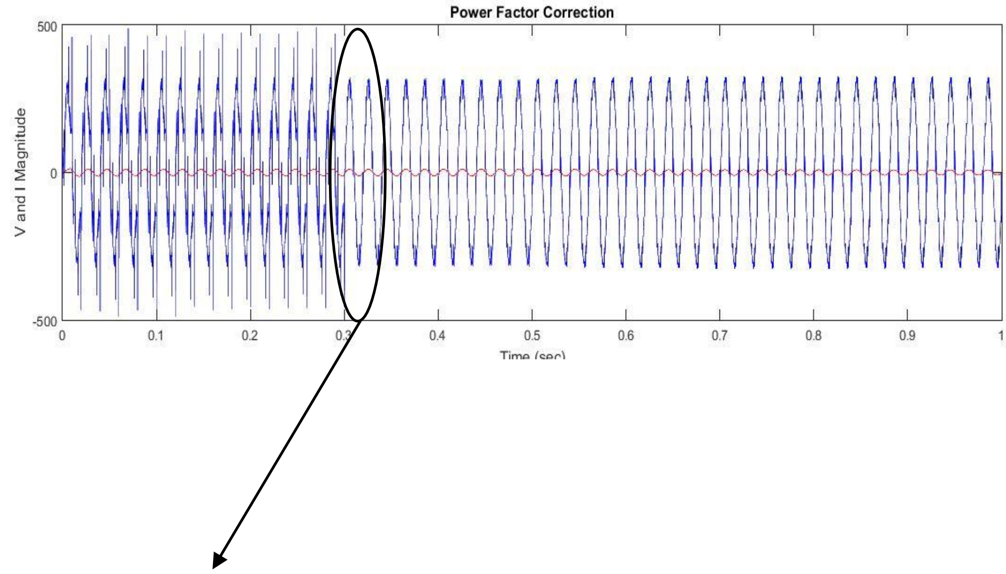

Fig.3.29: Reactive power compensation.

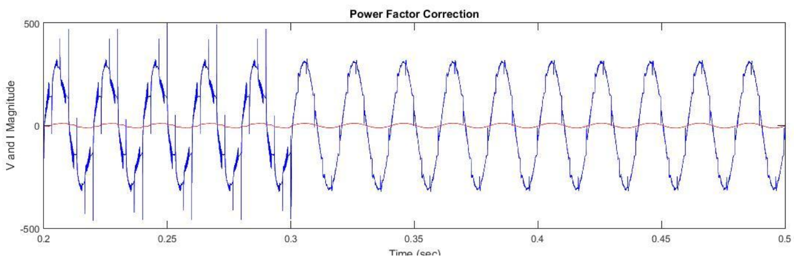

Fig.3.29 (a): Zoom for reactive power compensation**.**

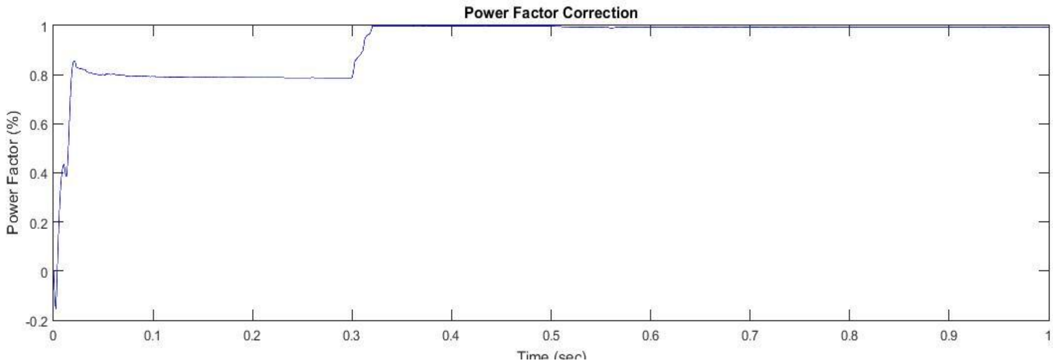

Fig.3.29 (b): Power factor correction curve.

3.10.3 Simulation Results for Series APF Control System.

The series active power filter (SAPF) is used to remove the harmonics in source voltage and to compensate the voltage drop at the point of common coupling (PCC).

The three phase reference signal is shown in Fig. 3.30, where Fig. 3.30 (a) shows the scope of reference signal generated to feed the inverter gates and perform the series APF tasks.

The three phase source voltage waveform is shown Fig.3.30, where Fig.3.31 (a) proved the correct working of harmonic mitigation task (at t=0.3S), the total harmonic distortion (THD) of source voltage is shown in Fig.3.31(b).

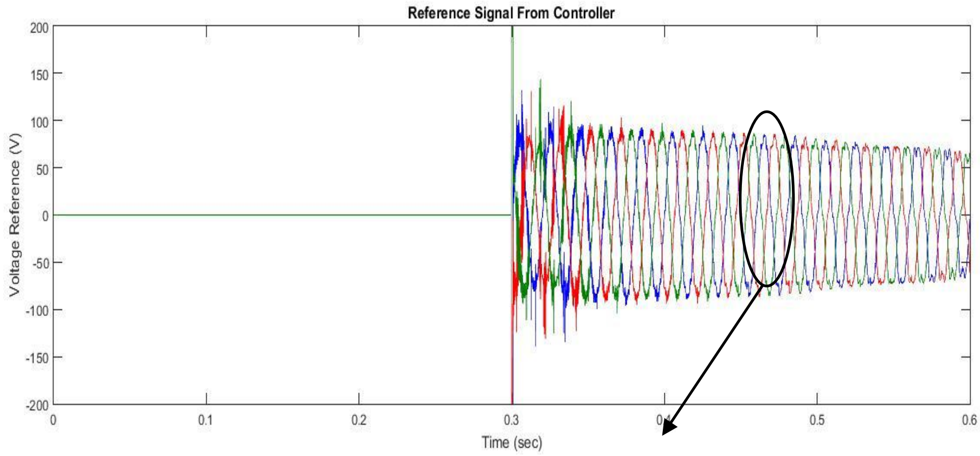

Fig.3.30: Three phase reference signal from controller**.**

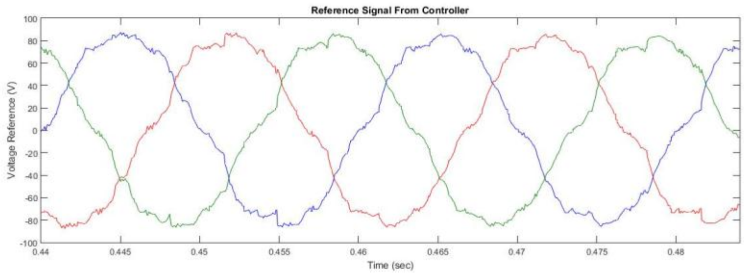

Fig.3.30 (a): Zoom for reference signal from controller.

As seen in Fig.3.30, at t=0.3 S the control system of series APF start generating a reference vector contains the filtering and compensation

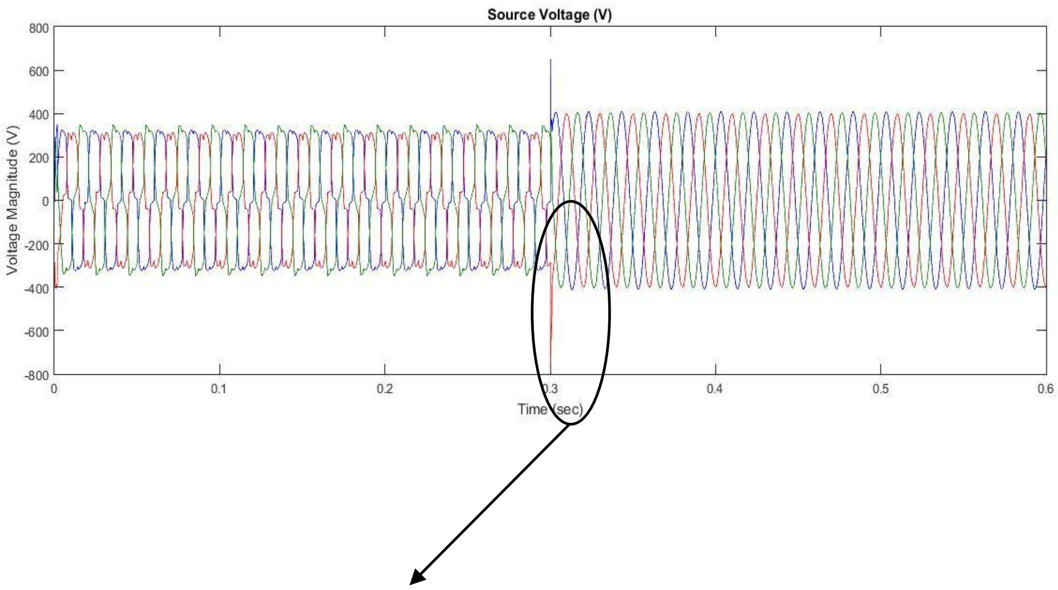

Fig.3.31: Three phase source voltage waveform**.**

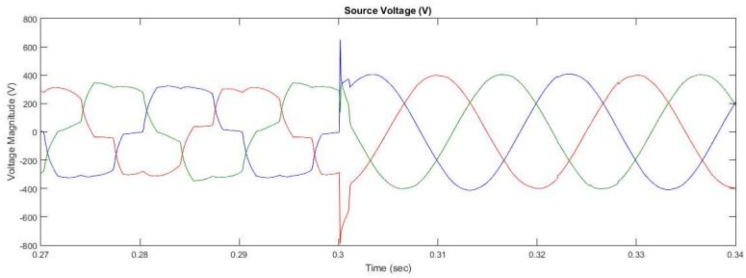

Fig.3.31 (a): Zoom for source voltage**.**

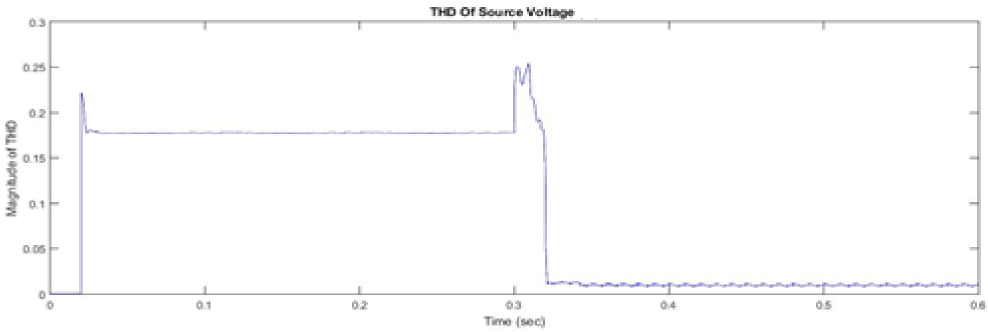

Fig.3.31 (b): Total harmonic distortion for source voltage.

As shown in Fig.3.31 (a) at t=0.3 S the series active power filter (Series APF) start harmonic mitigation and voltage drop compensation, the voltage at the point of common coupling (PCC) increased from 340voltsto its rated value (400volts) and became pure sinusoidal by reducing the total harmonic distortion (THD) from 18% to 1% as seen in Fig.3.31 (b).

3.10.4 Simulation Results for Active and Reactive Power Injection Control System.

To study the correct functioning of the active and reactive power injection control system, the results divided into three cases:

Case 1: frequency variation effect.

Case 2: state of charge (SOC) variation effect.

Case 3: poor power factor tracking.

The active power (P) controlled by adjusting the value of id-ref current, where id-ref current depends on the SOC of all battery packs and the frequency of the system.

The injection of reactive power (Q) depends on the tuning of iq-ref current, where iq-ref set to maintain a unity power factor.

Fig.3.32 shows the MATLAB SIMULINK for active and reactive power injection control algorithms using embedded MATLAB function.

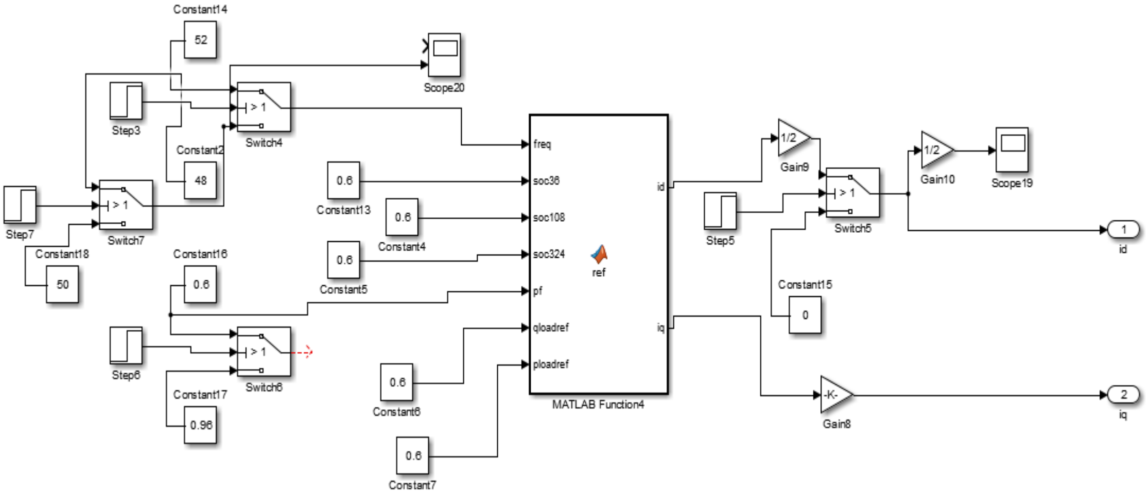

Fig.3.32; MATLAB SIMULINK for active and reactive power injection control algorithms.

Fig.3.33 shows the embedded MATLAB function program for active and reactive power injection control algorithms.

```
function [id,iq]  = ref(freq,soc36,soc108,soc324,pf,qloadref,ploadref)
double freq;
if  (ploadref) > 0

if (freq<49.5 &&  soc36>0.5 && soc108>0.5 && soc324>0.5)

    id=0.6*(174*36+174*108+304*324)/1000; %rated discharge current

elseif (freq>50.5 && soc36>0.5 && soc108>0.5 && soc324>0.5)

        id=0;

elseif (49.5<=freq && freq<=50.5 && soc36>0.25 && soc108>0.25 && soc324>0.25)

        id=0.6*(22*36+22*108+39*324)/800;%low discharge current

else
    id=0;
end
else
    id=0;
end

end
```

```
 if  (qloadref) ~=0

if (soc36>0.25 && soc108>0.25 && soc324>0.25)

    if pf<0.85
    iq=0.4*(174*36+174*108+304*324)/468;
    elseif pf<=0.98
    iq=0.4*(174*36+174*108+304*324)/50;
    else
        iq=0;
    end
else

    iq=0;
end
  else
      iq=0;
  end
```

Fig.3.33: Embedded MATLAB function program for active and reactive power injection control algorithms.

Case 1: Frequency Variation Effect.

The three phase source current waveform is shown in Fig. 3.34.

Fig.3.34 (a) shows the changing in source current when the system start active power injection at t=0.5 S, in case of normal frequency rang.

Fig.3.34 (b) demonstrate the changing in source current when the system start active power injection at t=0.7 S, in case of abnormal frequency rang.

The id reference signal generated from controller for filtering and active power injection shown in Fig.3.35.

The total harmonic distortion (THD) of source current is shown in Fig.3.36.

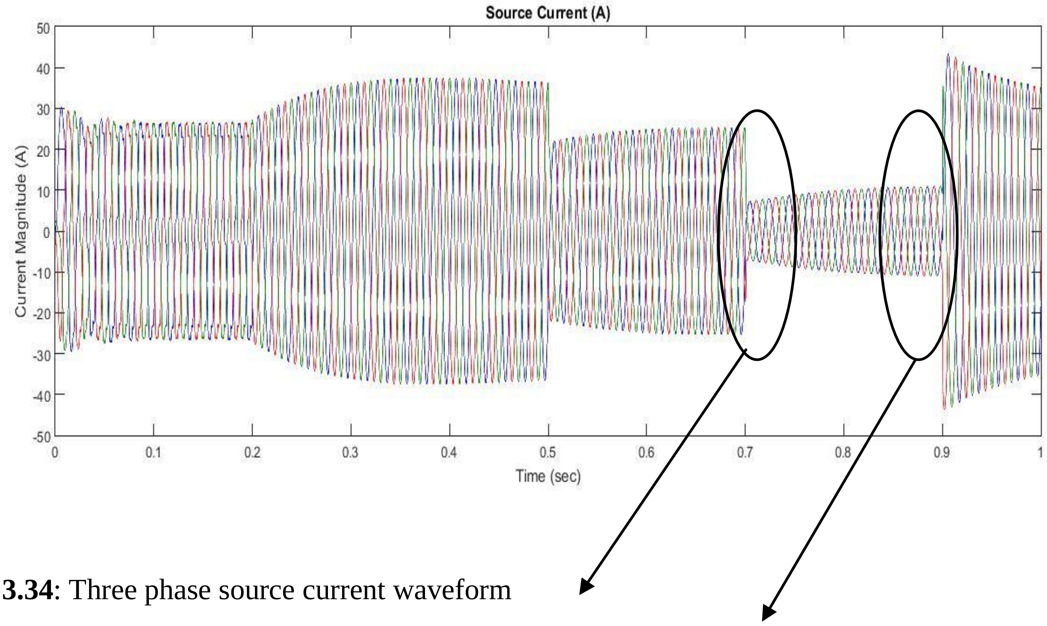

Fig. 3.34: Three phase source current waveform

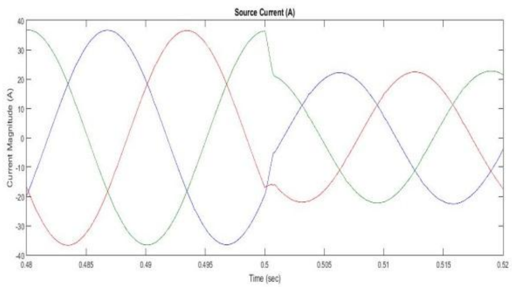

Fig. 3.34 (a): Zoom for source current

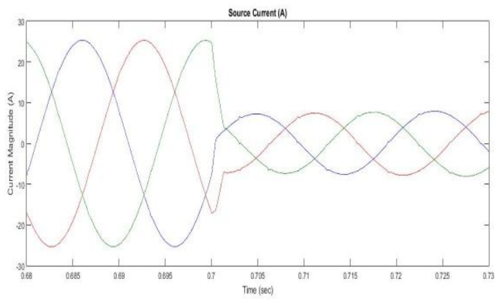

Fig. 3.34 (b): Zoom for source current

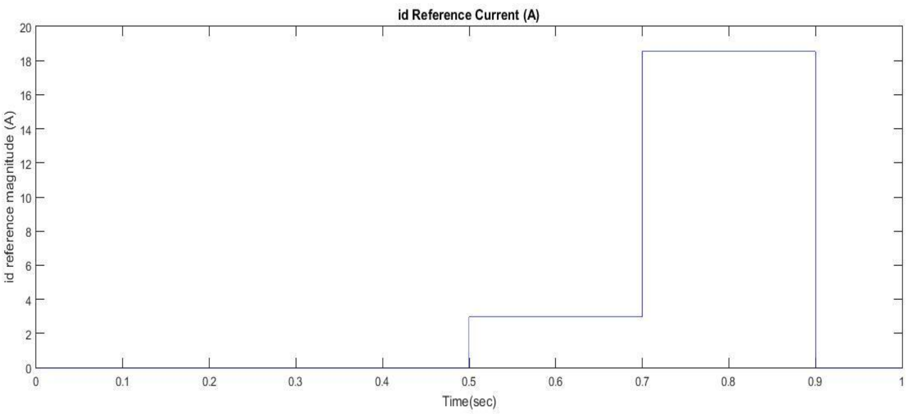

Fig.3.35: Changing in id reference current.

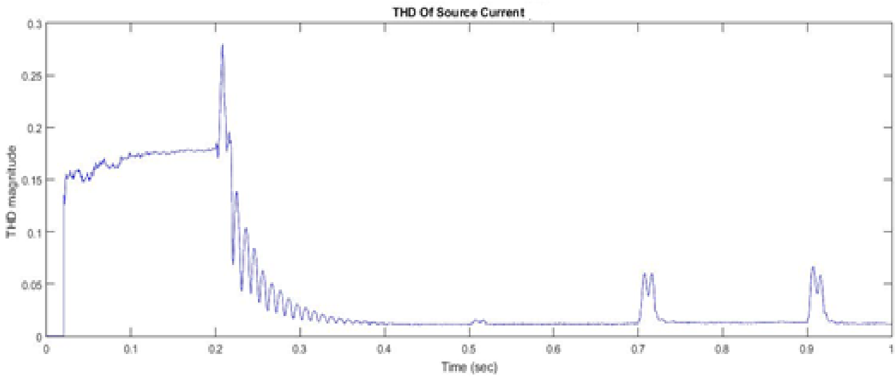

Fig.3.36: Total harmonic distortion variation**.**

When the network frequency between the normal limits (49.5<frequency<50.5) Hz, the system adjust id-ref to inject real power with a certain value depending on the state of charge (SOC) of batteries, Fig. 3.34 (a) demonstrate the current injection when the frequency in normal region, id-ref set to 15% from rated.

On the other hand, if we set the SOC to 0.9 (for example) and the network frequency down suddenly to 48 Hz, the controller will adjust id-ref to its maximum value and push the network frequency to normal region.

Fig. 3.34 (b) shows 19 A injected current to support the weak network source.

The reference current id-ref generated at the input of controller shown in Fig.3.35.

From Fig.3.36 we noted that the total harmonic distortion (THD) reduced from 16.5% to 1% and did not change when the controller inject a different levels of current to the point of common coupling. Hence the system is trusted and stable for all its tasks.

Case 2: State of Charge (SOC) Variation Effect.

The three phase source current signal is shown in Fig. 3.37.

Fig.3.37 (a) shows the changing in source current when the system start active power injection at t=0.5 sec and SOC =0.8.

Fig.3.37 (b) demonstrate the changing in source current when the system stop active power injection at t=0.7 sec and SOC=0.25. The state of charge variation shown in Fig.3.38

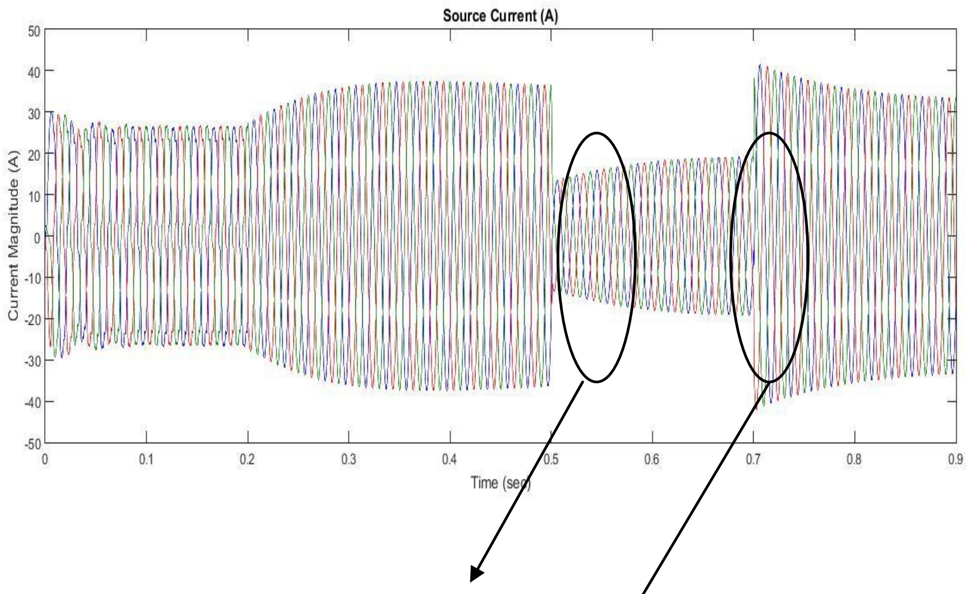

Fig. 3.37: The three phase source current signal

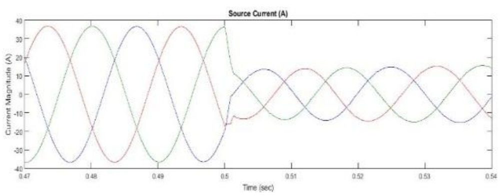

Fig.3.37 (a): Zoom for source current.

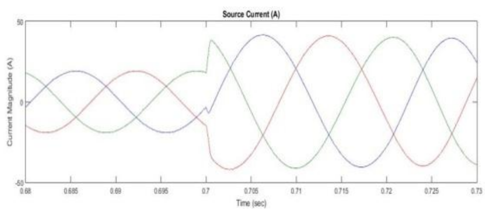

Fig.3.37 (b): Zoom for source current.

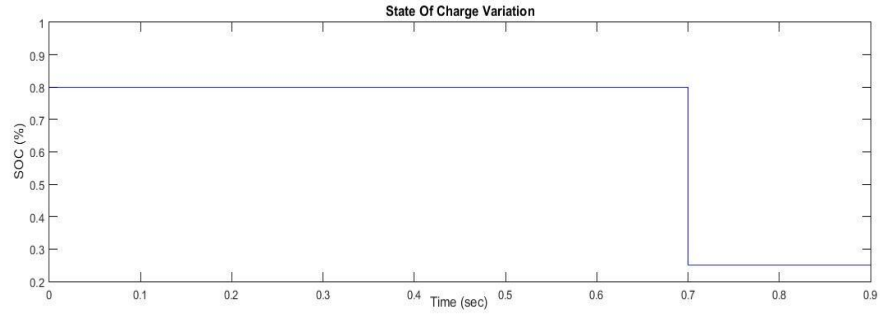

Fig.3.38: The state of charge variation

From the figures 3.37 (a) and (b) it's clear that the system start active power injection (at t=0.5 S) and from Fig.3.38 the SOC was 0.8,

On the other hand, at t=0.7 S the SOC decline to 0.25 and the controller stop active power injection to protect the batteries from deep discharging.

Case 3: Poor Power Factor Tracking.

The phase shift between the source voltage and current waveforms during control system operation is shown in Fig. 3.39.

Fig.3.39 (a) and Fig. 3.40 prove the correct and optimum working of power factor correction task.

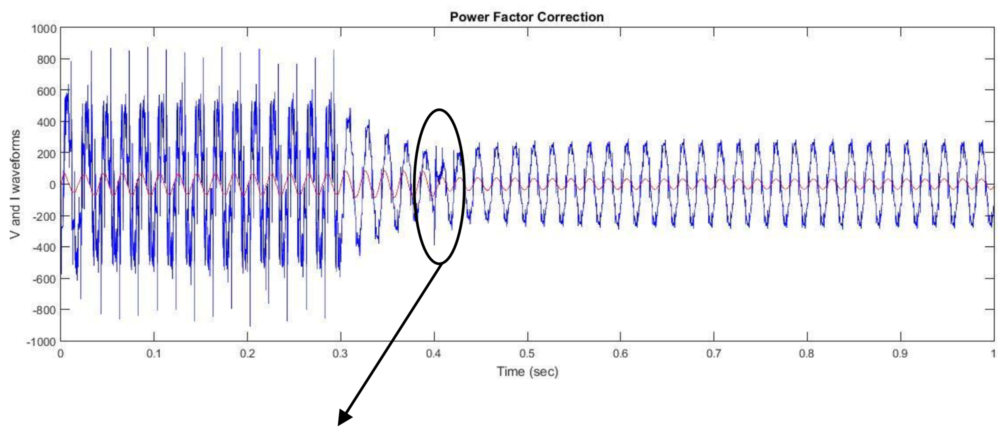

Fig. 3.39: Phase shift between the source voltage and current

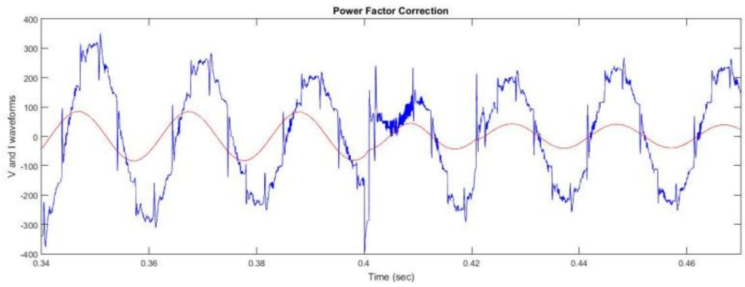

Fig.3.39 (a): Zoom for power factor correction**.**

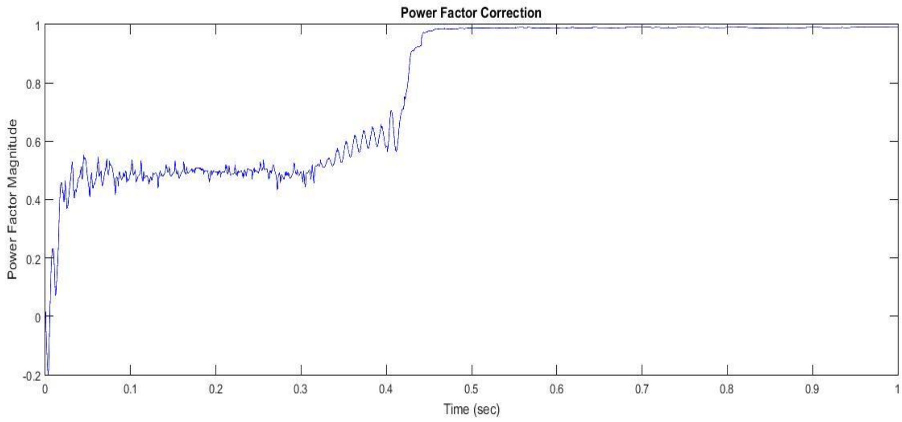

Fig. 3.40 Power factor correction**.**

From Fig. 3.39 (a), the controller start power factor correction at t=0.4 S, Its clear from figure that the phase shift angle between the voltage and current almost equal to zero. in addition Fig. 3.40 clarify that the power factor pushed from 0.5 to 0.99 after system working.

3.11 Chapter Summary.

The above section explained and tested the control algorithms for both shunt and series APF. It shows the control principle for APF to optimize the electrical power quality of distribution network. This chapter includes the mathematical explanation for both the series and shunt APF .In addition; this chapter extract the needed reference vectors for control algorithms. The control strategy is depend on Dual Instantaneous Electric Power Victoria algorithm for shunt and instantaneous reactive power (p-q) theory for series APF.

At the end of this chapter a simulation results for all control algorithms used in this project have been tested and discussed.

Chapter Four
Multilevel Converters

4.1 Introduction

A multilevel converter is power electronic controllable equipment, which is capable of supplying needed alternating voltage level at the output using multiple lower level DC voltages as an input source.

Multilevel converters have found an important position among applications as high-power converters. Also, they are widely used in renewable energy sources where multilevel converters appear as a link between renewable sources, such as wind, fuel cells, photovoltaic modules from one side and high-power loads from the other side. Power converters for high-power AC motors, systems for reactive power compensation, Flexible Alternative Current Transmission Systems (FACTS) devices photovoltaic power injection systems, and inverters in tracking vehicles have become typical applications in which multilevel converters are used.

4.2 Multilevel Converter Topologies

In the literature there are a large number of multilevel converter topologies, in this chapter the most popular topologies will be presented and discussed. The most typical multilevel converter topologies are: Diode-Clamped Converter (DCC) or (neutral point clamped), Flying Capacitor Converter (FCC) or capacitor clamped, and Cascaded Converter.

4.2.1 The Diode Clamped Multilevel Inverter.

The neutral clamped or diode clamped multilevel converter uses diodes to split the DC link voltage into sublevels [81] [82]. The schematic of this topology is depicted in Fig 9.2.

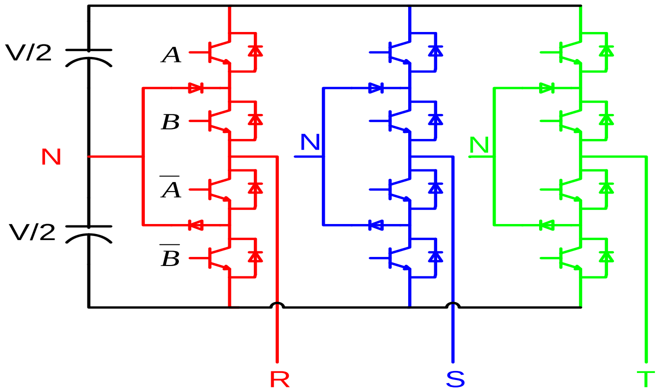

Fig.4.1: Three level neutral point clamped converter.

Different output voltage levels can be generated from each leg of the multilevel converter according to different switching states of the semiconductors switches as follows:-

Table.4.1 Switching possibilities in three level neutral point clamped converter.

A	B	$\bar{A}$	$\bar{B}$	V_{XN}
ON	ON	OFF	OFF	V/2
OFF	ON	ON	OFF	0
OFF	OFF	ON	ON	-V/2

The number of the levels in the output voltage waveform of the diode clamped multilevel inverter can be increased by increasing the number of the clamped points to DC link capacitors and the number of the semiconductor switches between these points. This gives the ability to generate the same voltage level by different switching patterns of the semiconductor devices which helps to keep the switching losses divided equally between the semiconductor devices and at the same time the storage DC components are utilized equally. The price that is paid as a result of increasing the number of the levels is the additional complexity in control and extra expenses [80].

Another disadvantage of the diode clamped multilevel converter appears to the high voltage applications as some of the clamping diodes must block high voltages. This may be solved by using many diodes connected in series which increases the losses and cost [80].

4.2.2 The Capacitor Clamped (Flying Capacitor) Multilevel Converter.

The schematic of the capacitor clamped multilevel converter is shown in Fig 9.3 with independent capacitors that clamp the semiconductors switches to one capacitor voltage level [80]. The output voltage levels that can be generated using the diode clamped multilevel converter are:-

Table.4.2 Switching possibilities in three level 'Flying' capacitor converter.

A	B	$\bar{A}$	$\bar{B}$	V_{XN}
ON	ON	OFF	OFF	V/2
OFF	ON	ON	OFF	0
ON	OFF	OFF	ON	0
OFF	OFF	ON	ON	-V/2

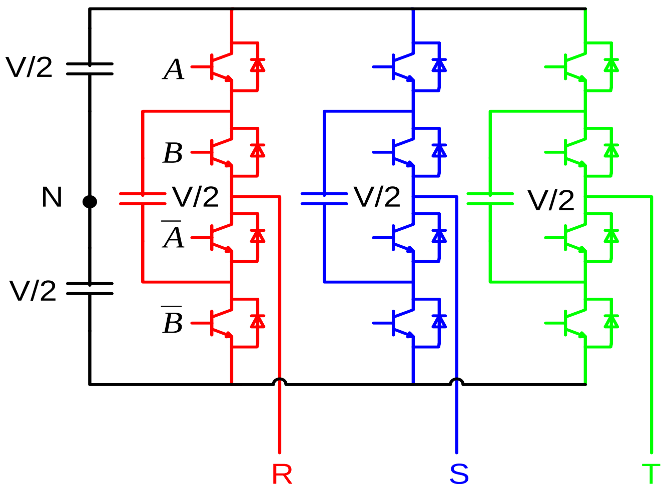

Fig.4.2: Three level flying capacitor multilevel converter.

Similar to the diode clamped multilevel converter, the number of levels can be increased by increasing the number of clamping point in the DC Link source and the number of semiconductor switches in each leg which will increase the cost and the complexity in control.

The other disadvantage of this multilevel converter is the need for additional circuitry in order to pre-charge and maintains the capacitor voltages.

4.2.3 The Cascaded H-Bridge Multilevel Converter with Separated DC Sources.

The schematic of the cascaded H-Bridge multilevel inverter is depicted in Fig 4.3. It is composed of a number of cells (H-Bridges) connected in series.

Each H-Bridge should be supplied from an isolated DC source (e.g from phase shift transformer)[80]. The possible outputs of each H-Bridge will be:-

Table.4.3 Switching possibilities in one H-Bridge cell.

A	$\bar{A}$	B	$\bar{B}$	V_{RX}
OFF	ON	ON	OFF	V/2
ON	OFF	OFF	ON	-V/2
ON	OFF	ON	OFF	0
OFF	ON	OFF	ON	0

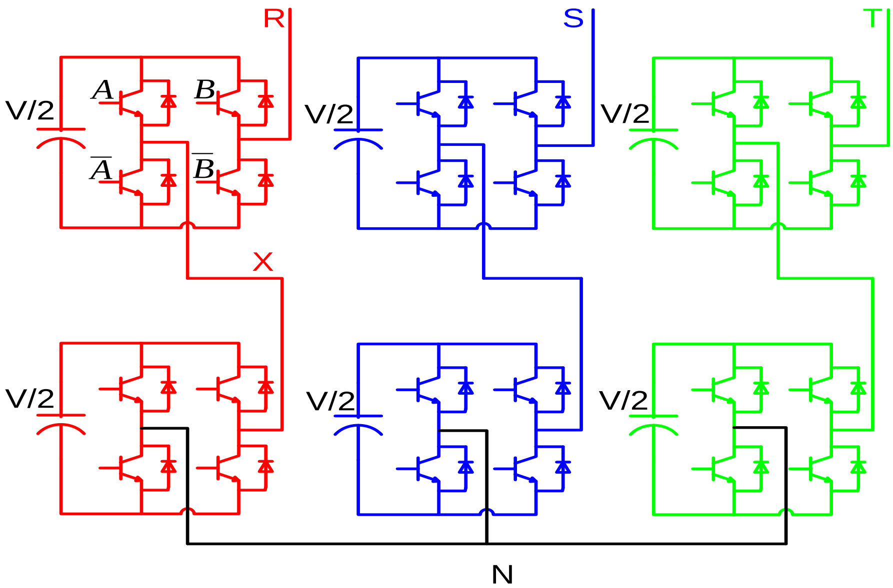

Fig.4.3: Five level cascaded H-bridge multilevel converter.

The following table summarizes the components required per phase in each topology; where n is the number of levels per phase [80].

Table.4.4 Comparison of components required per phase for each of the three multilevel topologies.

	Topology		
component	Diode Clamped	Capacitor Clamped	H-Bridge
Number of Switches	(n-1)*2	(n-1)*2	(n-1)*2
Diodes	(n-1)*2	(n-1)*2	(n-1)*2
diodes clamping	(n-1)*(n-2)	0	0
DC bus capacitors	(n-1)	(n-1)	(n-1)/2
Balancing capacitor	0	(n-1)*(n-2)/2	0

4.3 Modulation Techniques for the Cascaded H-bridge Multilevel Converter.

After studying the main multilevel topologies, the cascaded H-Bridge multilevel converter was chosen to be prototyped by which the application of the shunt and series active power filter introduced in chapter 2 were studied. To begin with, an overview of the modulation techniques that are used in cascaded H-Bridge converters will be introduced in this part.

The modulation techniques that can be used in the cascade H-Bridge converter [81][80] are :

- Phase-shifted multicarrier modulation
- Level shifted carrier PWM
- Staircase modulation
- Space vector modulation

This method is based on the natural PWM sampling where the gate signals are generated by directly comparing the modulating signals with the carrier waves [81][80].

4.3.1 Phase-Shifted Multicarrier Modulation.

Single triangular carrier wave as in the standard inverter, multiple carrier waves are used here depending on the number of the levels (M) in the multilevel inverter. All the carrier waves have the same frequency and amplitude but are phase shifted by an angle equal (360/(M-1)).

To illustrate this modulation technique the carrier waves shown in Fig 4.7 in (solid red and solid blue) are used to generate the gate signals for the switches S11 and S21 respectively while the carrier waves in dashed red and dashed blue are used to generate the gate signals for the switches S12 and S22.

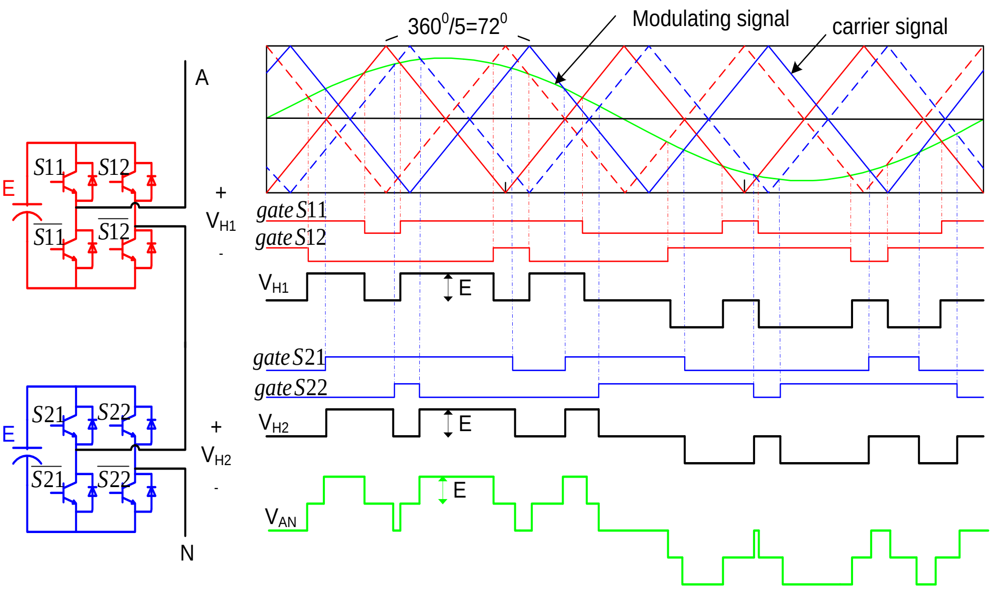

Fig.4.4: Five level, phase shifted carrier waveforms.

The power flow in each H-Bridge using this modulation method is equal. Also the switching frequency of each switching device is identical and equals the carrier frequency.

4.3.2 Level Shifted Carrier PWM.

This method is similar in principal to the previous method [81][80]. It uses a number of carrier waves to generate the gate signals of each switch. The carrier waves are identical in amplitude and frequency but they are arranged vertically such that the bands they occupy are continuous as depicted in Fig 4.8. The number of carrier waves used in this method is equal to that in the previous method.

One disadvantage of this method is that the conduction times and the power flow are not equal in all the cells and the switch devices.

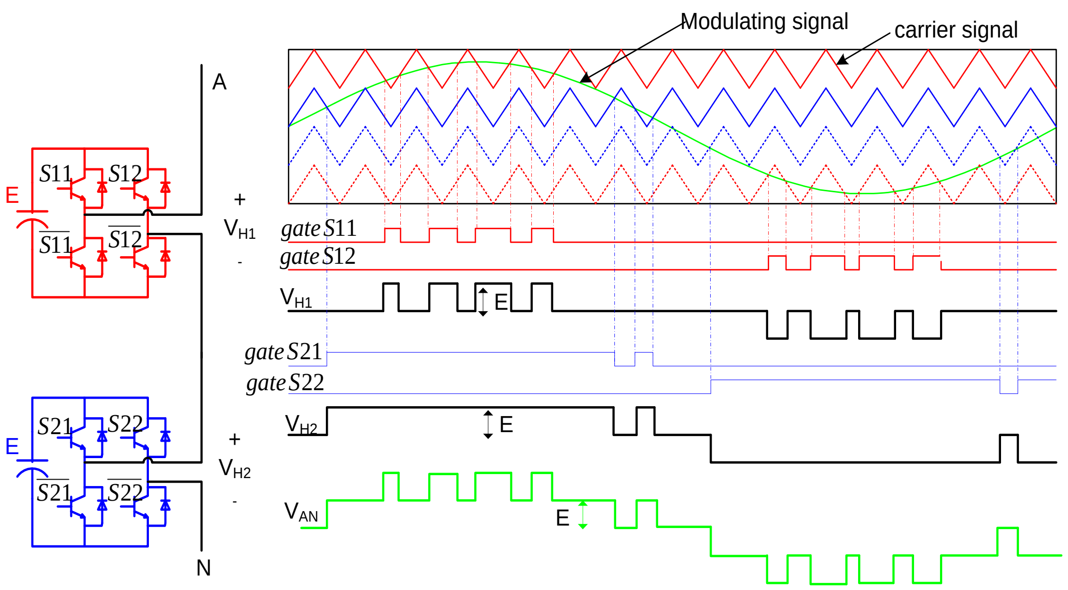

Fig.4.5: Five level, level shifted carrier waveforms.

4.3.3 Staircase Modulation.

This modulation method can be easily implemented in a cascade H-Bridge multilevel inverter and the semiconductor devices will have a switching frequency equal to the fundamental frequency of the output of the inverter [81][80]. The principle of this method is illustrated in Fig 4.9. The angles θ_1 and θ2 are optimized to eliminate specific harmonics from the output voltage waveform. Swapping of the conducting time of the switches is used in order to assure an equal power flow in each H-Bridge cell. This may introduce extra current ripple.

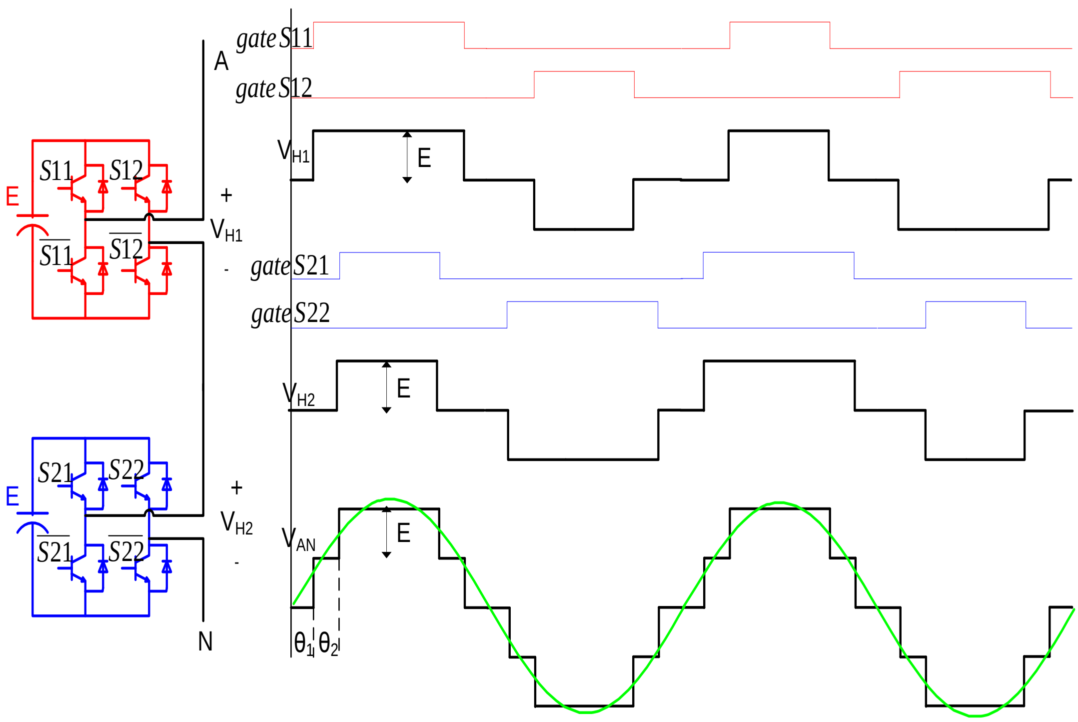

Fig.4.6: Five level, staircase modulation waveforms

4.3.4 Space Vector Modulation.

Among all the previous mentioned modulation methods, this method seems most promising due to the following reasons: 1) It offers more flexibility in optimizing the switching sequence; 2) It is suitable for digital implementation [82][83].

Consider the 7 level cascaded H-Bridge converters shown in Fig 4.10. The possible output voltages that can be generated from each leg are 3E, 2E, E, 0, -E, -2E and -3E. According to the switching state of each Cell in the multilevel converter, it is possible to generate 2^7 voltage vectors in space.

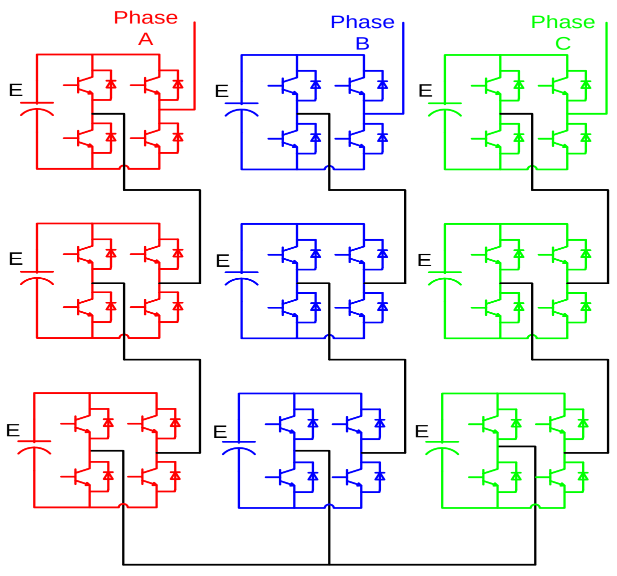

Fig.4.7: Seven level cascade H-Bridge multilevel converter.

4.3.5 Amplitude Modulation (AM)

4.3.5.1 Introduction.

Nowadays, multilevel cascaded H-bridge converters based on amplitude modulation are favorable candidates for big-scale photovoltaic power injection plants. They permit direct connection to medium-voltage electrical distribution networks without the existence of bulky line frequency power transformers.in addition, cheap and simplicity in deal and use.

Because of above the mentioned advantage, this method has been used and implemented for designing the complete task of APF.

4.3.5.2 Basic Principle of H-Bridge Cascaded Multilevel Converter

The cascaded H-Bridge converter is formed by two single-phase inverters with separated voltage sources. The circuit in Fig.4.4 demonstrates the basic topology of one phase of the three level cascaded converter, Each H-Bridge cell consists of four switches and four diodes as shown in the picture.

Same as each H-Bridge, several combinations of switch positions will get different voltages such as V+, V- and

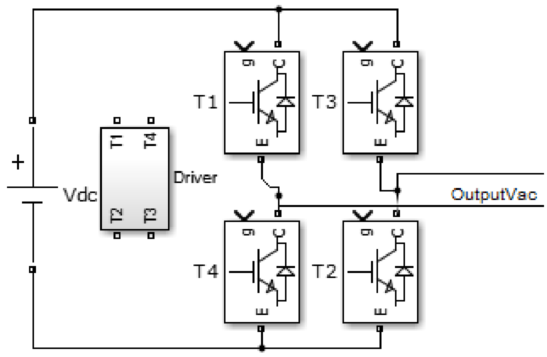

Fig.4.8: Three level converter

This three-level converter is the basic cell that is utilized to build multilevel cascaded converters. A multilevel cascaded converter is simply built by connecting basic three-level cells in series.

4.3.5.3 The 27-level Converter Operation Based on Amplitude Modulation.

This topology utilizes, at least, two conventional full-bridge single-phase inverters, usually designated H-bridges, connected in series, as shown in Fig. 4.5. Which shows a single-phase converter?

The topology needs each H-bridge to be sourced by an isolated DC source. Each bridge has three levels in the output voltage (V, 0 and –V); along these lines, keeping in mind the end goal to get a higher number of levels and a waveform with better quality it is needed more bridges connected in series.

For equal DC sources, the number of levels, NL, in the output voltage is given by (1), being S the number of H-bridges of the multilevel inverter.

$$NL=2*S+1 \qquad (1)$$

A higher number of levels can be obtained using DC sources with different and specific voltage levels, [1]. For example, with V1=V and V2=3V, a 9-level waveform can be combined instead of a 5-level one, with V1=V2=V.

Unlike conventional DC/AC inverters multilevel inverters are characterized by synthesizing a voltage waveform constituted by several steps, closer to a sine wave and so with a lower harmonic content. In multilevel topologies, the alternating voltages are obtained through the connection of several semiconductors that block or conduct a portion of the input power (current or voltage) and create several steps in the output voltages.

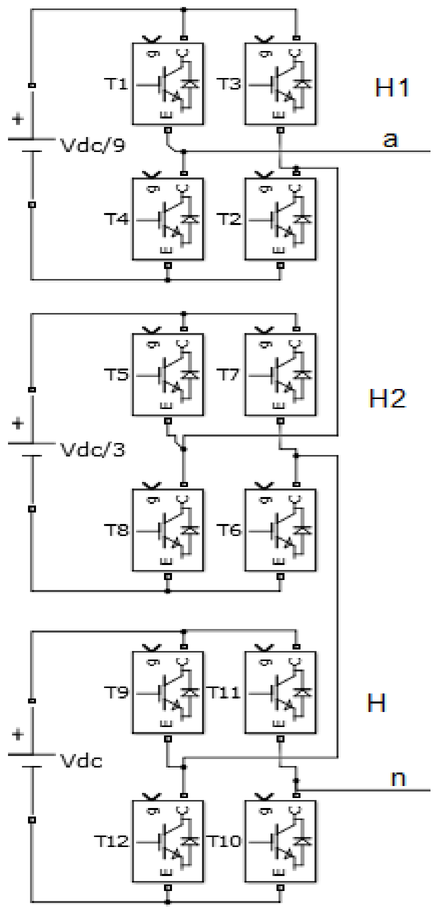

Fig.4.9: Single-phase converter.

Fig.4.6 (d) shows the switching frequency in each “H” bridge inverter of the multistage inverter implemented. It can be noted that the switching frequency of the main inverter, which manages more than 80% of the total power, is the same frequency of the system, in this case, only 50 Hz.

The frequency of the auxiliary inverters is also low but increases as the voltage level of the inverter becomes lower in the chain, as seen in Fig. 4.6 (d) The modulation algorithm to synthesize the waveforms shown in Fig.4.6 is described as follows: There is a three-digit binary number associated with the instantaneous amplitude of the voltage. The three-digit number could be +1,0, or −1 (positive, zero, or negative output at the corresponding “H” bridge). Each one of the three digits of the binary number is applied to each one of the Three “H” Bridges of the converter, which defines the output of the 27-level converter. For example, level 7 is obtained with the three-digit number {1, -1,1} or 1 Vdc - 3 Vdc + 9 Vdc = 7. The maximum positive level is {1, 1, 1} or 13 Vdc, and the minimum level (or maximum negative level) is {−1,−1,−1} or −13. It is important to mention that more complicated PWM strategies can also be applied in this kind of converters [20]–[22].

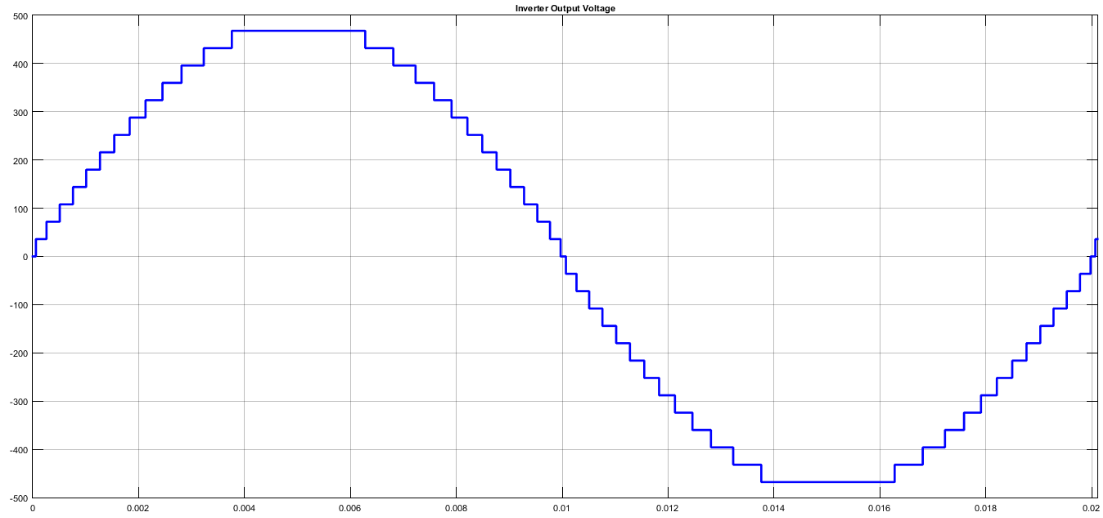

Fig.4.10 (a); Output signal from 27-level inverter**.**

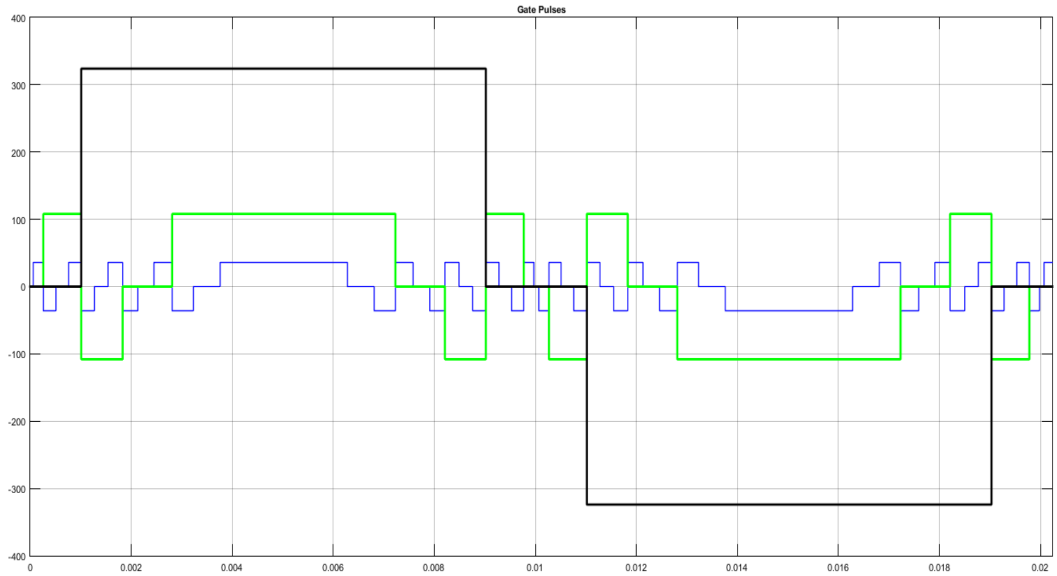

Fig.4.10 (b); Switching frequency of each “H” Bridge.

Table. 4.5 Shows the Switching sequence of cascaded “H” bridge multilevel inverter. The table below clarifies the working principle of modulation technique to generate 27 level output voltage waveform.

Table.4.5: Switching sequence of cascaded multilevel inverter.

V out	1 Vdc	3 Vdc	9 Vdc
13 Vdc	+ve	+ve	+ve
12 Vdc	Zero	+ve	+ve
11 Vdc	-ve	+ve	+ve
10 Vdc	+ve	Zero	+ve
9 Vdc	Zero	Zero	+ve
8 Vdc	-ve	Zero	+ve
7 Vdc	+ve	-ve	+ve
6 Vdc	Zero	-ve	+ve
5 Vdc	-ve	-ve	+ve
4 Vdc	+ve	+ve	Zero
3 Vdc	Zero	+ve	Zero
2 Vdc	-ve	+ve	Zero
1 Vdc	+ve	Zero	Zero
0 Vdc	Zero	Zero	Zero
-1 Vdc	-ve	Zero	Zero
-2 Vdc	+ve	-ve	Zero
-3 Vdc	Zero	-ve	Zero
-4 Vdc	-ve	-ve	Zero
-5 Vdc	+ve	+ve	-ve
-6 Vdc	zero	+ve	-ve
-7 Vdc	-ve	+ve	-ve
-8 Vdc	+ve	Zero	-ve
-9 Vdc	zero	Zero	-ve
-10 Vdc	-ve	Zero	-ve
-11 Vdc	+ve	-ve	-ve
-12 Vdc	zero	-ve	-ve
-13 Vdc	-ve	-ve	-ve

Multilevel inverters are able to produce current waveforms with negligible total harmonic distortion. Furthermore, they can work using both amplitude modulation and PWM strategies.

The amplitude modulation technique had been used in this system because it’s easy to use, the simplicity in implementation and it does not depend on the frequency of the input signal, it depends on the amplitude of signal only.

When the reference voltage signal generated is entered to the amplitude modulation block, it made pulses to the multilevel inverter to get output similar to the reference signal input, using 27 level inverters in both series and shunt active filter we can get the reference signal with negligible harmonic distortion and this completely eliminate the need for passive filters to support the working of active filters.

If the amplitude of reference signal changes the output of multilevel inverter will also change with the same ratio, so this composed topology can track the input signal from 1-level to 27 level output signal, so the system can deal with a large band of contaminating loads and this is an additional advantage of the system.

The amplitude modulation technique had been implemented using Embedded MATLAB Function block as seen in Fig.4.10 (c).

```
function y= f(u)

a=abs(u);
if a<0.015 %0
    p1=1;
    p2=0;
    p3=1;
    p4=0;
    p5=1;
    p6=0;
    p7=1;
    p8=0;
    p9=1;
    p10=0;
    p11=1;
    p12=0;
elseif a<0.07692
%1
    p1=1;
    p2=1;
    p3=0;
    p4=0;
    p5=1;
    p6=0;
    p7=1;
    p8=0;
    p9=1;
    p10=0;
    p11=1;
    p12=0;
elseif a<0.1538 %2
    p1=0;
    p2=0;
    p3=1;
    p4=1;
    p5=1;
    p6=1;
    p7=0;
    p8=0;
    p9=1;
    p10=0;
    p11=1;
    p12=0;
elseif a<0.2307 %3
    p1=1;
    p2=0;
    p3=1;
    p4=0;
    p5=1;
    p6=1;
    p7=0;
    p8=0;
    p9=1;
    p10=0;
    p11=1;
    p12=0;
elseif a<0.3077 %4
    p1=1;
    p2=1;
    p3=0;
    p4=0;
    p5=1;
    p6=1;
    p7=0;
    p8=0;
    p9=1;
    p10=0;
    p11=1;
    p12=0;
elseif a<0.3846 %5
    p1=0;
    p2=0;
    p3=1;
    p4=1;
    p5=0;
    p6=0;
    p7=1;
    p8=1;
    p9=1;
    p10=1;
    p11=0;
    p12=0;
elseif a<0.4615 %6
    p1=1;
    p2=0;
    p3=1;
    p4=0;
    p5=0;
    p6=0;
    p7=1;
    p8=1;
    p9=1;
    p10=1;
    p11=0;
    p12=0;
elseif a<0.5384 %7
    p1=1;
    p2=1;
    p3=0;
    p4=0;
    p5=0;
    p6=0;
    p7=1;
    p8=1;
    p9=1;
    p10=1;
    p11=0;
    p12=0;
else    %nul
    p1=0;
    p2=0;
    p3=0;
    p4=0;
    p5=0;
    p6=0;
    p7=0;
    p8=0;
    p9=0;
    p10=0;
    p11=0;
    p12=0;


    end
 if u<0
y=[p3,p4,p1,p2
,p7,p8,p5,p6,p
11,p12,p9,p10]
;
 else
y=[p1,p2,p3,p4
,p5,p6,p7,p8,p
9,p10,p11,p12]
;
 end
end
```

Fig.4.10 (c): Amplitude modulation program.

4.4 Results and Work

4.4.1 Introduction.

The proposed 27-level converter used for series and shunt APF is simulated with a non-linear balanced three phase load and the performance of the three level and 27-level converters is discussed and compared. The results include:

1- Shunt active power filter using:

-Three level converter.

- 27-level converter.

2-Series active power filters using:

-Three level converter.

- 27-level converter.

Increasing the number of levels of a multilevel converter will increase the filter efficiency, reliability and optimize the transient and steady state behavior.

4.4.2 Shunt Active Power Filter Using.

- Three level converter.

- 27-level converter.

To study the correct performance of the shunt APF using different converter levels, the waveform of source current and its total harmonic distortion (THD) must be seen and discussed.

4.4.2.1 Shunt APF Using Three Level Converters.

The three phase source current signal is shown Fig.4.11, where Fig.4.11 (a) proves the correct functioning of harmonic mitigation (at t=0.4S), and it's clear from Fig.4.11 (b) the filter capability for active power injection (at t=0.7S). The changing in total harmonic distortion (THD) of source current is clear in Fig.4.12.

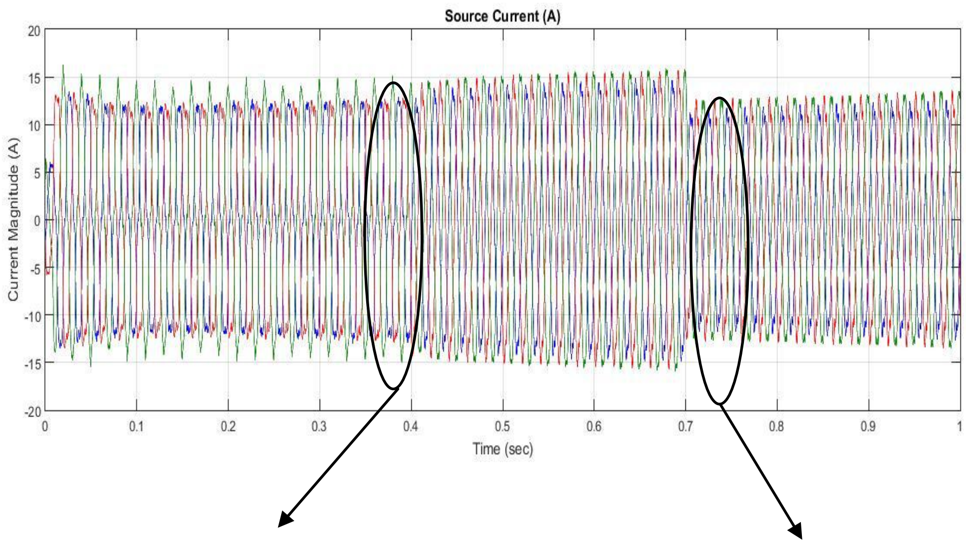

Fig. 4.11: Three phase source current waveform

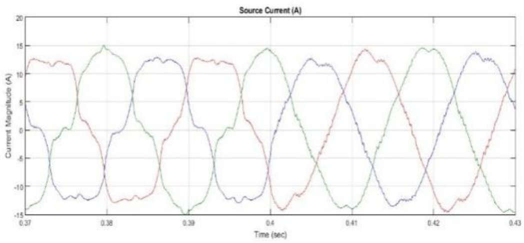

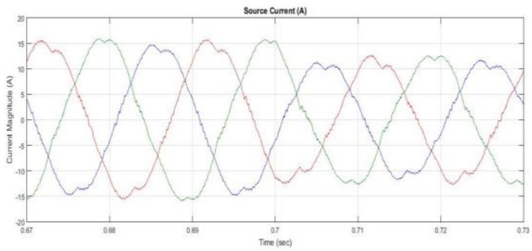

Fig.4.11 (a): Zoom for source current **Fig.4.11(b):** Zoom for source current

As shown in Fig.4.11 (a) at t=0.4 (sec) the shunt active power filter start working to mitigate the harmonic and the source current became close to sinusoidal.

The total harmonic distortion (THD) reduced from 15% to 4.8% as proved in Fig.4.12.

The active power injection starts at t=0.7 (sec) with 4 A current assistant as seen in Fig.4.11 (b), but the total harmonic distortion increased to 6% during active power injection, and this value of THD is over the IEEE 519 harmonic limit, which is 5%.so for the same control strategy we need to increase the output levels of converter to get the required results.

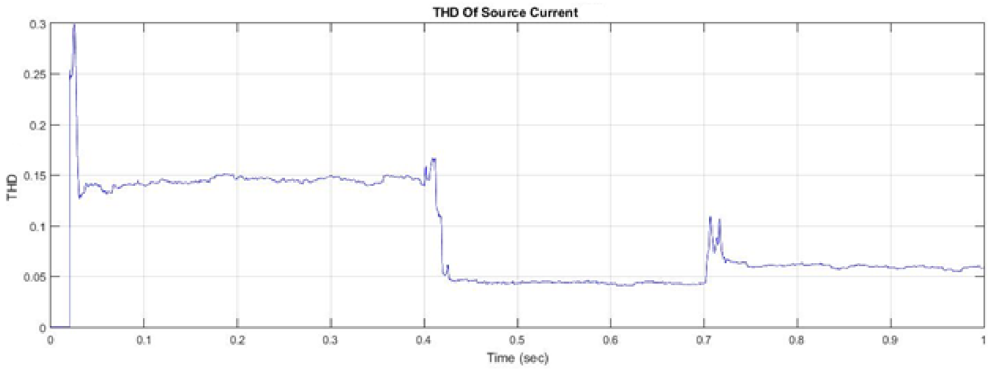

Fig. 4.12: Total harmonic distortion (THD) of source current.

4.4.2.2 Shunt Active Power Filter Using 27-Level Converter.

The three phase source current waveform is shown Fig.4.13, where Fig.4.13 (a) proves

The correct functioning of harmonic mitigation (at t=0.4 S), and it's clear from Fig.4.13 (b) the filter capability for active power injection (at t=0.7 S).

The changing in total harmonic distortion (THD) of source current is clear in Fig.4.14.

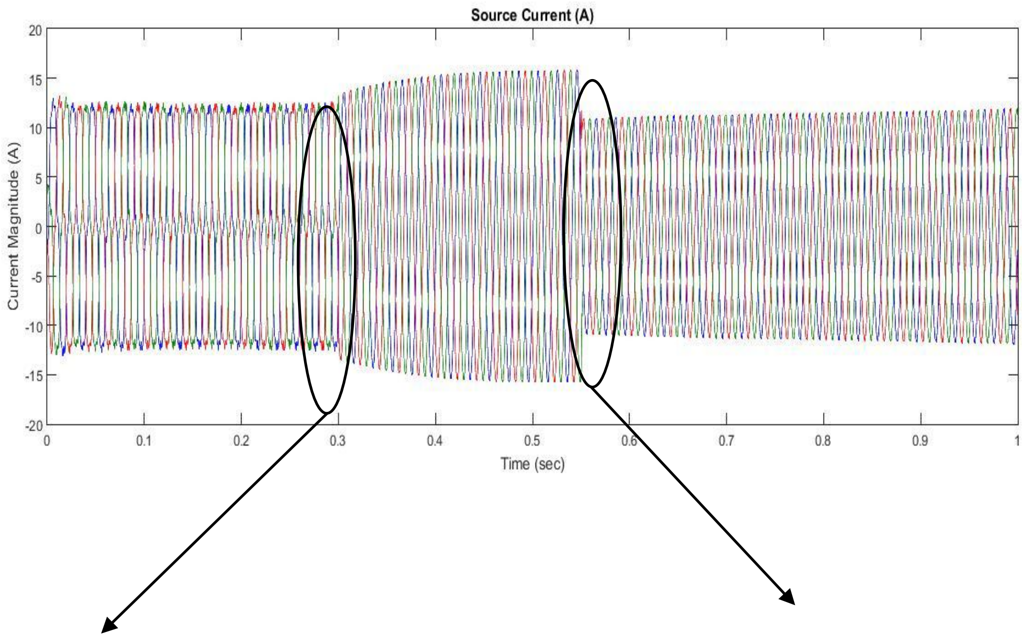

Fig. 4.13: Three phase source current waveform

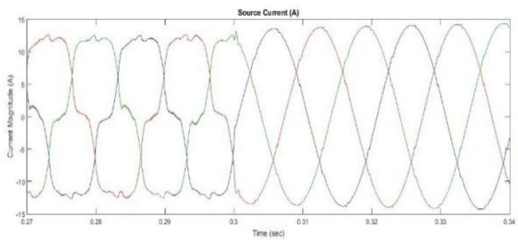

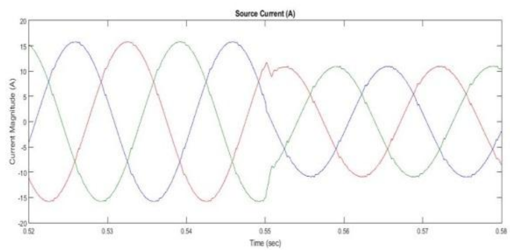

Fig. 4.13 (a); Zoom for source current

Fig. 4.13 (b): Zoom for source current

As shown in Fig.4.13 (a) at t=0.4 S the shunt active power filter start working to mitigate the harmonic and the source current became pure sinusoidal.

The total harmonic distortion (THD) reduced from 16% to 0.8% as seen in Fig.4.14.

The active power injection starts at t=0.7 S with 4 A current assistant as clear in Fig.4.13 (b), and the total harmonic distortion stay very low (1.3%) during active power injection.

It's clear from the simulation results, the using of 27-level converter more beneficial, reliable and trusted especially in high voltage levels where the total harmonic distortion (THD) need to be less than 2%.

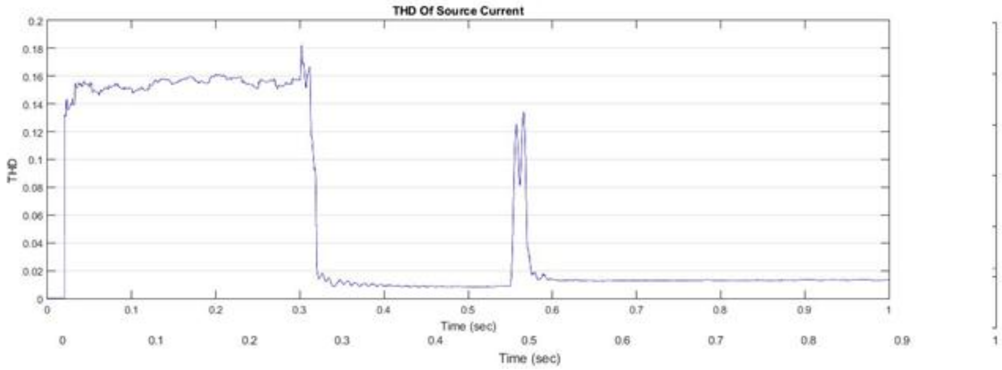

Fig. 4.14: Total harmonic distortion (THD) of source current.

4.4.3 Series Active Power Filter Using:

-Three level converter.

- 27-level converter.

To study the correct performance of the series APF using different converter levels, the waveform of source voltage and its total harmonic distortion (THD) will be seen and discussed.

4.5.3.1 Series APF Using Three Level Converters.

The three phase source voltage signal is shown Fig.4.15, where Fig.4.15 (a) proves the correct functioning of harmonic mitigation (at t=0.4 S). The variation in total harmonic distortion (THD) of source voltage is clear in Fig.4.16.

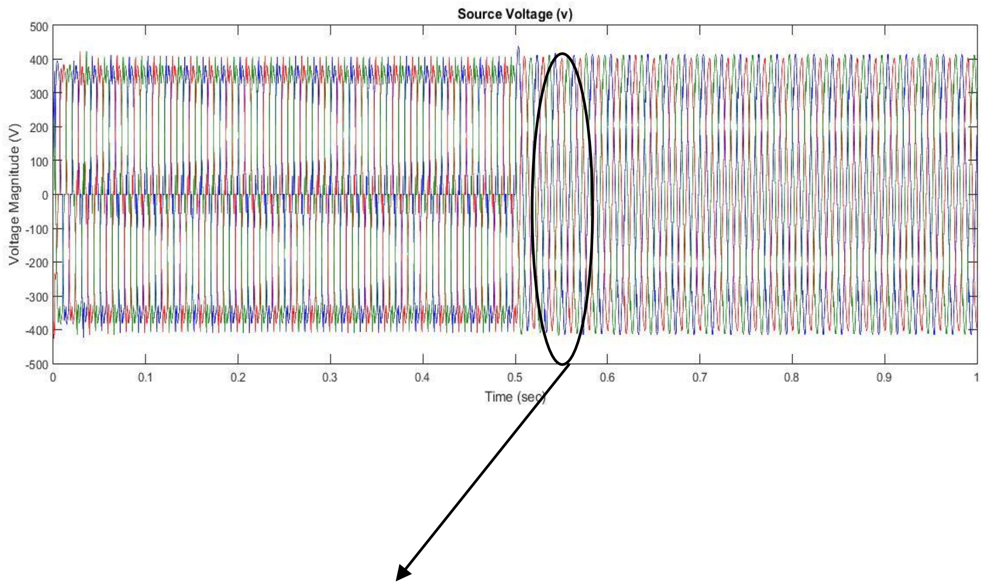

Fig. 4.15: Three phase source voltage waveform**.**

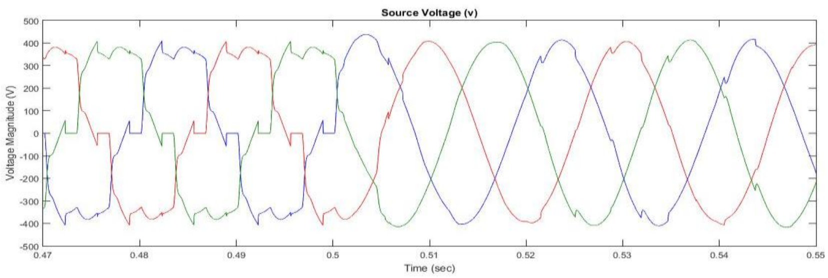

Fig. 4.15 (a): Zoom for source voltage.

As shown in Fig.4.15 (a) at t=0.5S the series active power filter start working to mitigate the harmonic in source voltage.

The total harmonic distortion (THD) reduced from 21% to 4.9% as seen in Fig.4.16.

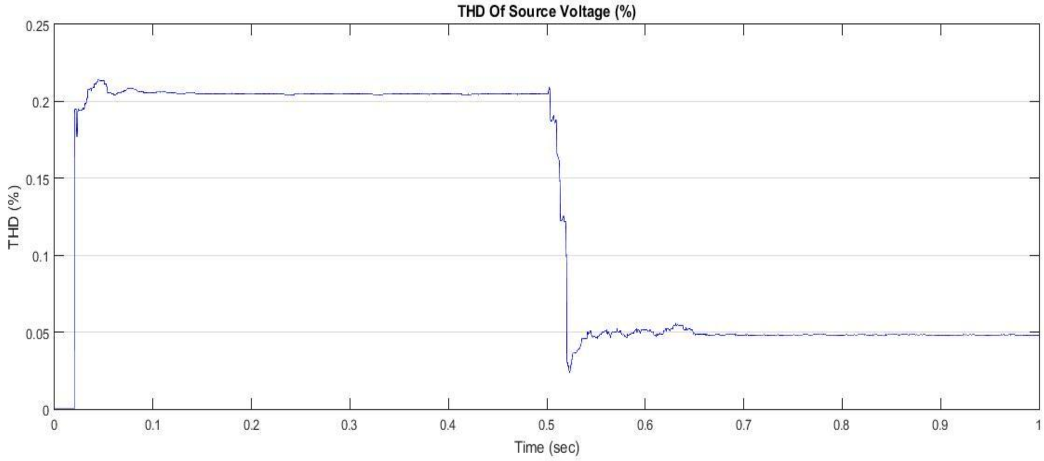

Fig.4.16: Total harmonic distortion (THD) of source current.

4.4.3.2 Series APF Using 27-Level Converter.

The three phase source voltage signal is shown Fig.4.17, where Fig.4.17 (a) proves the correct functioning of harmonic mitigation (at t=0.5S). The variation in total harmonic distortion (THD) of source voltage is clear in Fig.4.18.

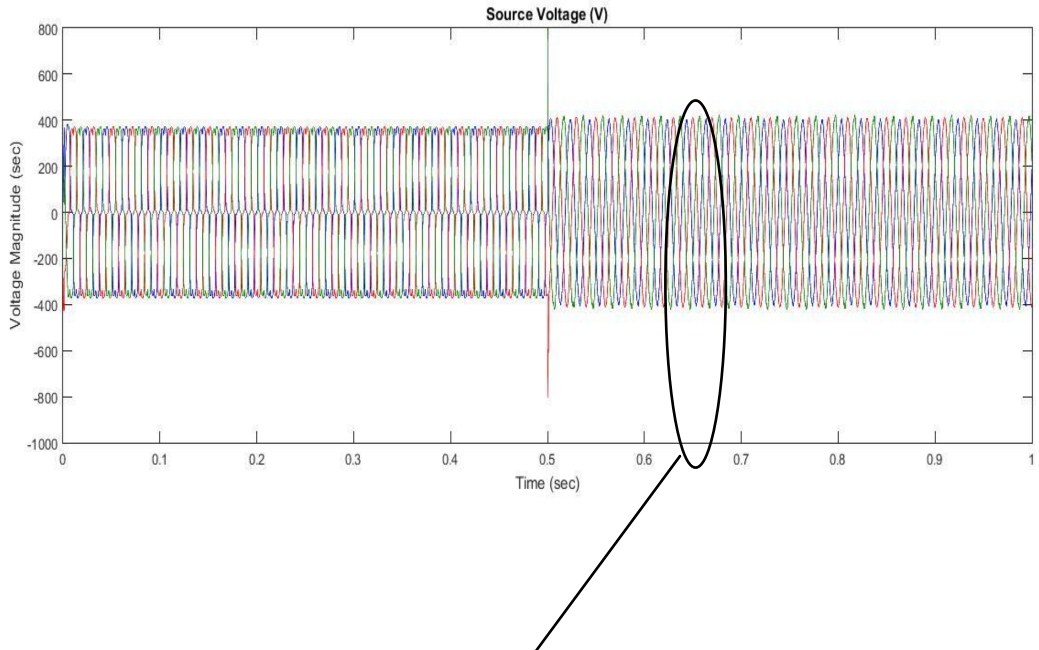

Fig. 4.17: Three phase source voltage waveform.

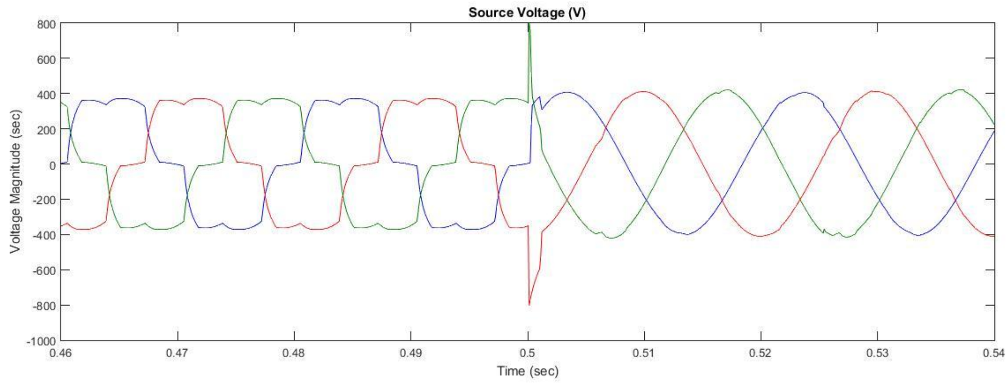

Fig. 4.17 (a): Zoom for source voltage**.**

As shown in Fig.4.17 (a) at t=0.5S the series active power filter start working to mitigate the harmonic and the source voltage became pure sinusoidal.

The total harmonic distortion (THD) reduced from 20.4% to 1.28% as seen in Fig.4.18.

It’s clear from the simulation results; the using of 27-level converter in series APF is more efficient, reliable and trusted.

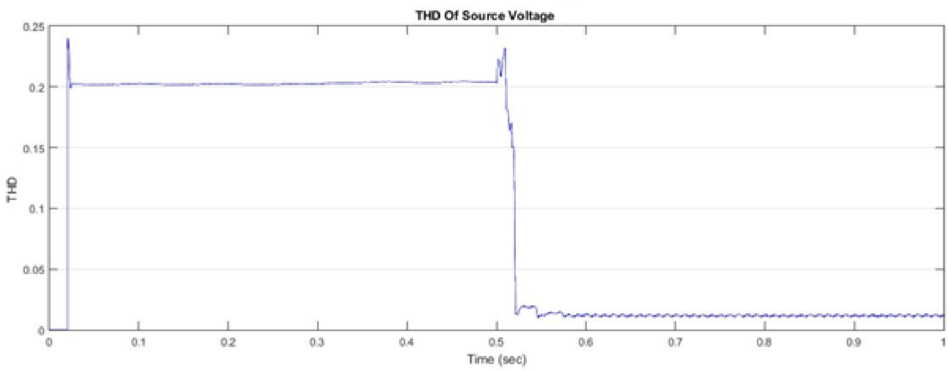

Fig. 4.18 (a): Total harmonic distortion (THD) of source current.

Fig.4.18 (b) shows the spectrum of source voltage signal, and proves the correct working of series APF.

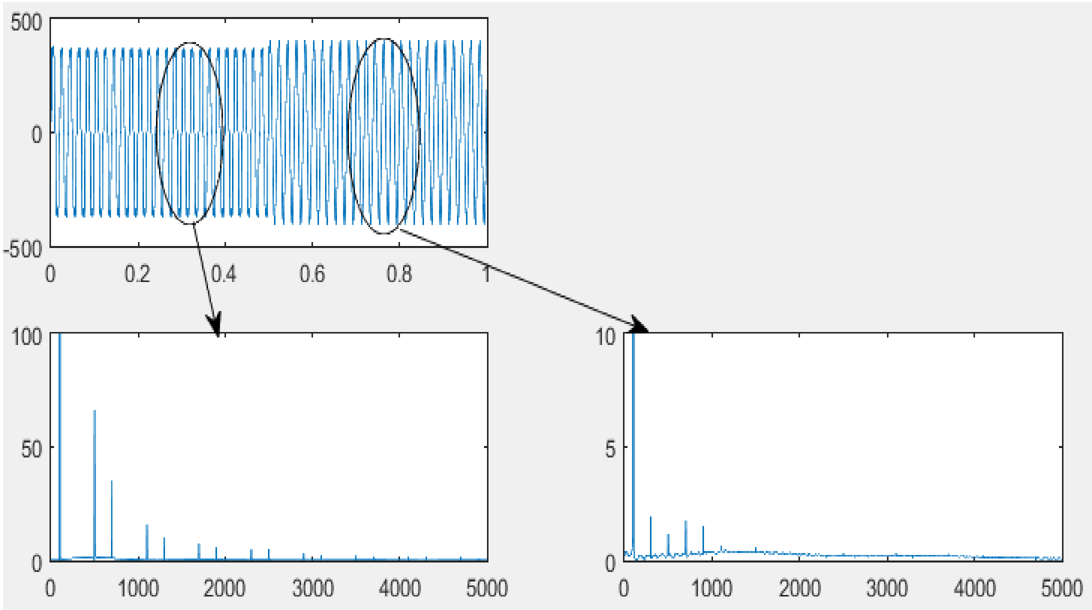

Fig.4.18 (b): Spectrum of source voltage signal.

4.5 Chapter Summary.

This chapter is focused on the study of multilevel converters. At first, an overview of the most typical converter topologies had been presented. Then the cascaded H-bridge 27 level inverter have been discussed and tested, the modulation techniques have been used in cascaded H-Bridge converters are presented, and finally a simulation results for shunt and series APF using three level and 27-level converters have been compared and tested with three phase nonlinear load .

Chapter Five

Dc Source PV System with MPPT

5.1 Photovoltaic System with MPPT.

There are two ways for connection of PV array to the grid:

- Way-1: the photovoltaic array linked to DC-DC step up converter and supplies a DC-AC converter for network linking.

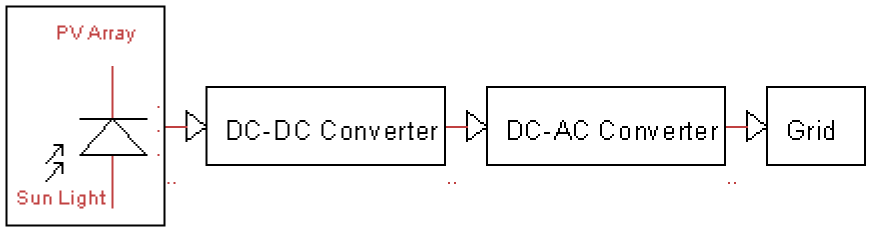

Fig.5.1: Photovoltaic array linked to the network through DC-DC converter and DC-AC converter

- Way2: the photovoltaic array could be linked to DC-AC converter then to electrical network.

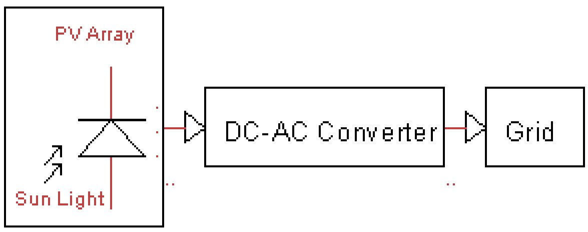

Fig.5.2: Photovoltaic array linked to the network with DC-AC converter.

Whereas the Photovoltaic system linked to electrical network using DC-DC converter and DC-AC inverter have been implemented and tested, because the DC-DC converters can be used for power bus regulation and noise isolation.

5.2 Photovoltaic Cell Theory.

The solar cell composed from a semiconductor silicon material to form a PN-junction. So the photovoltaic system builds basely from the PN-junction. A big number of electrons and holes are generated when the light stroked on the flat of PN-junction. Therefore, an electric field generated between the PN-junction terminals and positive and negative terminals are also formed.

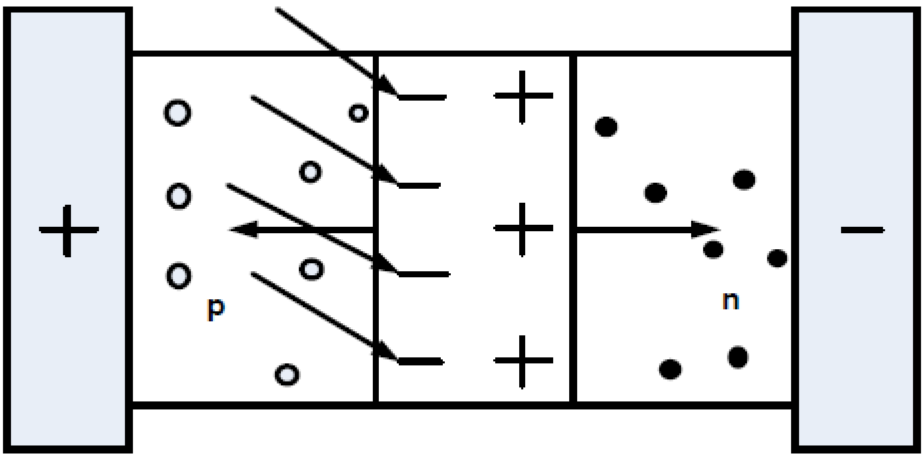

Fig.5.3: P-N junction clarification of PV cell.

As seen from the above figure. 5.3, when the junction exposed to the sunlight, a pairs of electrons and holes are formed by getting the needed energy from the sunlight.

Whereas the P-region is the house of holes and the n-region is the house of free electrons. Hence, positive and negative terminals are created as shown the middle portion of the Fig.5.3.

If we put an electrical load between junction terminals, the electrons will travel to P-type part and the holes travel to N-type part. That means, an electrical current motion generated through the PN-Junction and transfers the energy in sunlight to electrical energy.

5.3 Photovoltaic Cell, Module or Panel and Array.

The solar cell energy is so low, it's about 1.5 watts for mono crystalline type, so to make it useful, it is needed to get high solar power generation source.

The solar power generation source composed from a big number of series and parallel solar cells and it can be named as solar panel or module then named Array for high power systems.

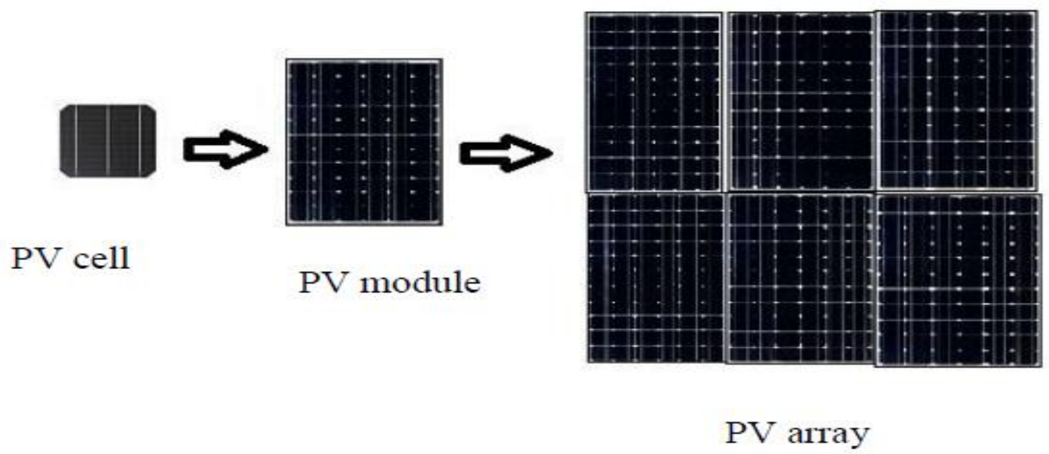

Fig. 5.4: Creation of solar module and solar array.

As seen in Fig. 5.4 the PV module is the summation of series connected solar cells to get applicable voltage for real life applications.

For high power applications, it’s needed to form the PV array which is the summation of series and parallel combinations of solar panels.

5.4 Modeling of Solar Cell.

To model the PV array, it’s important to analyze and study of the individual PV cells. Fig.5.5 below shows a good physical representation for solar cell.

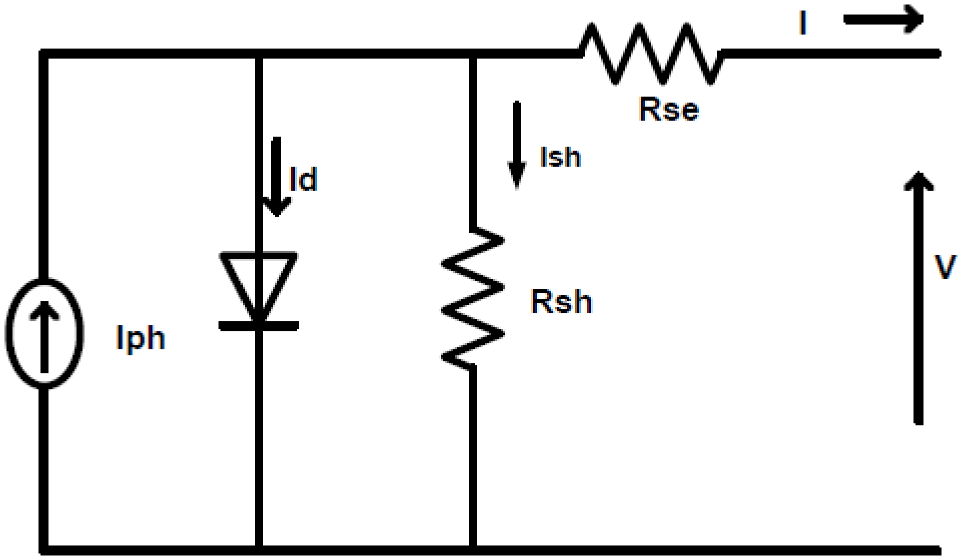

Fig.5.5: Equivalent electrical circuit for single solar cell.

Whereas,

Iph–Current produced from sunlight effect

Id – Diode current

I –The effective current of solar cell

K -Boltzmann constant (1.38 × 10-23 J/K)

Rse–Internal losses serial resistance

Rsh–Internal losses parallel resistance

V- The no-load cell voltage

The major impact of series resistance was to decrease the fill factor and when a short circuit happens between cell terminal, the series resistance acts as a small load and high values could protect the solar cell from short circuit current but with decreasing in cell efficiency and maximum power point. Also less values for internal shunt resistance will increase the internal power losses and then decrease the efficiency because it provide another easy path for the current generated in the cell.

The mathematical representation can be extracted figure 5.5 by using the nodal analyzes

The characteristics equation of the PV model given by equation (5.1)

$I=I_{ph}-I_{d}-I_{sh}$ or

$$I = I_{ph} – Io\ [\exp^{(q\ (V+IRs)/aKT)} -1] - (V+I_{Rs})/R_{sh} \qquad (5.1)$$

Where, *Ipv* is photocurrent; *Io* is diode saturation current; *q* is coulomb constant (1.602×10-19C); *K is* Boltzmann’s constant (1.381×10-23 J/K); *T* is cell temperature in ºC; *a* is P-N junction ideality factor; *Rs* and *Rsh* are the intrinsic series and shunt resistances of the cell, respectively. The shunt and series resistance of the module used equals to 66.3 and 0.255 ohms, respectively. These values increase the short circuit current capability for the module used. And as a result increasing the efficiency of the PV module. Because of all above mentioned advantages this module have been implemented for creation of all PV input arrays.

The shunt and series resistance used in the above model equals to 66.3 and 0.255 ohms, respectively. These values increase the short circuit current capability for the module used.

And as a result increasing the efficiency of the PV module. Because of all above mentioned advantages these modules have been implemented for creation of all PV input arrays.

5.5 Power against Voltage and Current against Voltage Characteristic Curves of (pv) Panel.

The short circuit current Isc of solar cell can be obtained by shorted both terminals of solar cell. In this case, the voltage across the solar cell equals to zero. In the same way, the open circuit voltage Voc can be obtained by keeping open circuit at the cell terminals. In this case, the current of solar cell equals to zero. Figure.5.6 show the I-V and P-V Characteristic Curves. Where the Voc happened when the cell current equal zero and the short circuit current Isc obtained when the cell voltage equal zero.

Where the cell power can be easily founded by multiplying both the cell current and voltage.

It's clear from figure below; the maximum power point (MPP) for photovoltaic module can work on it.

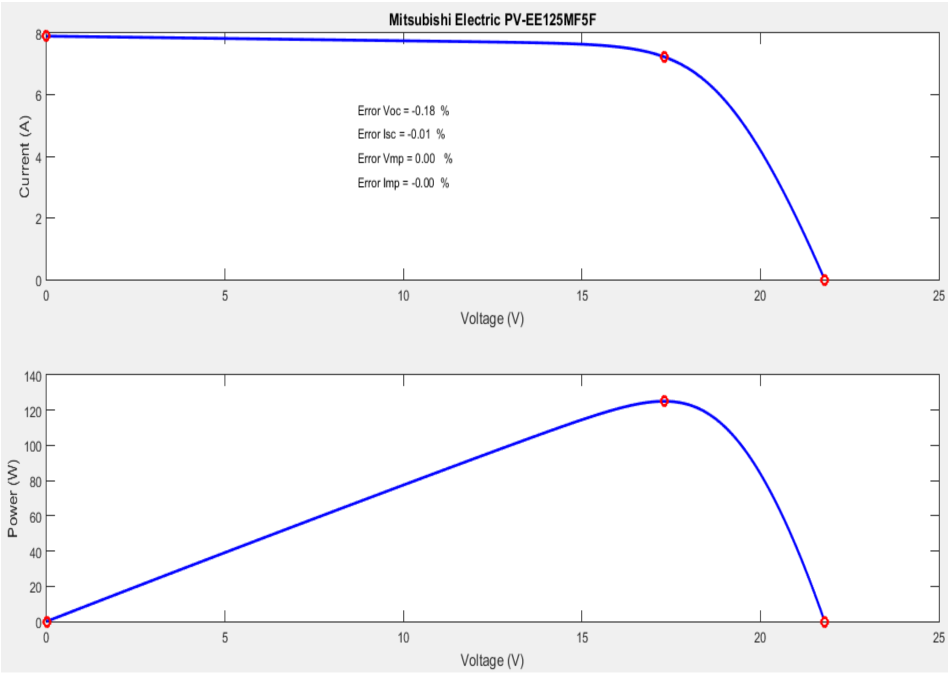

Fig.5.6: Mitsubishi PV-EE-125MF5F photovoltaic module I-V and P-V characteristic curves.

In this thesis, the Mitsubishi PV-EE-125MF5F photovoltaic module have been implemented and used to build all system solar arrays.

5.6 Influence of Solar Irradiance and Temperature on Solar Cell Characteristic Curves.

The idiom Irradiance definition is the amount of power density of sunlight received at a location on the earth with unit W/M2. While the irradiation is the measure of energy density of sunlight. During the day, the solar insolation varies continuously.

From figures.5.6 and 5.7, the solar irradiance decreased, both the short circuit current and open circuit voltage decreased accordingly. As a result the maximum power point of photovoltaic module decreased.

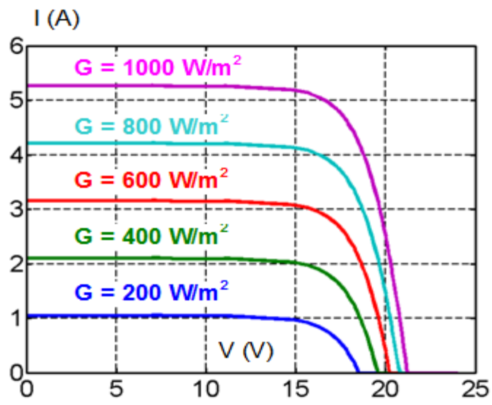

Fig.5.7 a: I-V Curve irradiance effect

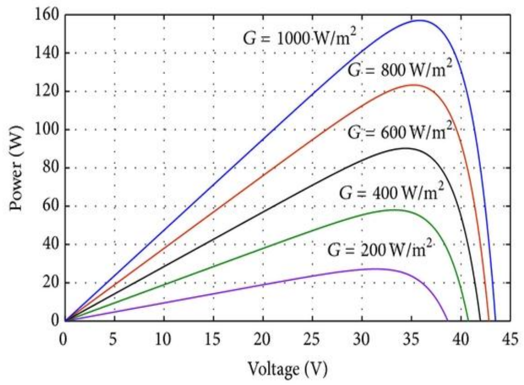

Fig.5.7 b: P-V Curve

As shown in fig. 5.6 the short circuit current of solar cell increased rapidly with the increasing of solar irradiance.

The short circuit current changed by the following equation (5.2)

$$Isc_{new}=Isc_{old}*(\text{new irradiance/old irradiance})\ W/m^2 \quad (5.2)$$

Whereas below 160W/m^2 the voltage increased rapidly and above 160w/m^2 the voltage increase by a small amount as shown in fig.5.6.

5.7 Temperature Effect.

Temperature plays an important role in determining the efficiency of photovoltaic modules. When the ambient temperature increased, the generation rate of electrons increased, therefore the diode saturation current increased quickly with reducing in energy band gab. This made a small increase in current and big decreasing of voltage.

Every decreasing in ambient temperature by one degree we got 2.4mV decreasing in voltage. So the performance of the solar cell decreases in hot days and we got an ideal performance in case of cold and sunny days.

The general voltage-temperature equation to calculate the new voltage when the ambient temperature changed is:

$$Voc_{mod} = Voc_{stc}\ (1+hv\ *(T_{cell}(c)-25\ c))\ V \qquad (5.3)$$

Where:

V_{ocmod} = the open circuit voltage at module temperature.

T_{cell}[°C] = temperature of the module.

Voc_{stc}= the open circuit voltage at standard conditions (STC)

hv: the temperature coefficient related to the voltage of the cell (-3.7mV/c)

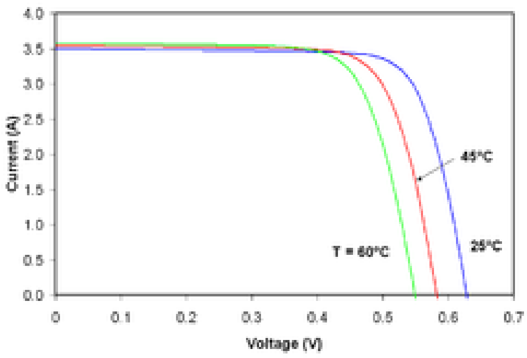

Fig.5.8: I-V Curve temperature effect

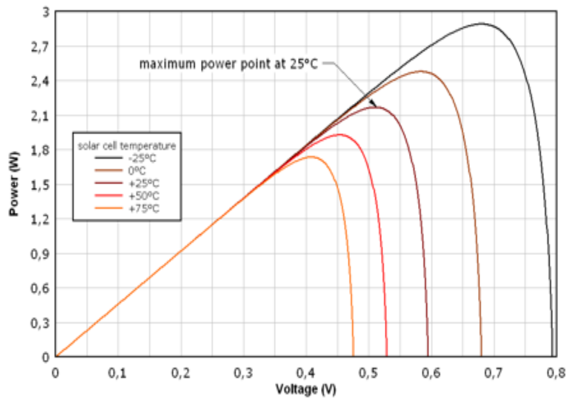

Fig.5.9: P-V Curve temperature effect

As shown in Fig.5.8, the open circuit voltage degreasing as temperature increasing with a very small increasing of short circuit current, and the maximum power point (mpp) varied according to fig.5.9 where the maximum power point (mpp) also degreased as the temperature increased.

5.8 Maximum Power Point Tracking.

In photovoltaic system Maximum power point tracking is a very essential part. In photovoltaic system there must be unique operating point which gives maximum power and this MPPT is used to track this operating point. MPPT is an electronic arrangement that is used to find out the voltage (VMPP) and current (IMPP) at which PV system gives maximum output power during change in environmental conditions. This method permits the PV modules to operate in such a way that can produce maximum power it is capable of. For implementation of the tracking algorithm to the dc-dc converter require some desired feature for the efficient use of MPPT.

These desired features of MPPT are described as below:

- Price is less.
- Implementation is easy.
- Rapid tracking response in dynamic analysis.
- There should not be any oscillations at the maximum power point during steady state condition analysis.
- The MPPT must have the capability for tracking the maximum power point with large range of change in solar irradiation and temperature.

DC to DC converters is needed for MPPT implementation as in Boost converter, input voltage (DC) is a smaller than output voltage (DC).That means input PV-voltage is lesser than the output voltage of boost converter. Hence, boost converter is required for MPPT to boost-up the voltage of the PV system.

MPPT works effectively during these conditions:

• **Cold or winter days:** Generally, PV system extracts less energy in winter seasons so MPPT (maximum power point tracker) is used more efficiently to extract maximum possible power presented.

• **During discharged condition of battery:** When the battery charge is less the MPPT extracts more current and able to charge the battery.

The maximum power point tracking (MPPT) have a very high efficiency (normally around 99% at 80 Vdc).

5.8.1 Importance of MPPT in Photovoltaic System.

Solar irradiation may change in a wide range depending upon the seasons, hours of a day, latitude, and orientation of the solar field. Hence, the solar irradiation that hits on the PV system may vary.

Considering these conditions, the MPPT is essential to identify the operating points at each instant on the V-I curve at which maximum power should be transferred to the grid system will occur at the PV generator.

Generally, the efficiency of solar panels is low but the energy to be generated from PV systems must be maximum.

Due to this reason PV systems are equipped repeatedly with maximum power point (MPP) tracker for tracking maximum possible power. Several maximum power point tracking techniques are proposed and implemented in recent years.

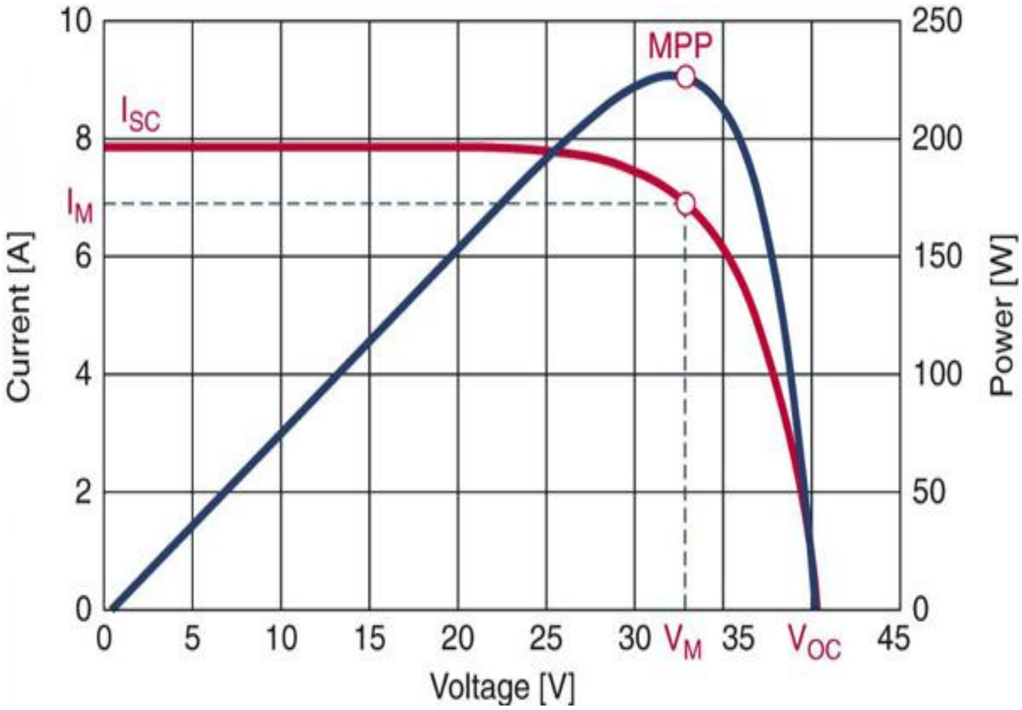

Fig.5.10: MPP in P-V and I-V curves for PV module.

Depending on the PV system control technique for generation methodology during steady state condition, it is normally classified into following groups:

1. Offline methods

- Open circuit voltage(OCV) method

- Short circuit current(SCC)
- Artificial intelligence

2. Online methods

- Perturb and observe(P&O) method
- Extreme seeking control method(ESC)
- Incremental conductance method (Inc. Cond.)

3. Hybrid methods.

The Perturb and observe (P&O) method designed and tested in this project.

5.9 Perturb and Observe (P&O) MPPT.

MPPT implemented by Enhanced Perturb and Observe (P&O) method to track the maximum power point.

The P&O algorithm is depends on the “hill-climbing” principle, which relies on moving the operation point of the PV array in the way of maximum power [8]. Hill-climbing algorithms are the top common MPPT methods referred to their ease of implementation and acceptable performance when the irradiation is constant. The advantages of P&O method are the simplicity and low power consumption needed. There are two drawbacks of this technique, the major one is that they can easily lose track of the maximum power point (MPP) if the irradiation changes quickly [9]. The minor disadvantage of P&O method is the unstable voltage and current around the maximum power point (MPP) in the steady state [10] and [11].To overcome these handicaps, we used enhanced P&O method; a diagram of this algorithm is shown in Figure 5.11

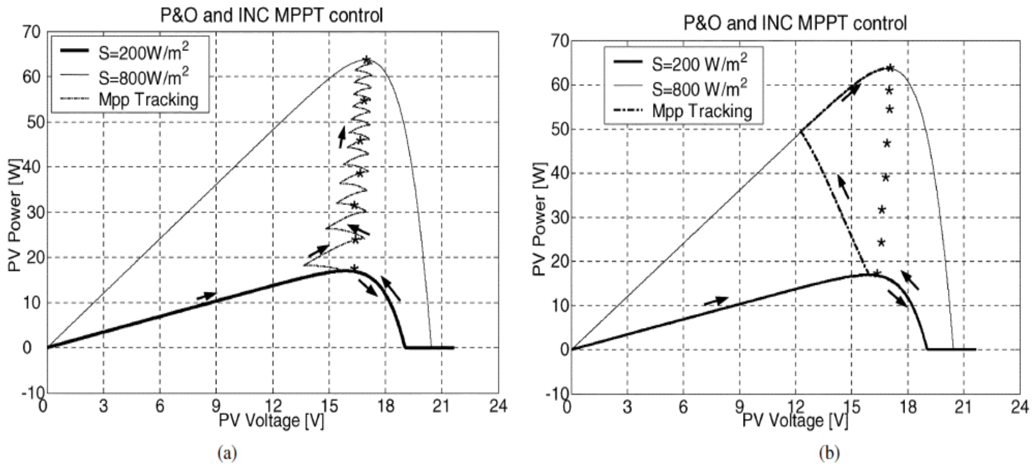

Fig. 5.11. P&O MPPT operating point path**.**

Tracking MPP for various levels of the irradiation: (a) slow change in atmospheric conditions and (b) rapid change in atmospheric conditions.

5.9.1 Flow Chart of (P&O) Algorithm.

Figure 5.11(a) shows the flowchart of the enhanced P&O Algorithm used in this project.

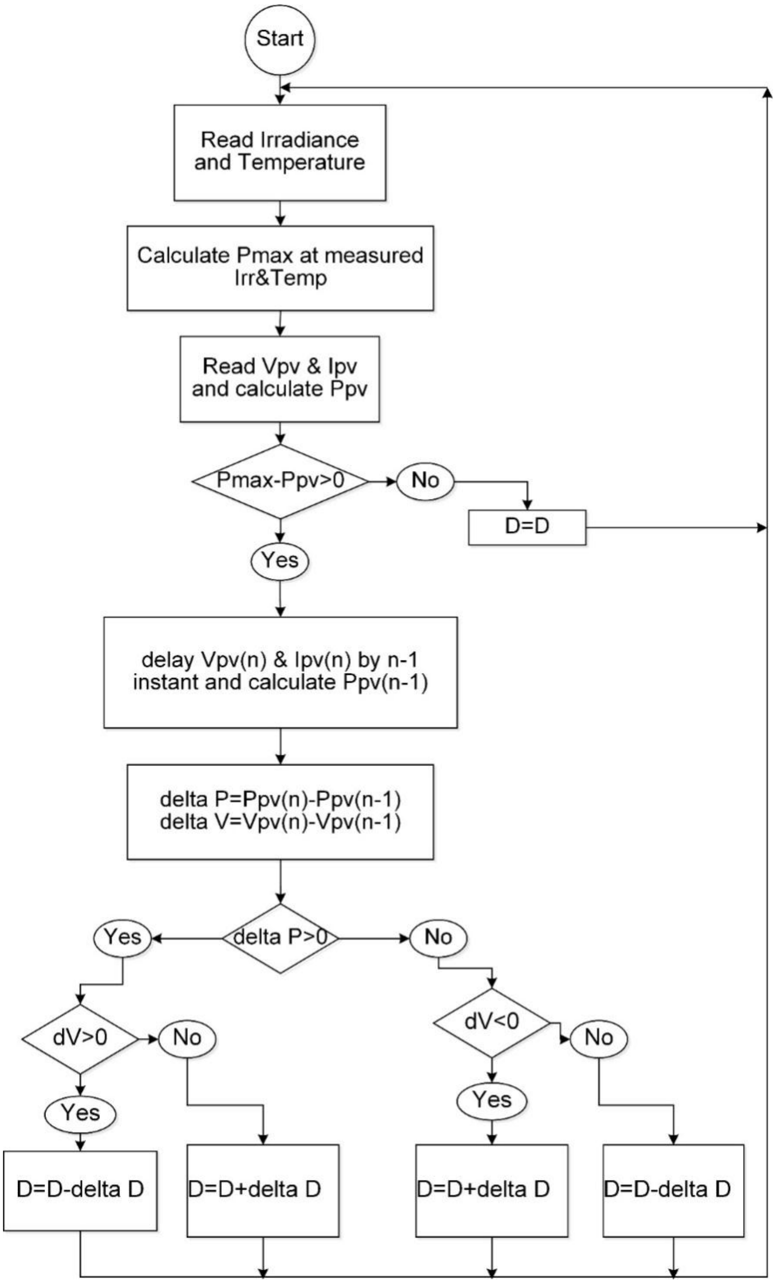

Fig.5.11 (a): Flowchart of the enhanced P&O algorithm.

Where:

Pmax – Maximum power needed from MPPT at present temperature and irradiance values.

Vpv (n) – voltage of the present perturbation

Ipv (n) – Current of present perturbation

Ppv (n) – Power of present perturbation

Vpv (n-1) – voltage of the previous perturbation

Ppv (n-1) - Power of previous perturbation

dV– Change in voltage between present and previous perturbation

Referring to the flowchart.

dP – Change in power between present and previous perturbation

D: is the duty cycle of boost converter.

According to the flowchart, if $\Delta p>0$ and $\Delta v>0$,thisindicates that the current power is present in the left side of the maximum power point.

Hence, increase in voltage occurs, similarly if $\Delta p<0$ and $\Delta v>0$ current power is present in right of the maximum power point then decrease in voltage occurs at this situation. At $\Delta p=0$ the available power is the maximum power point.

In this method, the Maximum Power was calculated according to the measurements of the Irradiance and the Temperature. After finding the maximum power at given conditions, we execute the classical P&O algorithm, and after each complete running cycle the variation between the power measured at the output of PV array(real power) and the max power estimated at the starting of the algorithm is calculated. If the difference is zero, then we have attained the max power, so the sitting duty cycle value is the optimum control signal. This value is fixed and is set as control reference signal for DC-DC boost converter until we get another reading of maximum needed power from MPPT. This method gives much more efficiency than the classical P&O algorithm.

Figure 5.11(b) shows the program of MPPT algorithm using embedded MATLAB function.

```
function [D,PMAX]  = SmartMPPT( V,I,irr,temp)

% MPPT by Perturb & Observe algorithm.
% V input = PV array terminal voltage (V)
% I input = PV array current (A)
% D output = Duty cycle of the boost converter
%pmax =the power of maximum power point=vmpp*impp


double pmax;
double irr;
double temp;
double P;


pmax=(0.7935*(109*(1-0.0036372*(temp-
25))))*(0.915*(23.7*(1+0.0004269*(temp-25))*(irr/1000)));


PMAX=pmax;
persistent Vold Pold Dold;

if isempty(Vold)
    Vold=0;
    Pold=0;
    Dold=0;
end
P= V*I;

if ((pmax-P)>0)
    dV= V - Vold;
    dP= P - Pold;
    if (dP>0)
        if (dV > 0)
            D = Dold - 0.001;
        else
            D = Dold + 0.001;
        end
    else
        if (dV < 0)
            D = Dold + 0.001;
        else
            D = Dold - 0.001;
        end
    end


else
    D=Dold;
end
if(D>1)
    D=1;
elseif (D<-1)
    D=-1;
else
    D=D;
end

Dold=D;
Vold=V;
Pold=P;

end
```

Fig.5.11 (b): Program of MPPT algorithm**.**

5.10 Boost Converter

The DC to DC converters is necessary for MPPT designing. As in Boost converter, input voltage (DC) is a less than output voltage (DC).That means input PV-voltage is smaller than the output voltage of boost converter. Hence, boost converter is required for the PV system with MPPT technique to boost-up the voltage of the PV system. DC-DC Converters are used for dc-input voltage which is then converted to desired dc-output voltages where the magnitude of the output voltage must differ than the input voltage magnitude. Normally, DC-DC converters are classified into three types namely: buck, boost and buck-boost Converter and here boost converter is preferred as we need to step up the PV output. DC-DC converters are also useful for noise isolation and power bus regulation. The DC-DC boost converter contains an inductor, capacitor, diode and an IGBT as it is a high frequency switch. It produces higher voltage during power supply to the load. Based on the switch duty cycle the output voltage may change. Generally transformer can step up the voltage, but there may be losses in the transformer. So to overcome this loss DC-DC Boost converter is used to get desired output voltage.

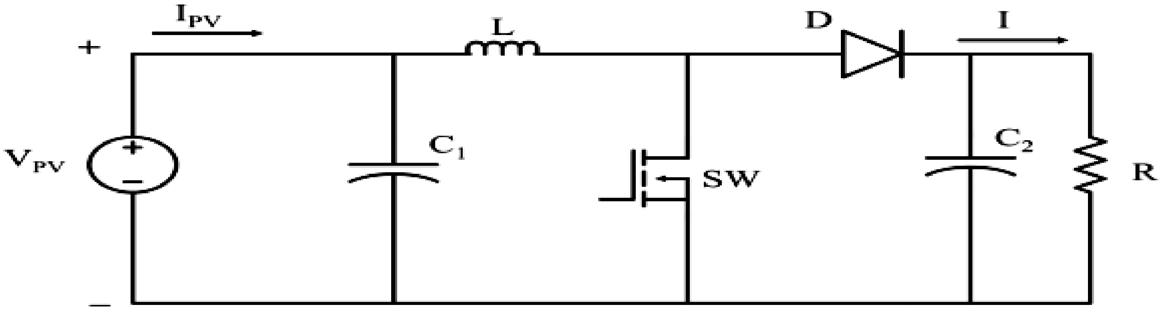

Fig.5.12: Circuit diagram of step-up converter

The four boost converters are designed and tested using MATLAB/SIMULINK.

Where:

V_{PV}= input voltage taken from PV system

$C1$= capacitor connected across the PV input (1.4mF) for all boost converters

The diode connected in series with Resistance (Ron) = 0.001Ω and forward voltage Vf = 0.8V

L = Inductor connected in series (0.012H for 12V converter 0.03H for 36V converter,0.05H for 108V converter,0.09H for 324V converter)

R = Resistance (12Ω) connected in parallel with capacitance $C2$ (1.43mF)

D = Duty ratio

The conversion ratio for the boost converter can be determined by assuming the inductor and capacitor having large value that can be enough to take voltages and currents as DC values. The switch can be replaced by an equivalent voltage source having value (1- D). The complementary duty cycle presents the duration during which the diode conducts can be expressed as D' = (1 - D). During this period it is assumed as an ideal diode, where the intermediate voltage is shorted to VL. The intermediate voltage is shorted to ground during on this condition of the switch. Hence, the average value is equal to (1 – D) Vout.

Since at DC condition, the inductor is short circuited hence,

V_{in} = (1-D) V_{out}

The above equation shows that the conversion ratio of the boost converter depends on duty cycle assuming constant-frequency operation. A boost converter can operate with both constant on-time and constant off-time switching. But in both the cases, change in duty cycle results in change in frequency. So here a constant-frequency boost converter is taken.

The duty cycle indicates the duration period for which the diode turns on. It can be expressed as D' = (1 - D). Through this period it is assumed as an ideal diode, where the intermediate voltage is shorted to $Vout$.

5.10.1 Modes of Operation.

In DC-DC boost converters two modes are available and depending on the switch (higher frequency) opening and closing operation these modes are decided. In 1st mode operation the inductor is charged as the switch is closed so this mode is called as charging mode of boost converters. In the 2nd mode the inductor is discharged as the switch is open and is called as discharging mode of boost converters.

5.10.1.1 Mode-1 or Charging Mode Operation.

In 1st mode the switch is closed, hence by using battery inductor is charged and so energy is stored as a result there is exponential rise in inductor current but we are assuming linear inductor current in both the modes (charged and discharged mode). The load current remains constant, supplied by discharging of the capacitor as the diode blocks the current flow during this mode.

5.10.1.2 Mode-2 or Discharging Mode of Operation.

In 2nd mode switch is opened which results in short circuit of diode. So the stored energy stored in 1st mode of inductor is discharged with opposite polarity during this mode and as a result the capacitor is charged. But the load current is at constant value always.

5.10.1.3 Waveforms

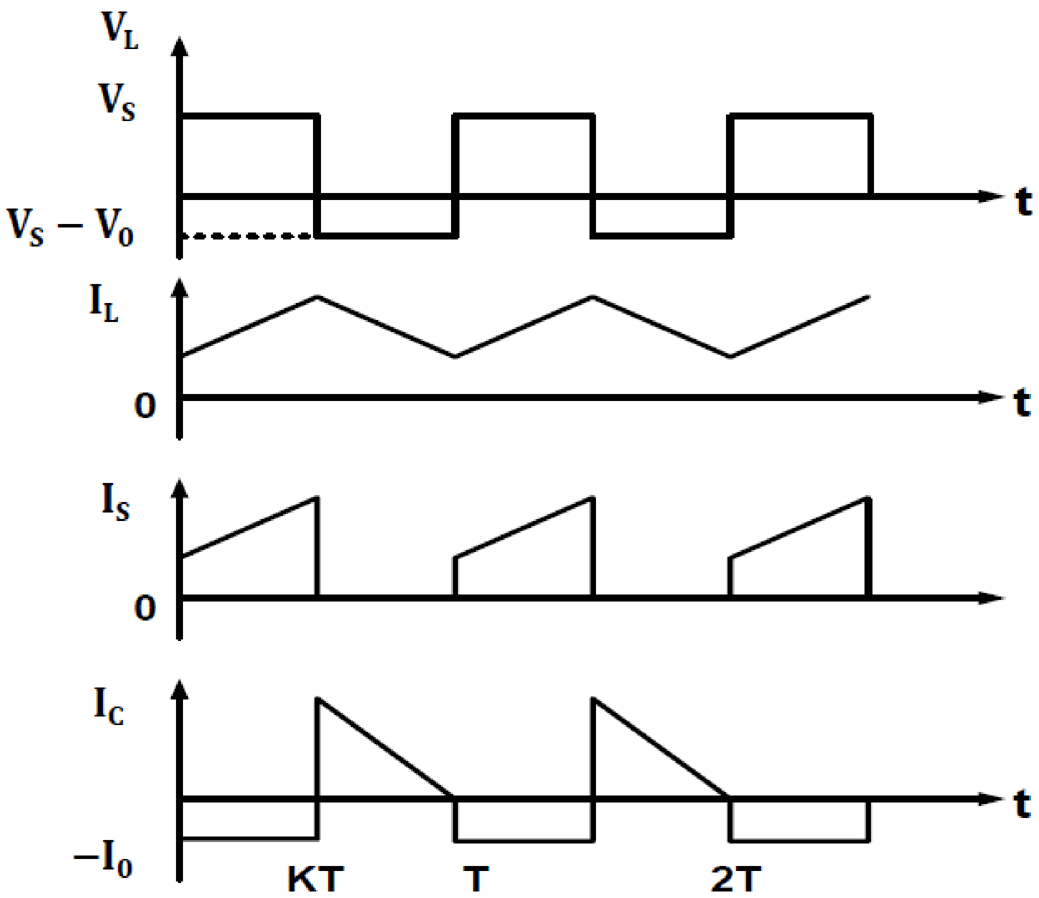

Fig.5.13: Waveforms of boost converter.

In the Fig.5.13 V_L represents the voltage across the inductor, V_S represents the input voltage of boost converter, I_L is the inductor current, Is the source current, and Ic the capacitor current.

When the switch is closed, by using battery inductor is charged and so energy is stored as a result there is exponential rise in inductor current and capacitor current at constant value. Hence, inductor voltage is at value equals to source voltage and supply current also increases. When the switch is opened, the stored energy in inductor is discharged with opposite polarity during this mode and as a result the capacitor is charged. So, the inductor current falls till the switch is closed again in the next half cycle.

5.11 Charge Controller.

The charger uses constant current / constant voltage (CC/CV) charging method, this way is an effective mode to charge lithium batteries. When a lithium battery is nearly empty, we used constant current mode to charge it. This current should be less than the max charging current that battery can accepted.

During constant current charging mode the voltage of battery is slowly increasing, when the voltage of the battery reaches the max charging voltage, charger will start the constant voltage mode and fix the charging voltage with reducing the charging current. When battery is fully charged the charge controller will stop charging and cut off the battery.

Fig.5.14 shows the flowchart of charge controller designed to charge all batteries.

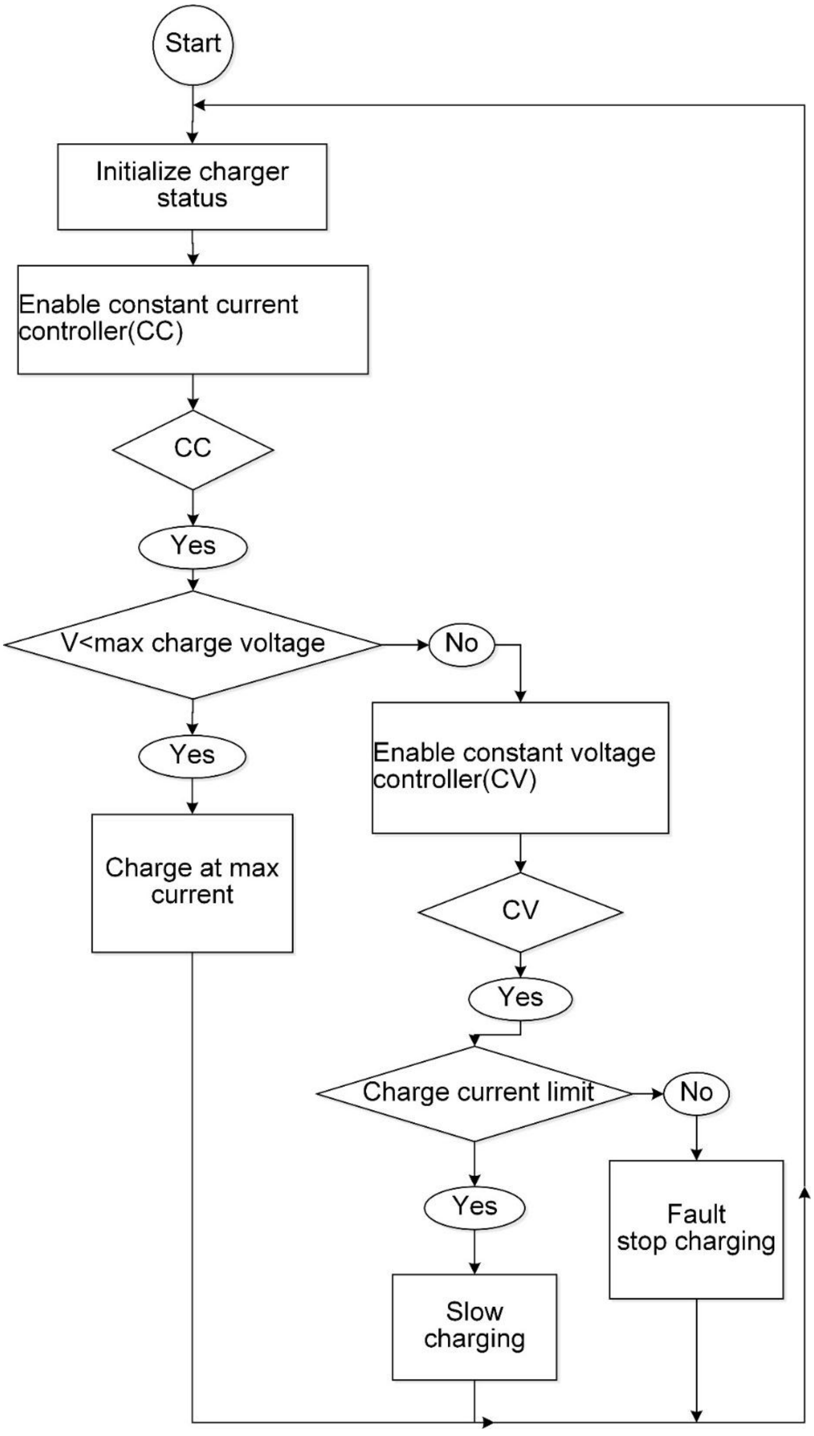

Fig.5.14: Flowchart of charge controller.

Figure 5.14(a) shows the program of charge controller algorithm using embedded MATLAB function.

```
function [Vref,Iref,signal,SD] = CHARGER(V,I,T)
persistent temp_i temp_v temp_signal temp_fault CC CV n ;
if isempty(temp_i)
    temp_i=0.2;
end
if isempty(temp_v)
    temp_v=0;
end
if isempty(temp_signal)
    temp_signal=1;
end
if isempty(temp_fault)
    temp_fault=1;
end
if isempty(CC)
    CC=1;
end
if isempty(CV)
    CV=0;
end
if isempty(n)
    n=0;
end
if (T>n*0.02) % sample time
    n=n+1;
    if CC
        if V<128
            temp_i=0.1;
            temp_v=0;
            temp_signal=1;
        else
            CV=1;
        end
    end
    if CV
        if I>5.0
            temp_i=0;
            temp_v=1;
            temp_signal=2;
        else
            temp_fault=0;
        end
    end
end
signal=temp_signal;
SD=temp_fault;
Iref=temp_i;
Vref=temp_v;
end
```

Fig.5.14 (a): Shows the program of charge controller algorithm.

5.12 Battery Backs.

In solar applications Batteries have to cover the requirements of unstable energy from the grid, heavy cycling during charging and discharging process and sometimes irregular full recharging. There are a many types of batteries suitable for these requirements. Taking into consideration the cost, life cycle, installation and maintenance, Lithium-ion batteries have been implemented in this project.

Lithium-ion batteries

Referring to a U.S. Solar Energy Monitor record, lithium-ion batteries are the extreme popular storage technology, negligent of application. There are three types: pouches such as in smart phones and tablets, cylindrical such as in power tools, and prismatic (which come in various shapes). The prismatic can have implementations in solar energy storage systems, precisely lithium iron phosphate (LFP) batteries.

Cycling: Lithium-ion batteries can typically deliver more cycles in their lifetime than lead-acid. This makes them a good choice for applications when batteries are cycled to provide ancillary services to the grid. The most important benefit lithium-ion provides for solar is its high charge and discharge efficiencies, which help harvest more energy. Lithium-ion batteries also lose less capacity when idle, which is useful in solar installations where energy is only used occasionally.

Maintenance/ Replacement: The main advantages of Lithium-ion batteries over lead-acid batteries are lighter and more self-contained, so may be easier to install and replaced. They can be wall-mounted and located indoors or outdoors. They are solid, so don’t require refills or maintenance.

To satisfy the rated voltages and ampere hour capacities (Ah) of needed batteries a combination of 100Ah/12V Lithium-ion batteries have been implemented and used.

Table (5.1) demonstrate the per phase combinations of battery packs, where the ampere hour capacity(Ah) calculated according to 18 hours working time without sun at rated discharging current. Equation 5.4

$$C_{ah}= \quad E_{out}/ (\eta_{ah}*DOD*VB) \qquad (5.4)$$

Where:

E_{out} is the output energy required per day, η_{ah} the ampere hour efficiency of the battery, DOD the depth of discharge of the battery and VB the rated battery voltage.

Table (5.1) Per phase combinations of battery packs.

Table(5.1)	Shunt Filter			Series Filter		
	Combination	Ah Capacity	Rated Voltage(V)	Combination	Ah Capacity	Rated Voltage(V)
AUX.1	3 in series*4 in parallel	400	36	1 in series*1 in parallel	100	12
AUX.2	9 in series*4 in parallel	400	108	1 in series*3 in parallel	100	36
MAIN	27inseries*7 in parallel	700	324	4 in series*4 in parallel	175	108

For 36 V system $C_{ah}= \quad 10000Wh/ (0.9*0.8*36) =400$ Ah needed

So if we use 100Ah/12V Lithium-ion battery we need 3 in series and 4 in parallel to achieve the requirements.

5.13 Combinations of PV Module Used for Designing Photovoltaic Arrays Sources.

The photovoltaic array fed the bottom inverter of both series and shunt active filters had the highest power ratio and will be called the main photovoltaic source. The rest of arrays will be the auxiliary sources (Aux1, 2).

The main source delivers most of the power (80%) [7], [8] but works at the lowest switching frequency, Where the AUX.2 deliver 15% and AUX.1 deliver the lowest power 5% but works at the highest switching frequency.

The switching frequency of the main source is nearly equal to the input reference voltage signal (50 Hz), where the switching frequency for AUX.2 around 150 Hz.

And for Aux.1 the switching frequency is around 550 Hz which is relatively small, which is an additional advantage of this topology.

Fig.4 shows the I-V, P-V characteristic curves for the 125W poly crystalline PV module (Mitsubishi Electric PV-EE125MF5F) have been used to design all photovoltaic arrays.

The maximum power point occurs at module voltage (17.3 V) and module current (7.23 A),this give a Fill Factor equals to 72.6 % ,and it have an efficiency higher than 14%,on the other hand this module behaves good at high temperatures.

Table (5.2) demonstrates the combinations of PV module for designing photovoltaic arrays sources.

Table (5.2): Combinations of PV module for designing photovoltaic arrays sources.

Table5.2	Shunt Filter			Series Filter		
	Combination	Power(w)	Percent (%)	Combination	Power(w)	Percent (%)
AUX.1	1 in series*4 in parallel	500	5%	1 in series*1 in parallel	125	5%
AUX.2	3 in series*4 in parallel	1500	15%	1 in series*3 in parallel	375	15%
MAIN	11 in series*6 in parallel	8000	80%	4 in series*4 in parallel	2000	80%
Total(W)	10kVA			2.5kVA		

The total number of 125W PV modules used in this project is 102 modules, and its equivalent to 12.5 kVA solar system.

5.14 Results and Work.

Simulation Results for Photovoltaic System Alone.

The photovoltaic system with maximum power point tracker (MPPT) and battery charger have been simulated and the performance of the system is analyzed independently.

Figure 5.15 below shows the simulated part

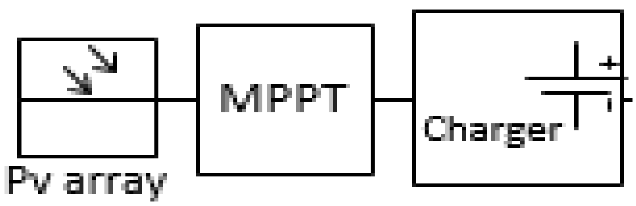

Fig.5.15: Photovoltaic DC source.

According to the required voltage levels at the input side of multilevel converters in both series and shunt filter, we used (36V, 108V, 324V) for each phase of shunt active filter and (12V, 36V, 108V) for active series filter. So we need to design four different voltage levels which were (12V, 36V, 108V, 324V) to satisfy the system requirements.

The simulation results taken and tested for 1s simulation time, which is equivalent to one real day.

For each phase of shunt and series active filter a three independent dc input sources required, these sources scaled in the power of three.

For shunt active filter 36,108,324 Volts have been used as input dc sources for inverter legs (AUX.1, AUX.2 and MAIN) respectively .whereas 12, 36, 108 Volts used in series filters same as the above arrangement.

Figure 5.15(a) shows the MATLAB SIMULINK of photovoltaic system part.

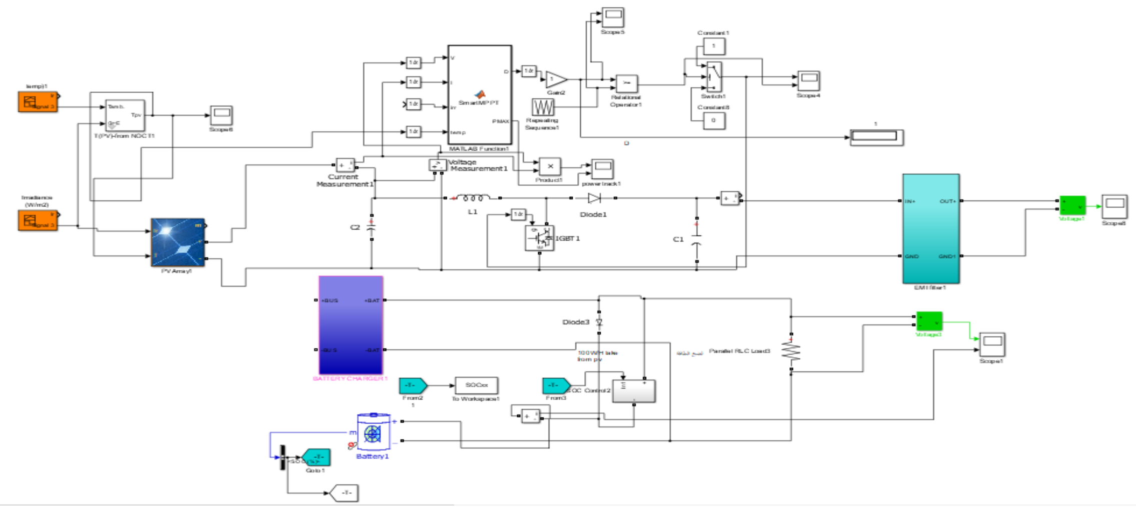

Fig.5.15 (a): Shows the MATLAB SIMULINK of photovoltaic system.

5.14.1 12V System.

The 12V battery pack used in series APF only. As shown in figure 5.16 (a) the maximum power point tracker(MPPT) start working at t=0.2 S, it founds the maximum power point under real daily ambient temperature and solar irradiance curve, also it keeps the output voltage constant by using DC-DC boost converter.

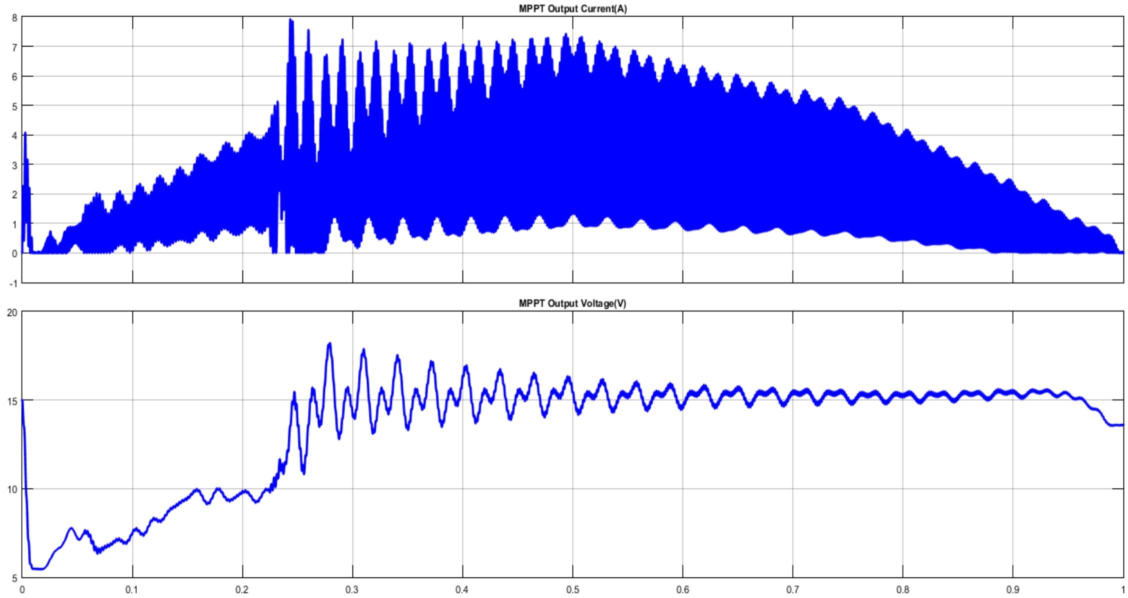

Fig.5.16 (a): MPPT output current and voltage.

The input of dc to dc boost converter shown in Fig.5.16 (b), where the voltage and current changed according to the temperature and solar irradiance respectively.

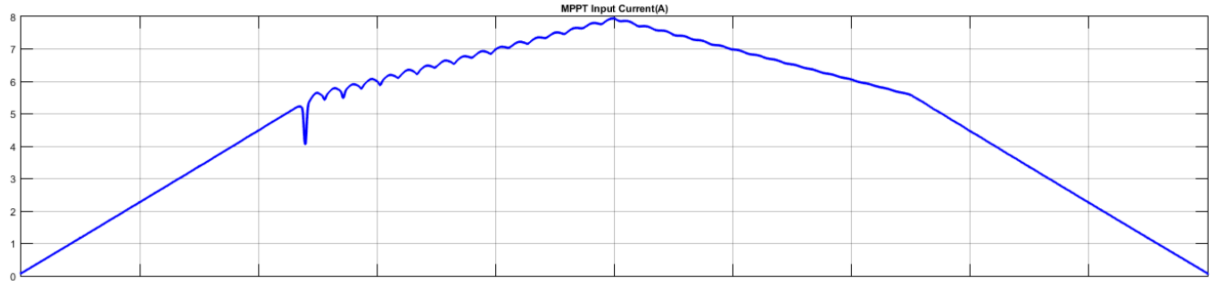

Fig.5.16 (b): MPPT input current.

Fig.5.16 (c) proves the battery was fully charged at t=0.86 S from state of charge (SOC) indicator, so we have a good margin to take into account cloudy days.

The irradiance and temperature daily curves are also shown in figure below, these curves were used as input information to Perturb and Observe method (P&O) to calculate the maximum instantaneous power available from PV modules.

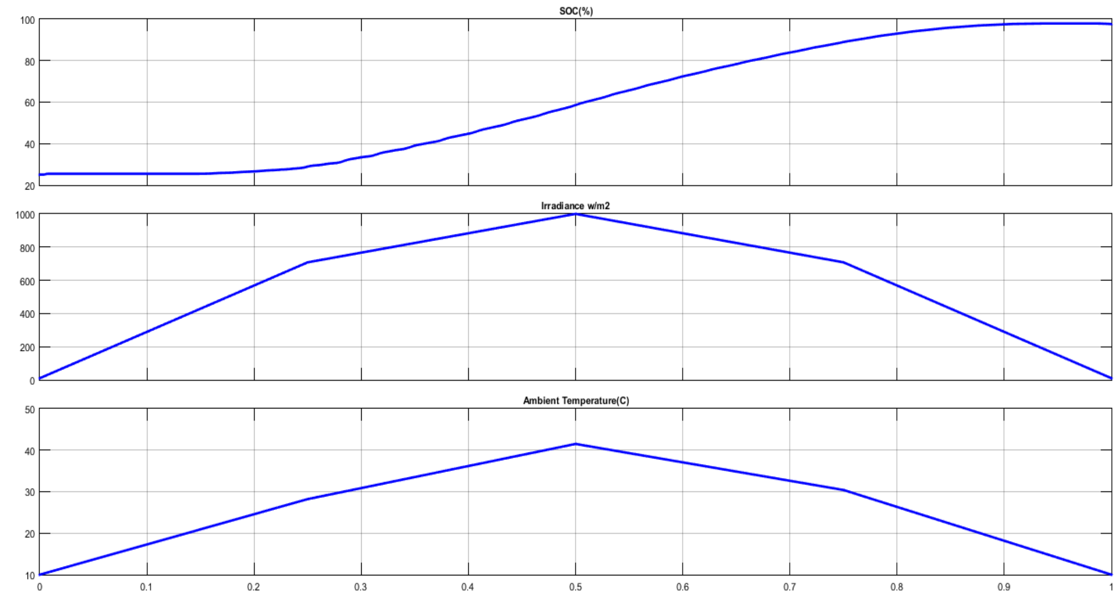

Fig.5.16 (c): SOC status during standard sunny day.

The most sensitive step in photovoltaic source is the output of battery charger, the main task of battery charger is to charge and protect the battery from over charged and deep discharged, Fig.5.16 (d) shows the output voltage and current of battery charger for 12 V battery pack.

It's clear that the charger maintains constant voltage (14.2V) and charge with current curve similar to irradiance curve.

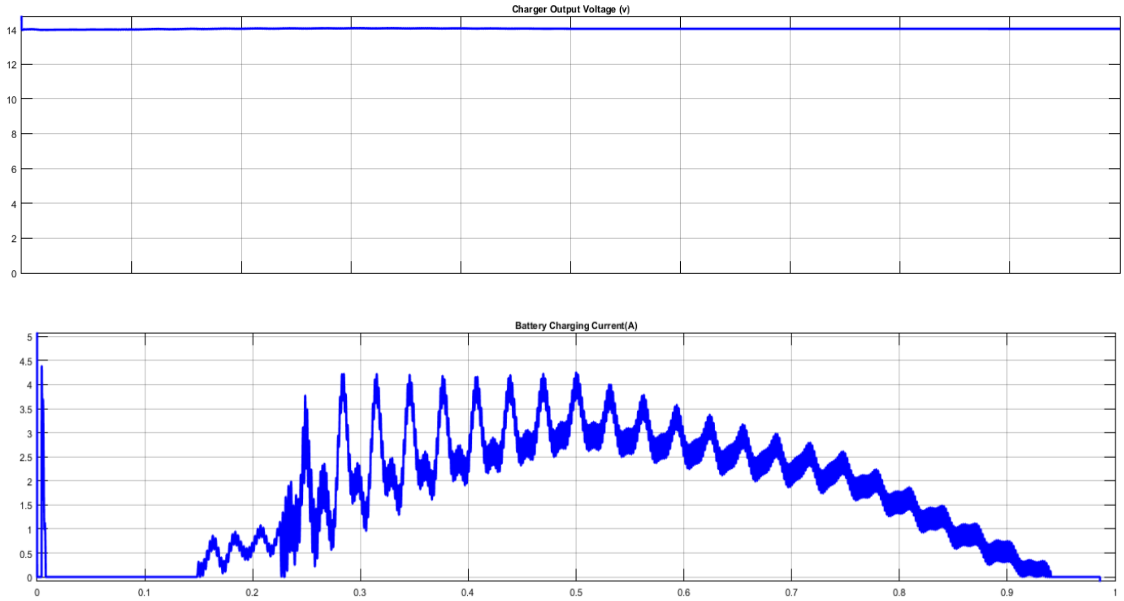

Fig.5.16 (d): Battery charging current and voltage.

5.14.2 36 V system

The 36 V battery pack used in both shunt and series APF. As shown in figure 5.17 (a) the output of maximum power point tracker (MPPT) start working at t=0.2 S, it found the maximum power point under real daily temperature and solar irradiance curve.

To maintain constant output voltage the MPPT will change the pulse width according to ambient temperature and solar irradiance measured by the system.

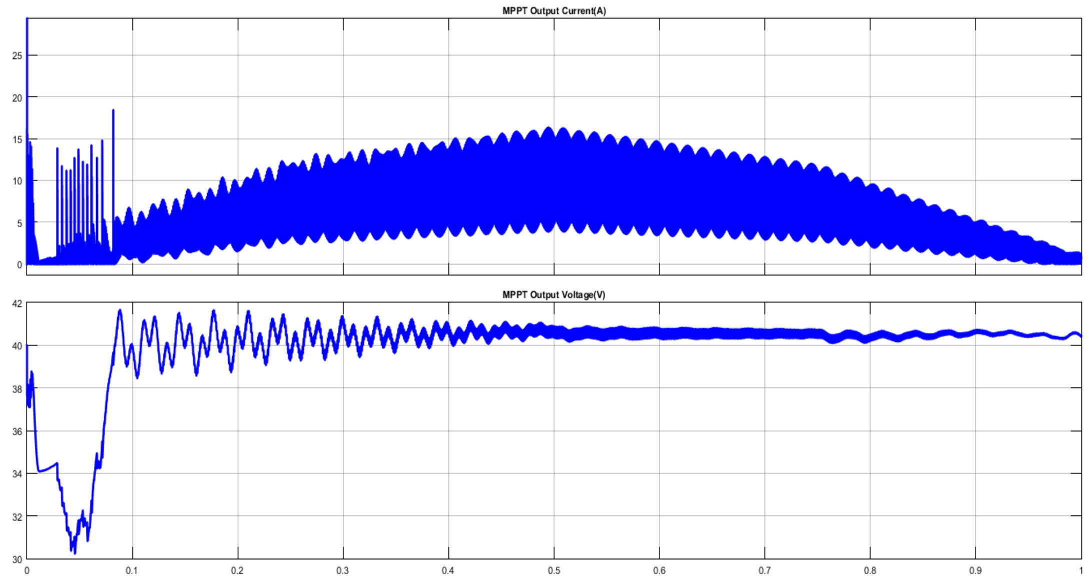

Fig. 5.17 (a): MPPT output voltage and current.

The input of dc to dc boost converter shown in Fig.5.17 (b), where the voltage and current changed according to the ambient temperature and solar irradiance respectively.

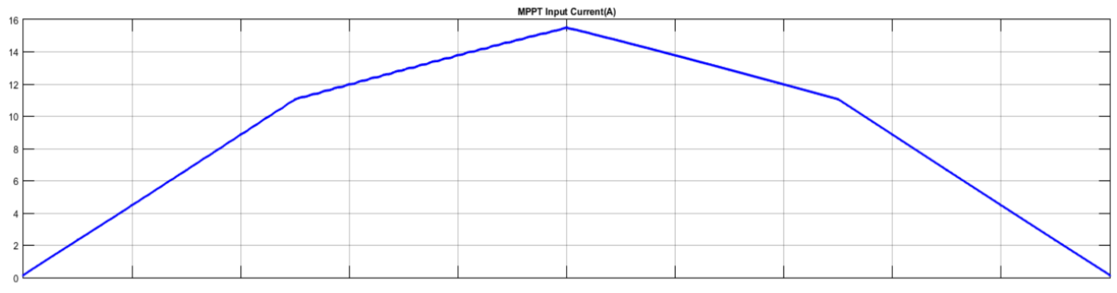

Fig. 5.17 (b): MPPT input current.

Fig.5.17 (c) shows the battery was fully charged at t=0.84 S from state of charge (SOC) indicator, so we have a good margin to take into account cloudy days.

The irradiance and temperature daily curves are also shown in Fig.5.17 (c) below, these curves were used as input information to Perturb and Observe method (P&O) to calculate the maximum instantaneous power available from PV modules, and then generate a signal to dc-dc boost converter to maintain constant output voltage.

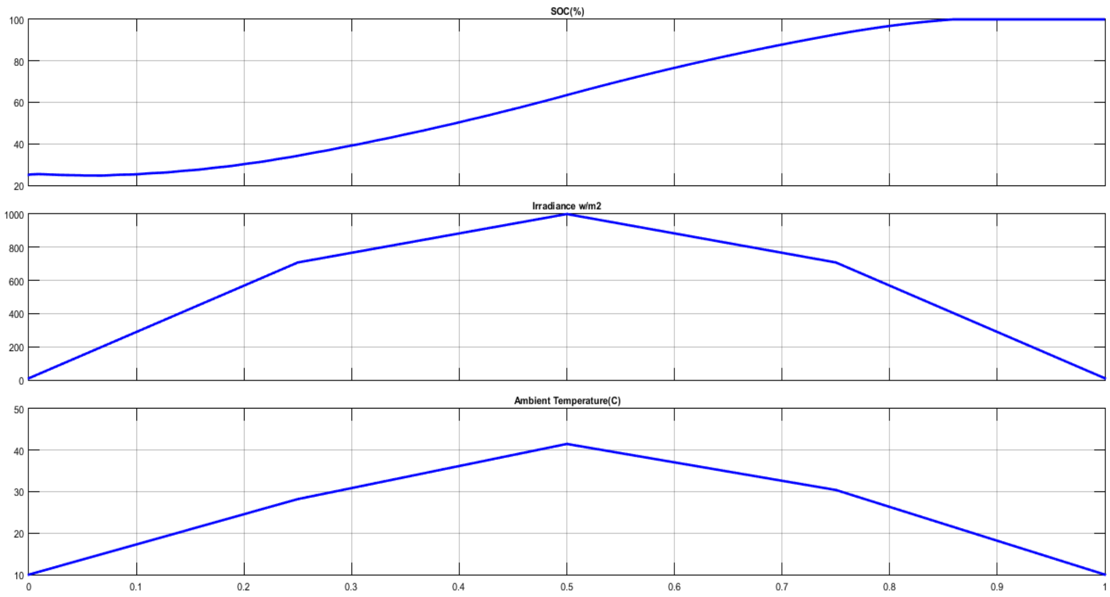

Fig. 5.17 (c): SOC status during standard sunny day.

The most important step in photovoltaic source is the output of battery charger, the main task of battery charger is to charge and protect the battery from over charged and deep discharged, Fig.5.17 (d) shows the output voltage and current of battery charger for 36 V battery pack.

It's clear that the charger maintains constant voltage (41.8 V) and charge with a current curve similar to irradiance curve.

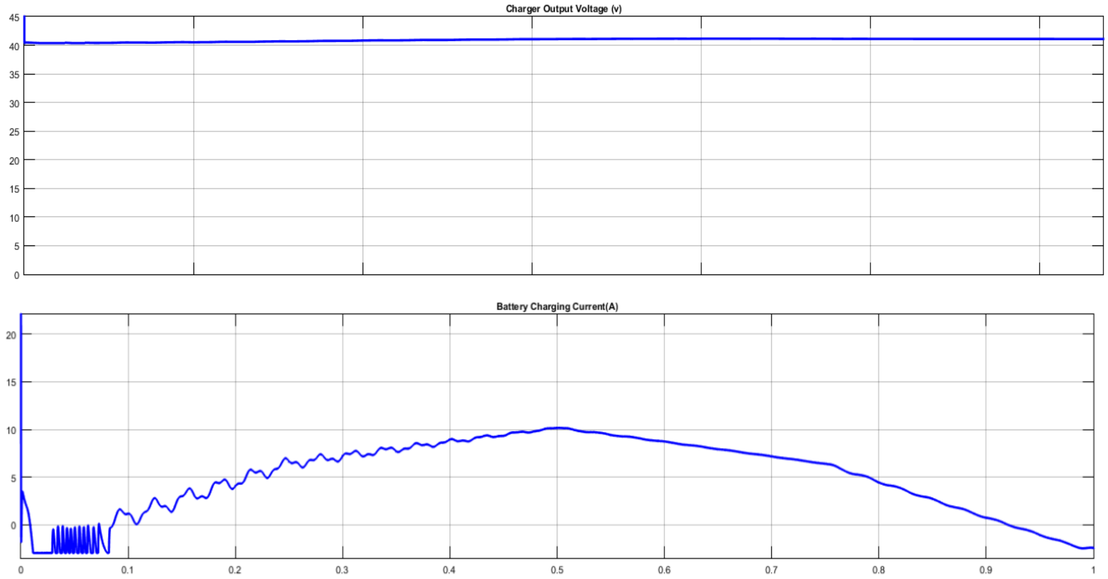

Fig. 5.17 (d): Charger output voltage and current.

5.14.3 108 V System.

The 108V battery pack used in both shunt and series APF. As shown in figure 5.18(a) the output of maximum power point tracker (MPPT) start working at t=0.1S, it found the maximum power point under real daily temperature and solar irradiance curve.

To maintain constant output voltage the MPPT will change the pulse width according to ambient temperature and solar irradiance measured by the system.

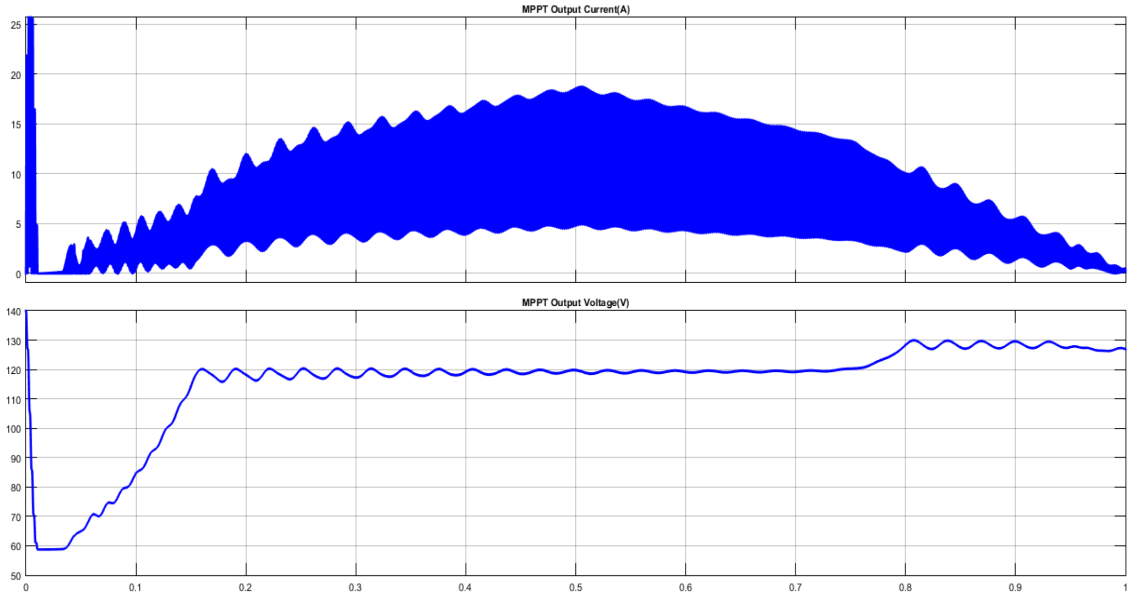

Fig. 5.18 (a): MPPT output current and voltage**.**

The input of dc to dc boost converter shown in Fig.5.18 (b), where the voltage and current changed according to the ambient temperature and solar irradiance respectively.

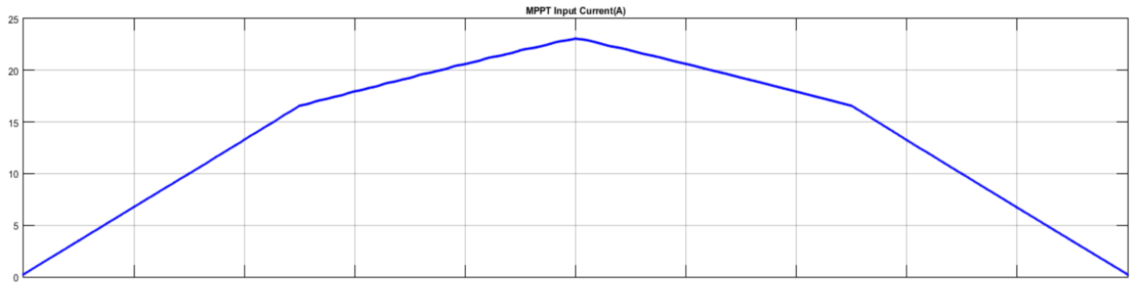

Fig. 5.18 (b): MPPT input current.

Fig.5.18 (c) shows the battery was fully charged at t=0.78 S from state of charge (SOC) indicator, so we have a good margin to take into account cloudy days.

The irradiance and temperature daily curves are also shown in Fig.5.18 (c) below, these curves were used as input information to Perturb and Observe method (P&O) to calculate the maximum instantaneous power available from PV modules, then generate a signal to dc-dc boost converter to maintain constant output voltage.

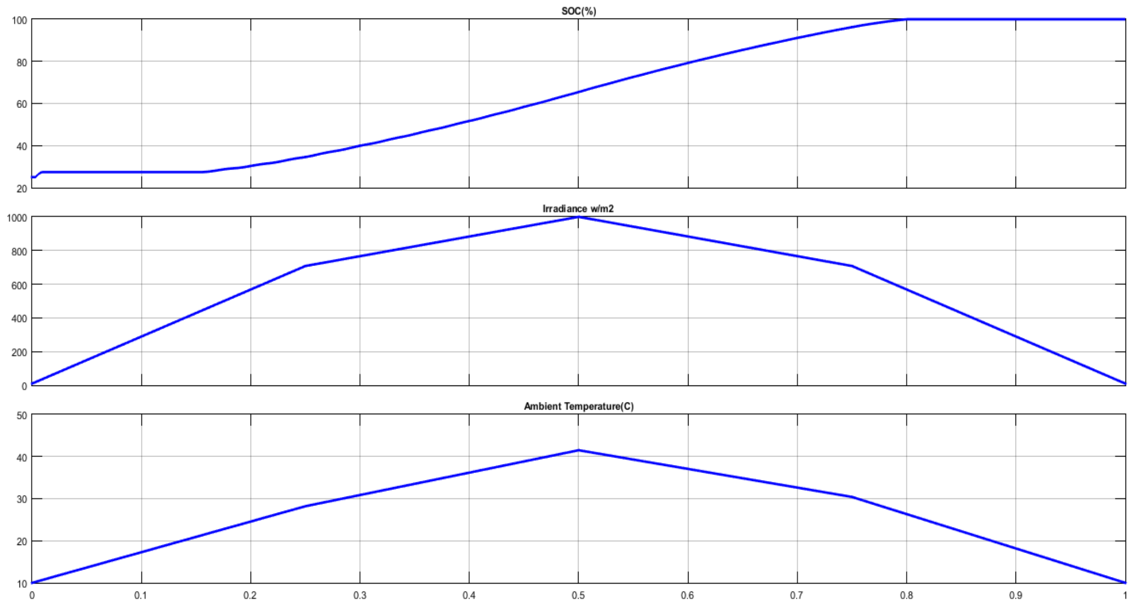

Fig. 5.18 (c): SOC status during standard sunny day.

The most important step in photovoltaic source is the output of battery charger, the main task of battery charger is to charge and protect the battery from over charged and deep discharged, Fig.5.18 (d) shows the output voltage and current of battery charger for 108V battery pack.

It's clear that the charger maintain constant voltage (129V) and charge with a current curve similar to irradiance curve.

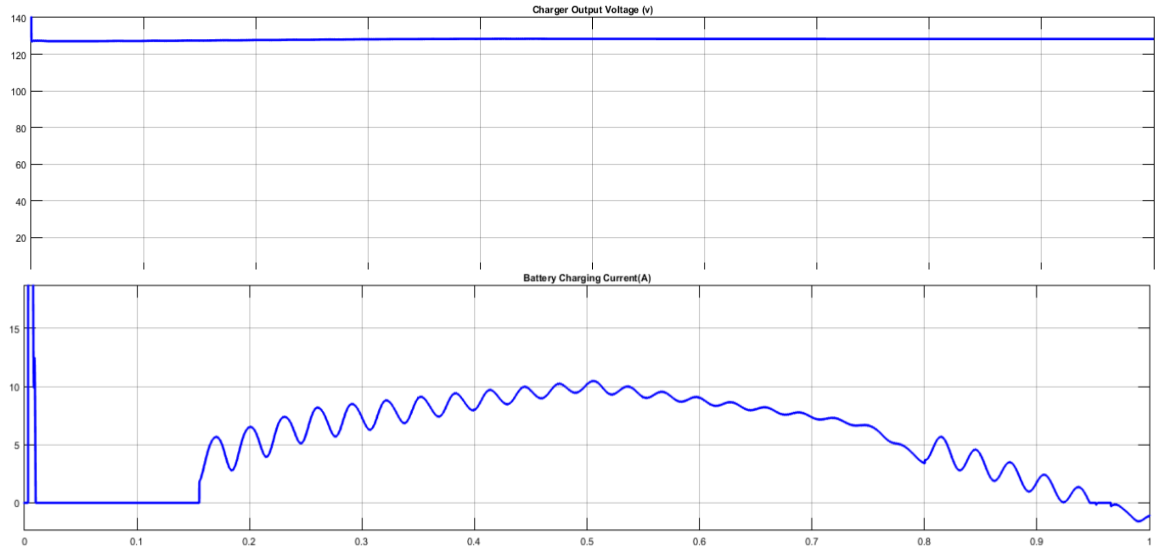

Fig. 5.18 (d): Charger output voltage and current.

5.14.4. 324 V System.

The 324V battery pack used in both shunt and series APF. As shown in figure 5.19(a) the output of maximum power point tracker (MPPT) start working at t=0.1 S, it found the maximum power point under real daily temperature and solar irradiance curve.

To maintain constant output voltage the MPPT will change the pulse width according to ambient temperature and solar irradiance measured by the system.

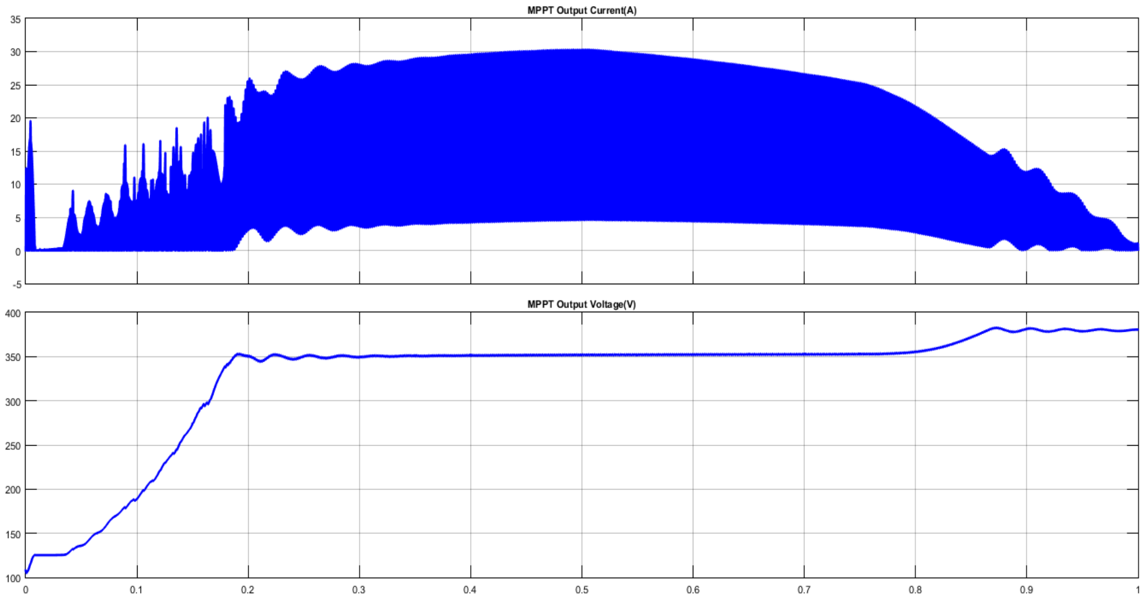

Fig. 5.19 (a): MPPT output current and voltage.

The input of dc to dc boost converter shown in Fig.5.19 (b), where the voltage and current changed according to the ambient temperature and solar irradiance respectively.

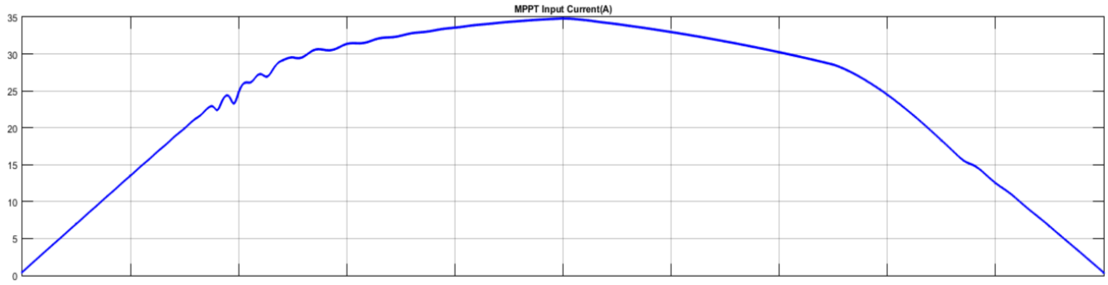

Fig. 5.19 (b): MPPT input current.

Fig.5.19 (c) shows the battery was fully charged at t=0.85 S from state of charge (SOC) indicator, so we have a good margin to take into account cloudy days.

The irradiance and temperature daily curves are also shown in Fig.5.19 (c) below, these curves were used as input information to Perturb and Observe method (P&O) to calculate the maximum instantaneous power available from PV modules, and then generate a signal to dc-dc boost converter to maintain constant output voltage.

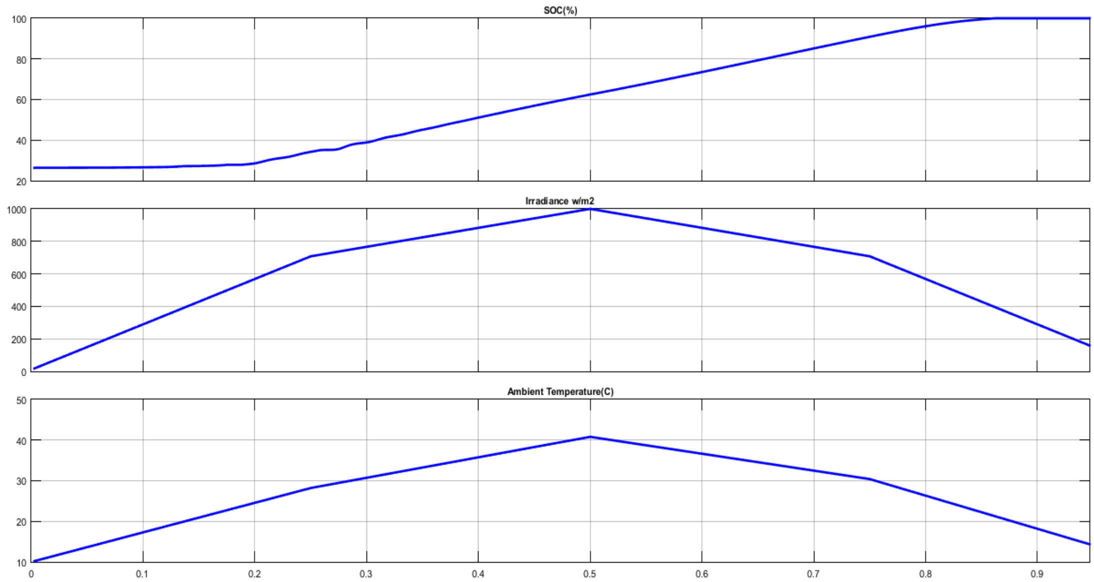

Fig. 5.19 (c): SOC status during standard sunny day.

The most important step in photovoltaic source is the output of battery charger, the main task of battery charger is to charge and protect the battery from over charged and deep discharged, Fig.5.19 (d) shows the output voltage and current of battery charger for 324V battery pack.

It’s clear that the charger maintains constant voltage (388 V) and charge with a current curve similar to irradiance curve.

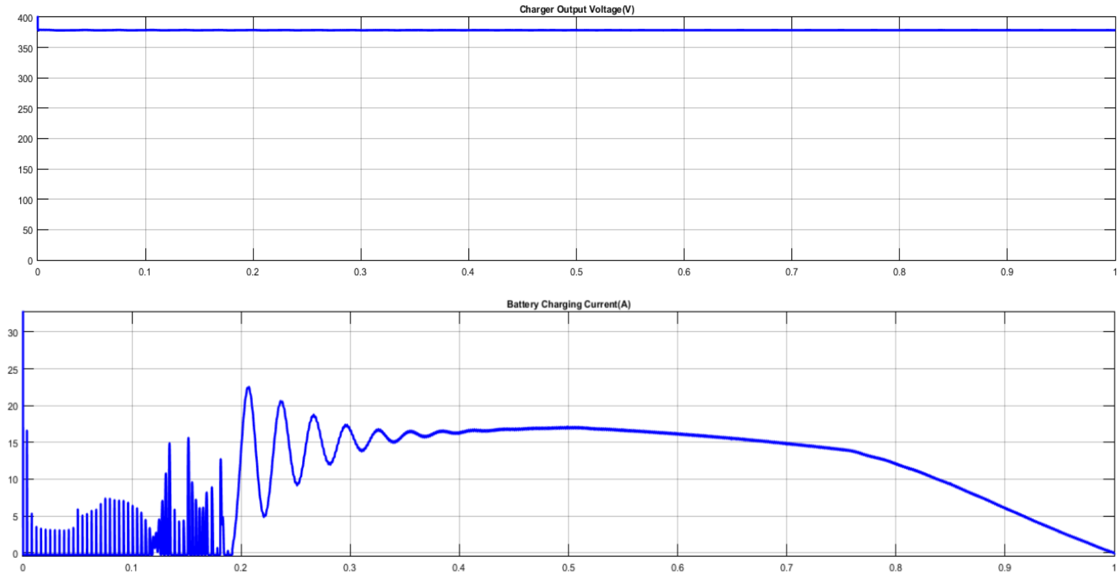

Fig. 5.19 (d): Charger output voltage and current.

5.15 Chapter Summary

This chapter described generation of PV cells and their connections.

This chapter described generation of PV cells and their connections. It also represented the modeling of PV cell and effect of solar irradiations and temperature on it and described the grid connected PV system with MPPT, P & O algorithm and DC-DC boost converter along with its modes of operation and waveforms.

The MATLAB SIMULINK results for boost converter with maximum power point tracker tested and analyzed.

Chapter Six

Simulation Results and Discussions

6.1 Introduction.

The proposed system is simulated in MATLAB SIMULINK environment to check the performance and the correct working of complete system. The simulation of hybrid active power filter (HAPF) tested to insure correct working of all system parts composed together.

Also the Injection of reactive power by inserting capacitor banks during empty batteries included in the results.

On the other hand, the performance of the system at each stage is discussed in details in the following section.

6.2 System Components.

As shown in Fig. 6.1 the main components of the three-stage Hybrid Active Power Filter (HAPF) that has been used in this work. The figure only shown one of the three phases of the complete system. The (APF) used 27-level asymmetrical inverters. Each phase of these inverters was composed of three ‘H’ bridges, supplied by three independent photovoltaic arrays Scaled in the power of three, delivering 12.5KW to each phase, 10kva for shunt active filter and 2.5KW for series active filter.

The outputs of inverters connected directly through a transmission line. In addition to the capability of harmonic elimination of both current and voltage drawn from the source, the combined system can produce real and reactive power to feed the loads during prolonged voltage outages or source shortage.

A battery pack used as dc link, which was charged from photovoltaic array connected to the battery through a maximum power point tracker and charge controller.

The injection of real and reactive power depends on the state of charge (SOC) of batteries, the frequency of the system, real and reactive power of the load, and power factor at the point of common coupling (PCC).

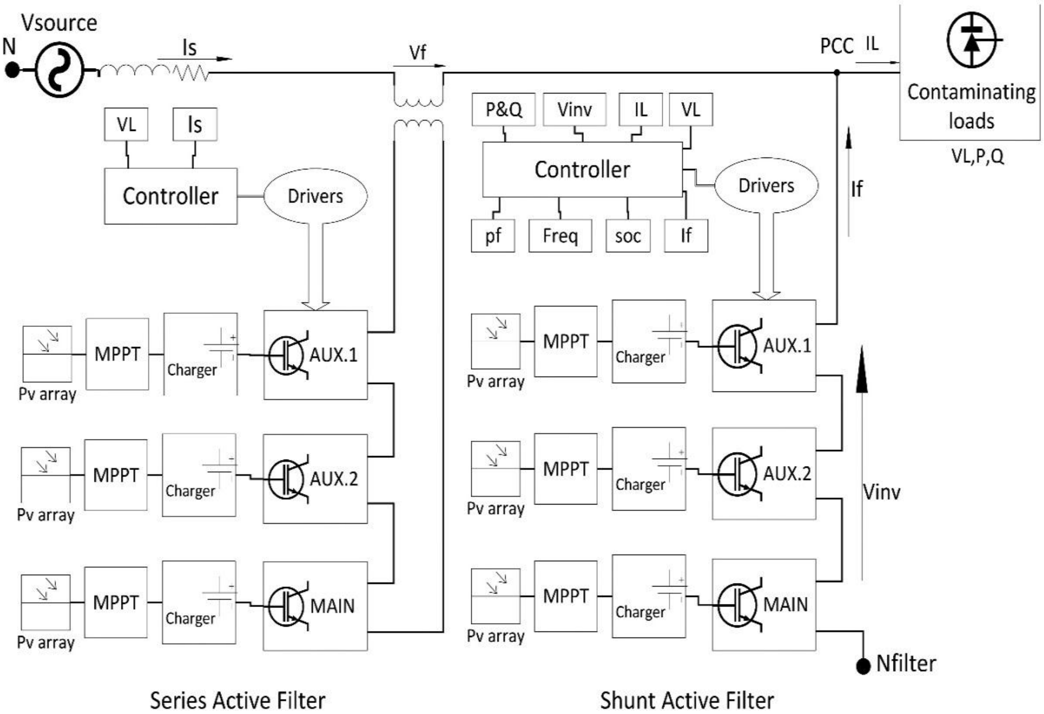

Fig.6.(a): Main components of complete system**.**

6.3 Simulation Results for Active Power Filter (APF).

The photovoltaic system fed the H-bridges of multilevel converters for shunt and series active APF. Also the total system controlled under precise and smart control system to get the needed results.

In this section, the behavior of the complete system included the photovoltaic part, shunt APF and series APF seen and discussed and tested as seen in Fig.6 (b).

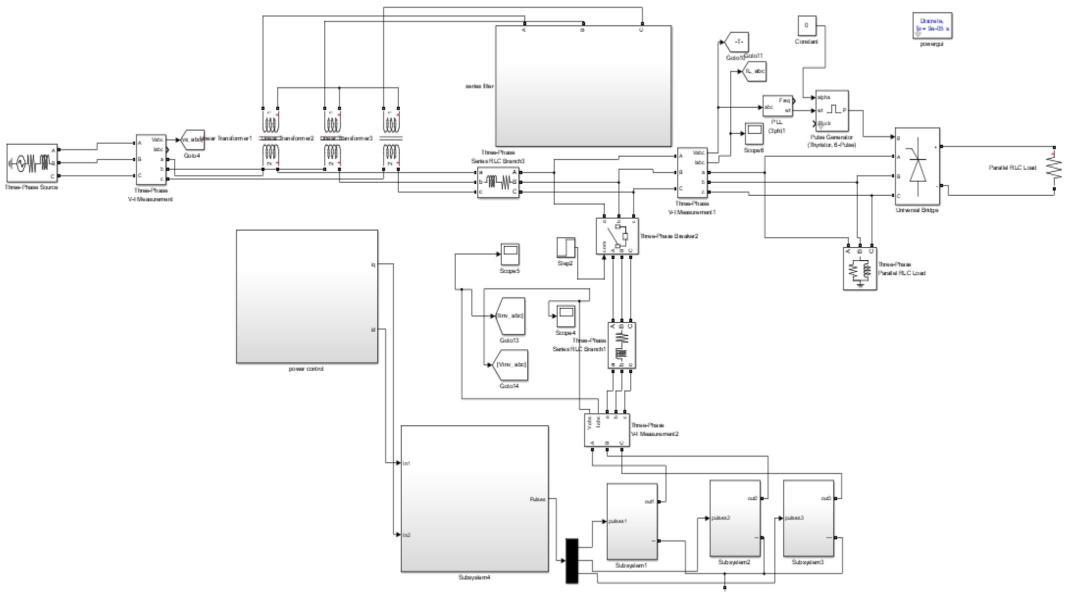

Fig.6 (b): Complete proposed system using MATLAB SIMULINK.

6.3.1 Photovoltaic DC Source.

In this part 36V photovoltaic system have been taken as a sample to check the correct working of photovoltaic source part and its effect on the complete system.

As shown in figure (6.1), the charger maintains constant voltage under variable irradiance-temperature curves.

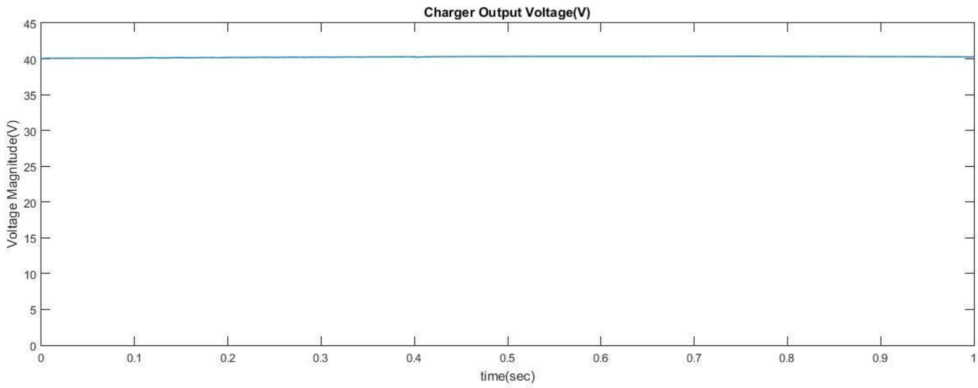

Fig.6.1: Battery charger output voltage.

As clear from Fig.6.2 the charging current curve toke the shape of irradiance curve to charge the battery and inject the excess power to the electrical network.

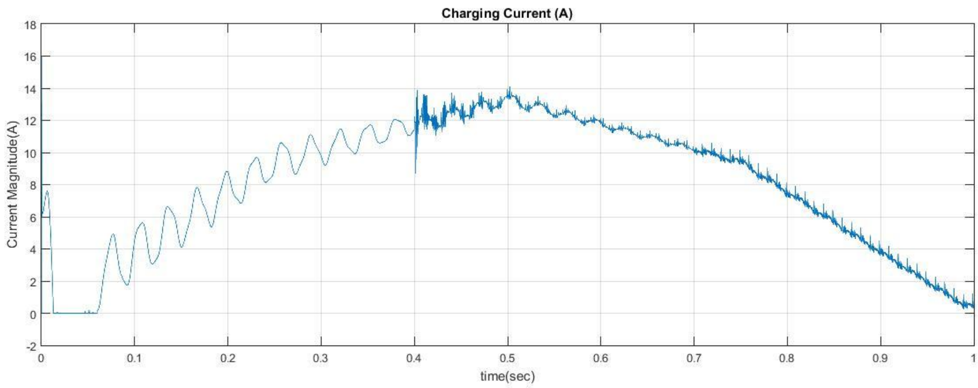

Fig.6.2: Battery charging current.

The main stability point of the photovoltaic system, was for getting a fully battery before the end of the sunny day. As seen from Fig.6.3 we got a fully battery at 0.82 S and its equivalent to real time 3:50 pm, which was a good indicator of stability.

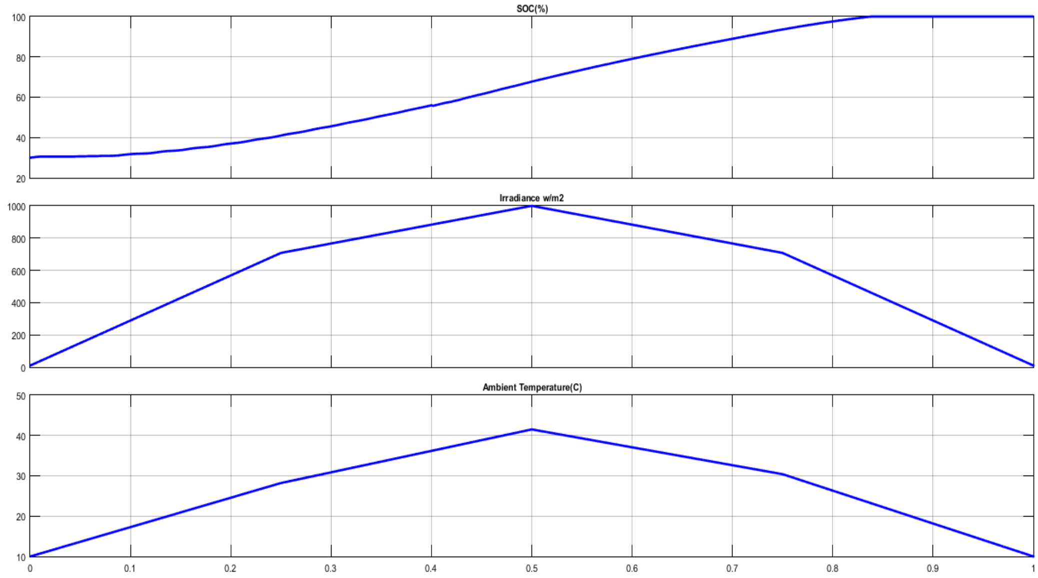

Fig.6.3: SOC, irradiance and temperature daily curves.

It's clear from the above results that the photovoltaic dc source worked perfectly with complete system and we did not have any mismatch between system parts.

6.3.2 Current Compensation.

As shown in Fig.6.4 (a) at t=0.4 S the active power filter starts working to mitigate the harmonic and the source current became pure sinusoidal.

The total harmonic distortion (THD) reduced from 18% to 0.4% as clear in Fig.6.5.

The active power injection starts at t=0.7 S with 6 A current assistant as seen in Fig.6.4 (b), and the total harmonic distortion remained very low (0.5%) during active power injection.

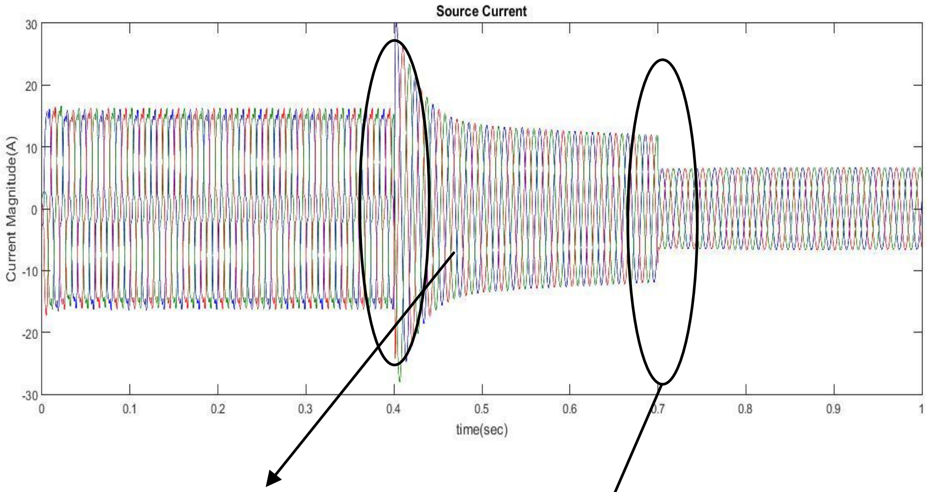

Fig.6.4: Current compensation

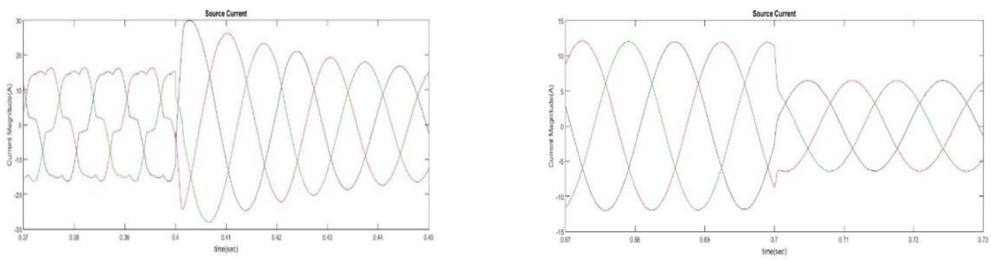

Fig.6.4 (a): Zoom for current compensation

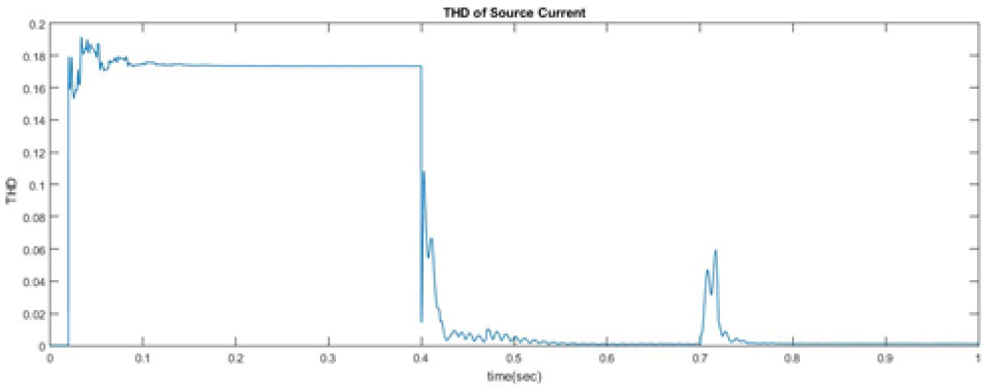

Fig.6.5: THD of Source Current**.**

It's clear from the simulation results, the behavior of Shunt APF improved and the capability of harmonic mitigation became ideal because the positive effect of series APF.

6.3.3 Voltage Compensation.

The three phase source voltage signal is shown below, where Fig.6.6 (a) proves the correct functioning of harmonic mitigation (at t=0.4 S). The variation in total harmonic distortion (THD) of source voltage shown in Fig.6.7.

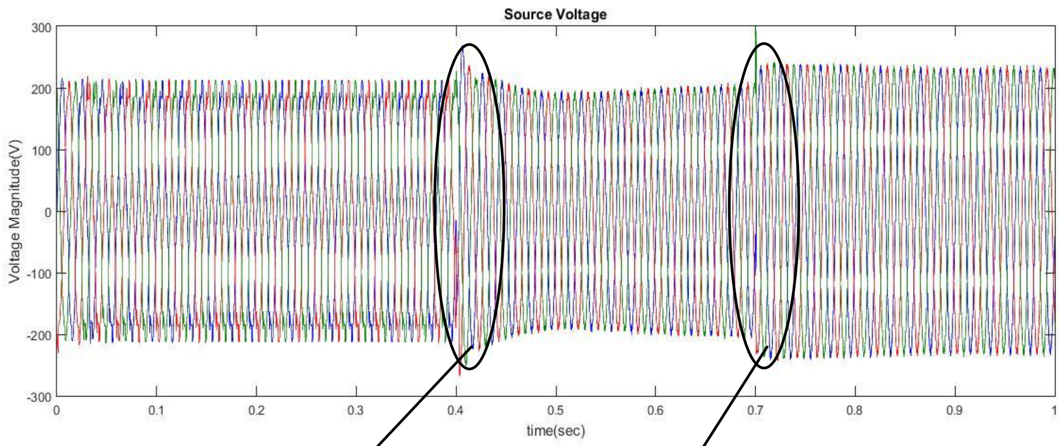

Fig.6.6: Voltage compensation

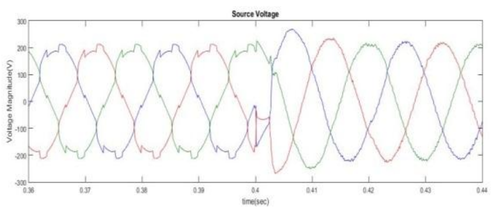

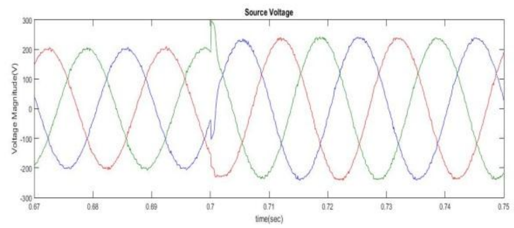

Fig.6.6 (a): Zoom for voltage compensation**.**

At t=0.7 S the system step up the source voltage to 230V and made the electrical network ideal with total harmonic distortion 1% in source voltage.

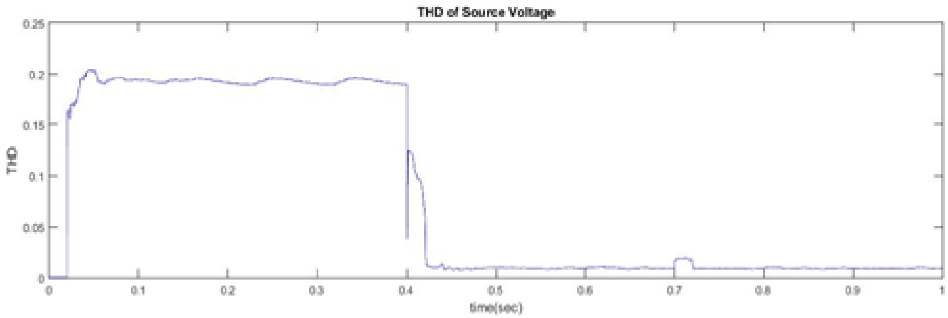

Fig.6.7: THD of source voltage.

It’s clear from the above results, the behavior of Series APF became better and the capability of harmonic mitigation and voltage compensation became ideal because the positive effect of shunt APF.

6.3.4 Power Factor Correction.

Figure below proves the capability of shunt active power filter (SAPF) for keeping a unity power factor at the point of common coupling (PCC).

It’s clear from Fig.6.8 (a) and 6.8 (b) that the power factor improved from low value to unity.

By injecting the required reactive power to the distribution network and tracking the reactive power of the load to generate the needed reference vector signal.

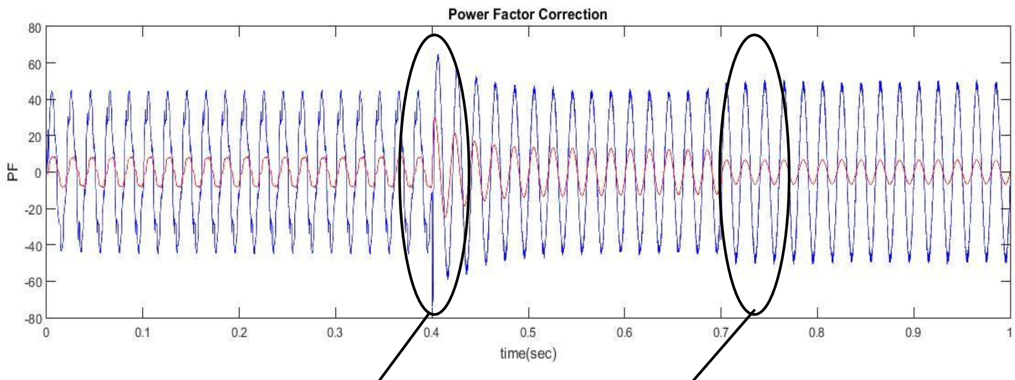

Fig.6.8: Power factor correction

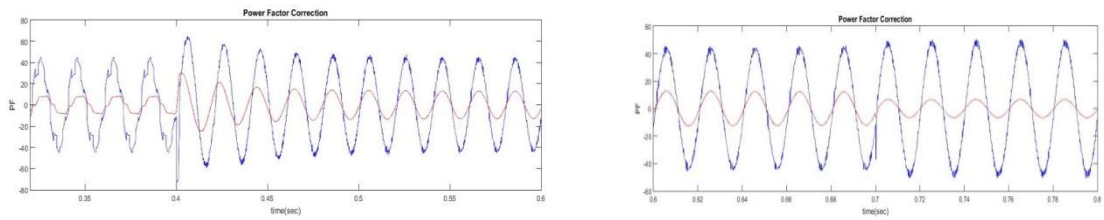

Fig.6.8 (a): Zoom for power factor correction

The power factor correction task did not effect, because the reactive power injection only controlled and injected from shunt APF.

6.3.5 Real Power Injection.

The active power (P) controlled by adjusting the value of id-ref current, where id-ref current depends on the SOC of all battery packs and the frequency of the system.

The injection of reactive power (Q) depends on the tuning of iq-ref current, where iq-ref set to maintain a unity power factor.

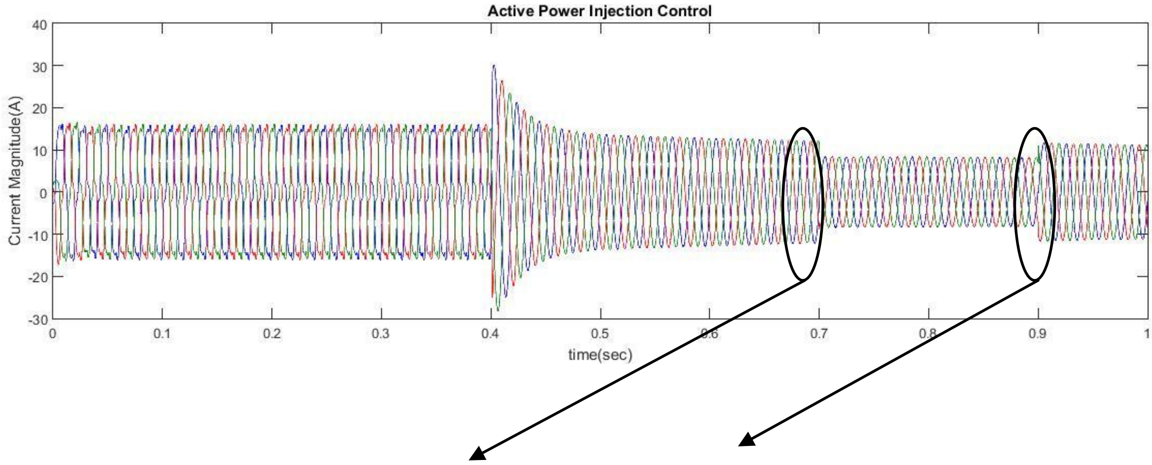

Fig.6.9: Real power injection

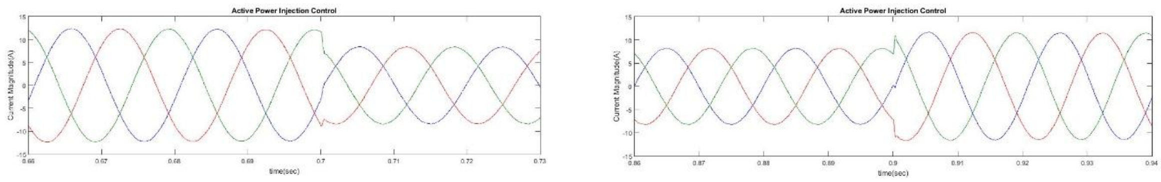

Fig.6.9 (a): Real power injection

Fig.6.9 (a) shows the changing in source current when the system start active power injection at t=0.7 S.

Fig.6.9 (b) shows that the injection of real power stopped working at t=0.9S due to one of abnormal reasons have been mentioned in chapter 3.

The active power injection task did not effect, because the active power injection only controlled and injected from shunt APF.

6.3.6 Capacitor Banks.

In case of empty batteries, the capacitor banks automatically inserted to the dc link and inject reactive power to the system.

As shown in Fig.6.10 the capacitor banks entered the system at t=0.2 S and worked as reactive power source.

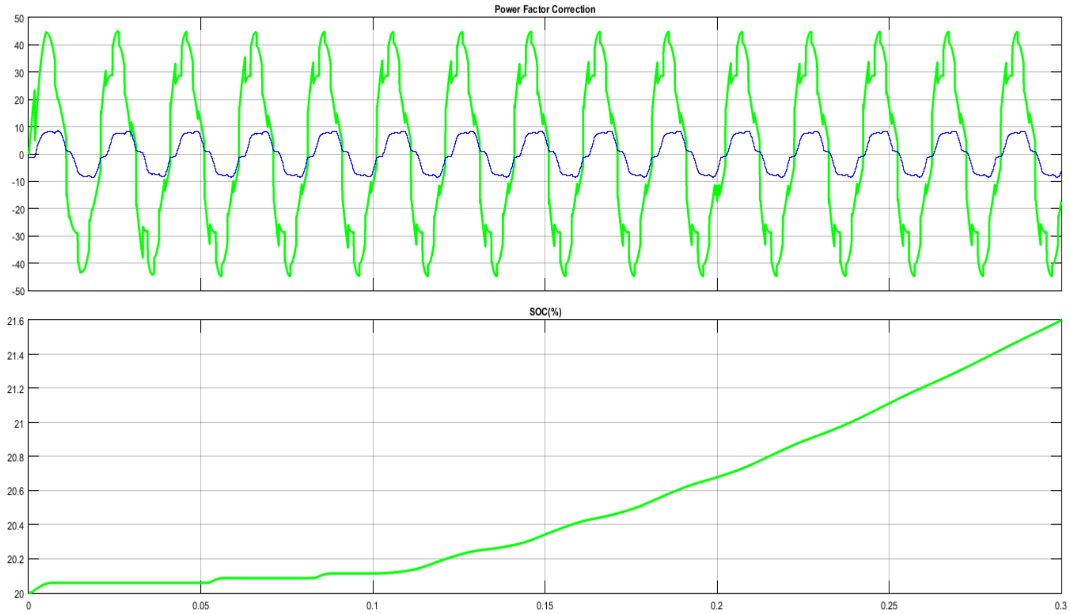

Fig.6.10: Reactive power compensation using capacitors.

The controllable existence of the capacitor banks at the dc link to permit the injection of reactive power in case of empty batteries, increase the efficiency and the reliability of the complete system and make it more applicable in real life application.

Fig.6.11 shows the switching circuit between batteries and capacitor banks depending on the state of charge control.

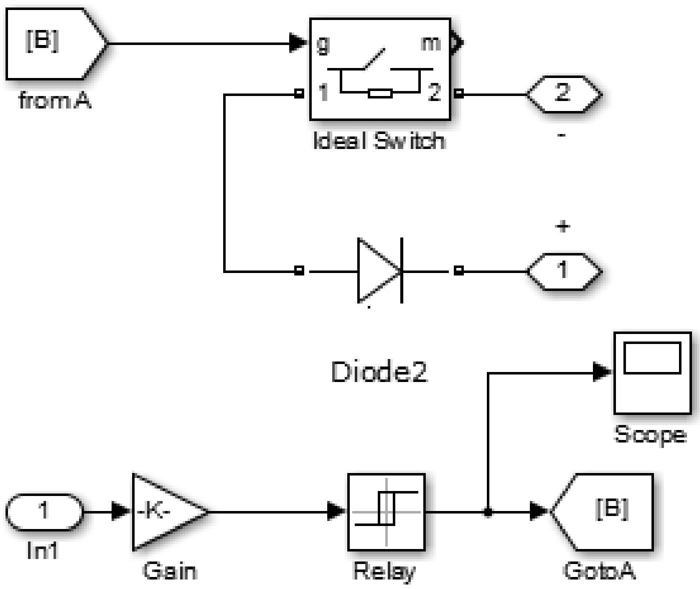

Fig.6.11: Switching circuit between batteries and capacitor banks.

6.4 Chapter Summary

This chapter presents the MATLAB SIMULINK results of the proposed Hybrid APF. The system is simulated and tested to maintain pure current and voltage signals seen by the source. From the results it is inferred that the Hybrid APF is very helpful in enhancement the power quality of the distribution network by filtering out the harmonics in current and voltage, improve the power factor and real power injection.

Chapter Seven
Conclusion and Practical Aspect

7.1 Recommendations and Conclusions.

The need of electric power is increasing with the evolution of life, and the term power quality turned out to be most outstanding in the power sector and both the electric power supply company and the end clients are interested in it.

Therefore, the elimination of harmonics and optimizing the power factor of the distribution network is very important. In this research a solution to enhance the electric power quality and inject real power to help the source by the use of Hybrid Active Power Filter is analyzed. From the results of Hybrid Active Power Filter for optimizing the quality of power we summarize the following conclusions

- The power electronics based nonlinear loads are expanded significantly in the distribution networks, which are the main source of harmonics in the electrical networks.

- The non-linear load consumes non-linear voltage and current from the electrical source, and this affecting the function of end costumer equipment.

- To clear the load current harmonics and optimize the power factor a shunt active filter is connected at the PCC which injects the compensating current.

- the shunt active filter can inject real power to the electrical network depending on the status of the system.

To compensate the voltage harmonics a series connected active power filter is implemented .To fulfill this a Hybrid active power filter with series connected active power filter and shunt connected active power filter is used.

- The shunt active power filter is controlled based on the “Generalized Theory of the Instantaneous Reactive Power in Three-Phase Circuits (p-q theory)", to compensate the load harmonics.

- The series active power filter is controlled based on the Dual Instantaneous Reactive Power Theory to compensate the load harmonics.

- Simulation of the proposed system show the behavior and the results of each part of the system separately, then a complete simulation results for Hybrid Active Power filter was discussed and analyzed.

- The simulation of complete system verify the correct operation of the Hybrid Active Power Filter for the ability to compensate voltage and current harmonics, inject the real power to the electrical network, and improve the power factor at PCC with taking into account the system status as well as the electrical network stability.

Multilevel inverters with more than 20 levels can deliver current waveforms with negligible total harmonic distortion. So they can implement in active filter application without the need of filters.

By using voltage reference generation control we will overcome the voltage matching problems, reduce the total harmonic distortion (THD) to minimum and eliminate the need of transformers.

The use of photovoltaic arrays and battery packs to inject real and reactive power make the system more applicable and reliable.

7.2 Economic Considerations.

The transformer less topology for shunt active filter makes the system much more efficient and cheaper,

However, because of matching voltages and isolation problems, this is not always a viable solution.

to solve the problem of matching voltages this topology generates a voltage signal reference that keep the inverter output voltage larger than source voltage by small amount to insure power injection to the network and correct working of inverter options. The shunt active filter designed to filter some voltage harmonic (by impedance effect) and the rest of harmonics filtered by the series active filter.

So low power series active filter was needed with using unity low power transformers (1:1) this is an additional advantage of this topology and make the system more cheaper Moreover, with transformer less topologies, nine independent and isolated solar panels are required for the three phases, and additional control strategies to separately manage each of them must be implemented.

To overcome this problem and to take the advantage of this system in real life we can make central big inverters unit for each 18 houses and arrange the percentages to fit our inverter inputs.

This idea can solve big problems in real life like make the electrical network clean and more stable even at distances away from the source, save the equipment's in houses from unstable current and voltages, and use the available resources

Where we need inverters to inject real power from solar panel so by adding small price we can take all these advantages

The utilization of transformers is an option but it make the system less efficient and expensive (39)

It should be noted that the main idea here is to make Unified Power Quality Conditioner (UPQC) more useful by adding active power sources at the dc link instead of a typical capacitor.

7.3 Future Scope.

The work achieved in this research can be further extended, and it's great to have a chance to apply the system in practice.

The feasible options are-

- To apply the filter in complete electrical distribution network and simulate the proposed filter type with grid faults.

To use new control strategies that improve the reference signals and optimize the transient response of the system

References.

[1] B. Singh,K. Al-Haddad and A. Chandra**, "A new control approach to 3- phase active filter for harmonics and reactive power compensation",-** IEEE Trans. on Power Systems, vol. 46, no. 5, pp. 133 – 138, Oct. 1999.

[2] W.M.Grady, M.J.Samotyj, A.H.Noyola **"Survey of active power line conditioning methodologies"**, IEEE Trans on Power Delivery, vol.5, no.3, pp.1536-1542, July.1990.

[3] J. Dixon and L. Morán, "**A clean four-quadrant sinusoidal power rectifier, using multistage converters for subway applications,"** IEEE Trans. Ind. Electron., vol. 52, no. 5, pp. 653–661, May/Jun. 2005.

[4] F.-S. Kang, S.-J. Park,M. H. Lee, and C.-U. Kim, "**An efficient multilevel-synthesis approach and its application to a 27-level inverter,**" IEEE Trans. Ind. Electron., vol. 52, no. 6, pp. 1600–1606, Dec. 2005.

[5] S. Lakshminarayanan, G. Mondal, P. N. Tekwani, K. K. Mohapatra, and K. Gopakumar, **"Twelve-sided polygonal voltage space vector based multilevel -inverter for an induction motor drive with common-mode voltage elimination,"** IEEE Trans. Ind. Electron., vol. 54, no. 5, pp. 2761–2768, Oct. 2007.

[6] Chi-Seng Lam, Man-Chung Wong, **"Design and control of hybrid active power filter,"** Springer Briefs in Electrical and Computer Engineering, 2014

[7] Hirofumi Akagi, **"Trends in active power line conditioners",** IEEE transactions on power electronics, vol.9, MAY 1994

[8] Hirofumi Akagi, **"New trends in active filters for power conditioning**". IEEE transactions on industry applications, vo1.32, NOVEMBER 1996.

[9] H. Fujita, H. Akagi, **"A practical approach to harmonic compensation in power systems-series connection of passive and active filters,"** Industry Applications Society Annual Meeting, 1107 - 1112 vo1.2, 1990

[10] F.Z. Peng, H. Akagi, A. Nabae, **"A new approach to harmonic compensation in power systems-a combined system of shunt passive and series active filters"**, IEEE Transactions on industry applications.

vol. 26, no. 6. NOVEMBERI990

[11] L. Chen, A.Y. Jouanne, **"A comparison and assessment of hybrid filter topologies and control Algorithms,**" Power Electronics Specialists Conference, 2001. PESC. 2001 IEEE 32nd Annual,Vol.2, 2001

[12] F.Z. Peng, H. Akagi, A Nabae**, "Compensation characteristics of the combined system of shunt passive and series active filters."** IEEE Transactions on industry applications, vol. 29, no. I, January 1993

[13] P. Salmer6n, S.P. Litfiln, "**A control strategy for hybrid power filter to compensate four-wires three-phase systems."** IEEE Transactions on power electronics, vol. 25, no. 7, JULY 2010

[14] P. Salmeron, S.-P. Litran, **"Improvement of the electric power quality using series active and shunt passive filters"** IEEE Transactions on power delivery, vol. 25, no. 2, APRIL 2010

[15] V.F. Corasaniti, M.B. Barbieri, P.L. Arnera, M.1. Valla, **"Hybrid active filter for reactive and harmonics compensation in a distribution network"**, IEEE Transactions on industrial electronics, vol. 56, no. 3,

MARCH 2009.

[16] S.T. Senini, P.l. Wolfs, "**Systematic identification and review of hybrid active filter topologies"**. Power Electronics Specialists Conference,vol.l,pp.394 - 399

[17] A Nakagima, J. Nishidai, and T. Shiraishi, **"Development of active filter with series resonant circuit,"** Power Electronics Specialists Conference,voI.2,pp.1168 - 1173,1988.

[18] Fujita, H.; Akagi, H. **"A practical approach to hannonic compensation in power systems-series connection of passive and active filters".** Industry Applications Society Annual Meeting, 1990., Conference Record of the 1990 IEEE,voI.2,pp.1107 - 1112,1990

[19] Vinod Khadkikar**,"Enhancing Electric Power Quality Using UPQC:A Comprehensive Overview"**. IEEE Transactions on power electronics, vol. 27, no. 5, MAY 2012

[20] Keng-Weng Lao, Man-Chung Wong, NingYi Dai, Chi-Kong Wong, Chi-Seng Lam. **"A Systematic Approach to Hybrid Railway Power Conditioner Design With Harmonic Compensation for High-Speed Railway"**. IEEE Transactions on industrial electronics, vol. 62, no. 2, FEBRUARY 2015

[21] Khairul Nisak Binti Md. Hasan, Kalle Rauma, Alvaro Luna, J. Ignacio Candela, Pedro Rodriguez, **"Hannonic Compensation Analysis in Offshore Wind Power Plants Using Hybrid Filters",** IEEE Transactions on industry applications, vol. 50, no. 3, MA Y/JUNE 2014

[22] Ayman Blorfan, Patrice Wira, Damien Flieller, Guy Sturtzer ,Jean Merckl':, **"A Three-Phase Hybrid Active Power Filter with Photovoltaic Generation and Hysteresis Current Control**".

[23] Yi Lei, Wei Xu, Chaoxu Mu, Zheng ming Zhao, Hongbing Li, and Zhiyong Li. **"New Hybrid Damping Strategy for Grid-Connected Photovoltaic Inverter With LCL Filter".** IEEE Transactions on applied superconductivity, vol. 24, no. 5, OCTOBER 2014

[24] Ahmed Faheem Zobaa**."Optimal Multiobjective Design of Hybrid Active Power Filters Considering a Distorted Environment**".IEEE Transactions on industrial, vol. 61, no. I, JANUARY 2014

[25] Wai-Hei Choi, Chi-Seng Lam, Man-Chung Wong, Ying-Duo Han. **"Analysis of DC-Link Voltage Controls in Three-Phase Four-Wire Hybrid Active Power Filters".** IEEE Transactions on power electronics, vol. 28, no. 5, MAY 2013

[26] Chi-Seng Lam, Wai-Hei Choi, Man-Chung Wong, Ying-Duo Han. "**Adaptive DC-Link Voltage-Controlled Hybrid Active Power Filters for Reactive Power Compensation**". IEEE Transactions on power electronics, vol. 27, no. 4, APRIL 2012

[27] M.EI-Habrouk, M.K.Darwish and PMehta."**Active power filters: A review"**. IEE Proc.-Elertr. Power Appl., vol. 147, no. 5, September 2000

[28] B. Singh, Y. Verma, A Chandra and K. AI-Haddad."**Hybrid filters for power quality improvement"**. IEE Proc.-Gener. Transm. Distrib., vol. 152,no. 3, MAY 2005.

[29] H. Akagi, "**Active Harmonic Filters".** Proceedings of the IEEE, vol. 93, no. 12, DECEMBER 2005.

[30] S. Rahmani,Ab. Hamadi,K. AI-Haddad**,"A Comprehensive Analysis of Hybrid Active Power Filter for Power Quality Enhancement".** IECON 2012 - 38th Annual Conference on IEEE Industrial Electronics SocietY,pp.6258 - 6267,2012.

[31] TugyeDemirdelen,MustafaInci, K. <;:agatayBayindir, Mehmet Tumay."**Review of Hybrid Active Power Filter Topologies and Controllers"**.4th International Conference on Power Engineering, Energy and Electrical Drives Istanbul, Turkey, 13-17 May 2013

[32] Balbo, N.; Sella, D.; Penzo, R.; Bisiach, G.; Cappellieri, D.; Malesani, L.; Zuccato, **A"Hybrid active filter for parallel harmonic compensation**". Power Electronics and Applications, Pages: 133 - 138

voI.8, 1993.

[33] Dixon, .I.; Moran, L.; Rodriguez, .I.; Domke, R. **"Reactive Power Compensation Technologies: State-of-the-Art Review"**, Proceedings of the IEEE, vol: 93, pp.144 - 2164, 2005.

[34] Corasaniti, Y.F.; Barbieri, M.B.; Arnera, P.L.; Valla, M.I.. **"Hybrid Power Filter to Enhance Power Quality in a Medium-Voltage Distribution Network"**, IEEE Transactions on Industrial Electronics, vol: 56, pp. 2885 - 2893,2009.

[35] Silva, c.; Cordova, L.A; Lezana, P.; Empringham, L. **"Implementation and Control of a Hybrid Multilevel Converter With Floating DC Links for Current Waveform Improvement"**, IEEE Transactions on Industrial Electronics ,vol: 58, pp.2304 - 2312, 2011

[36] An Luo, Shuangjian Peng, Chuanping Wu, Jingbing Wu, ZhikangShuai. **"Power Electronic Hybrid System for Load Balancing Compensation and Frequency-Selective Harmonic Suppression**", IEEE Transactions on Industrial Electronics, vol: 59, pp.723 - 732, 2012.

[40] J. G. Pinto1, R. Pregitzer1, Luís F. C. Monteiro1, João L. Afonso1 “**3-Phase 4-Wire Shunt Active Power Filter with Renewable Energy Interface”.**

[41] Patricio Flores, Juan Dixon, Micah Ortúzar, Rodrigo Carmi, Pablo Barriuso, and Luis Morán “**StaticVar Compensator and Active Power Filter With Power Injection Capability, Using 27-Level Inverters and Photovoltaic Cells”**.

[42] Rajasekar.S, Rajesh Gupta, **“Photovoltaic Array Based Multilevel Inverter for Power Conditioning”**.

[43] Singh, Bhim; Al-Haddad, K.; Chandra, A., "**A review of active filters for power quality improvement,"** Industrial Electronics, IEEE Transactions on , vol.46, no.5, pp.960,971, Oct 1999 doi: 10.1109/41.793345.

[44]Axente, N. G. Jayanti, M.Basu, and M. F. Conlon, **“A 12 kVA DSPcontrolled laboratory prototype UPQC capable of mitigating unbalance in source voltage and load current,”** IEEE Trans. Power Electron. , vol. 25, no.6, pp. 1471–1479, Jun. 2010.

[45] Ravikant Pandey *, Ravi Nath Tripathi and Tsuyoshi Hanamoto ‘’**Comprehensive Analysis of LCL Filter Interfaced Cascaded H-Bridge Multilevel Inverter-Based DSTATCOM’’.**

[46] Keith A. Corzine, Member, IEEE, Mike W. Wielebski, Student Member, IEEE, Fang Z. Peng, Senior Member, IEEE, and Jin Wang, Student Member, IEEE **‘’ Control of Cascaded Multilevel Inverters’’.**

[47] R. Taleba,*, D. Benyoucefa , M. Helaimia , Z. Boudjemaaa , H. Saidib ‘’ **Cascaded H-bridge Asymmetrical Seven-level Inverter Using THIPWM for High Power Induction Motor’’**

[48] T.Prathiba* ,P.Renuga ‘’ **A comparative study of Total Harmonic Distortion in Multi level inverter topologies’’**.

[49] JavadEbrahimi, Student Member, IEEE, EbrahimBabaei, Member, IEEE, and Gevorg B. Gharehpetian, Senior Member, IEEE **‘’ A New Multilevel Converter Topology with Reduced Number of Power Electronic Components’’.**

[50] Baharuddin Ismail1 , Syed Idris Syed Hassan1 , RizalafandeChe Ismail2 , Abdul Rashid Haron1 , Azralmukmin Azmi1 ‘’ **Selective Harmonic Elimination of Five-level Cascaded Inverter Using Particle Swarm Optimization’’**

[51] M. Suresh , S.S.Patnaik, Y. Suresh, Prof. A.K. Panda, **“Comparison of Two Compensation Control Strategies for Shunt Active Power Filter in Three-Phase Four-Wire System”**, Innovative Smart Grid Technology, IEEE PES, 17-19 Jan. 2011, pp. 1 – 6

[52] Marcelo A. Pérez, Member, IEEE, Patricio Cortés, Member, IEEE, and José Rodríguez, Senior Member, IEEE ‘’ **Predictive Control Algorithm Technique for Multilevel Asymmetric Cascaded H-Bridge Inverters’’**

[53] Sung Geun Song, Feel Soon Kang, Member, IEEE, and Sung-Jun Park ‘’ **Cascaded Multilevel Inverter Employing Three-Phase Transformers and Single DC Input’’**

[54] Zhong Du, Member, IEEE, BurakOzpineci, Senior Member, IEEE, ‘’ **DC-AC Cascaded H-Bridge Multilevel Boost Inverter with No Inductors for Electric/Hybrid Electric Vehicle Applications’’**

[55] Bindeshwar Singh1 , Nupurmittal 3 , Dr. K.S.Verma 2 , Dr. Deependra Singh2 , S.P. Singh1 , Rahul Dixit3 , Manvendra Singh3 , and Aanchal Baranwal4 ‘’ **Multi-level Inverter: A Literature Survey on Topologies and Control Strategies**’’

[56] Jingang Han, Zhiyuan Ma and Dongkai Peng ‘’ **Analysis of Model Predictive Current Control for Voltage Source Inverter’’**

[57] Park, Young-Min; Ryu, Han-Seong; Lee, Hyun-Won; Jung, Myung-Gil; Lee, Se-Hyun; ‘’ **Design of a Cascaded H-Bridge Multilevel Inverter Based on Power Electronics Building Blocks and Control for High Performance’’**

[58] Madhav D. Manjrekar Thomas A. Lip0 ‘’ **A Hybrid Multilevel Inverter Topology for Drive Applications’’**.

[59] MadhukarWaware and Pramod Agarwal **‘’ A Review of Multilevel Inverter Based Active Power Filter’’**.

[60] HaiwenLiu1 , Leon M. Tolbert1, 2 , Surin Khomfoi3 , Burak Ozpineci2 , Zhong Du **‘’ Hybrid Cascaded Multilevel Inverter with PWM Control Method’’.**

[61] Er. MamathaSandhu ,Dr.Tilak Thakur ‘’ **Multilevel Inverters: Literature Survey – Topologies, Control Techniques & Applications of Renewable Energy Sources - Grid Integration’’ [62] ‘’ Symmetrical Hybrid Multilevel DC–AC Converters With Reduced Number of Insulated DC Supplies’’**.

[63] C.R. Balamurugan*, S.P. Natarajan, R. Bensraj‘’ **Elucidation of Various PWM Techniques for a Modified Multilevel Inverter’’**.

[64] Hina B. Chandwani and MeetaK.Matnani‘’ **A Review of Hybrid Multilevel Inverter Configurations and Their Comparison’’**.

[65] M. Murugesan1 , R.Pari2 , R.Sivakumar3 and S.Sivaranjani4 ‘’ **Different Types of Multilevel Inverter Topologies – A Technical Review’’**

[66] M. Murugesan1 , R.Pari2 , R.Sivakumar3 and S.Sivaranjani4 ‘’ **A Novel 40kW ZVS-SVM Controlled Three-Phase Boost PFC Converter’’**.

[67] Goran S. Miljković, Ivana S. Stojković, Dragan B. Denić. ‘’ **Generation and Application of Pseudorandom Binary Sequences Using Virtual Instrumentation’’.**

جامعة النجاح الوطنية

كلية الدراسات العليا

تصميم مرشح قدرة فعال له القدرة على توليد طاقة فعالة وغير فعالة باستخدام عاكس كهربائي متعدد المستويات وخلايا شمسية

إعداد

نائل نجيب حنتولي

إشراف

د. كامل صبحي صالح

قدمت هذه الاطروحة استكمالاً لمتطلبات الحصول على درجة الماجستير في هندسة القوى الكهربائية، بكلية الدراسات العليا، في جامعة النجاح الوطنية، نابلس– فلسطين.

2018

تصميم مرشح قدرة فعال له القدرة على توليد طاقة فعالة وغير فعالة باستخدام عاكس كهربائي متعدد المستويات وخلايا شمسية

إعداد

نائل نجيب حنتولي

إشراف

د. كامل صبحي صالح

الملخص

يتكون مرشح الطاقة الفعال من إتحاد مرشح طاقة توازي ومرشح طاقة توالي عند نفس نقطة الربط، ويعمل هذا المرشح بطريقة مثالية حيث أنه يجمع بين إيجابيات مرشح التوازي ومرشح التوالي مما يعني إمكانية ترشيح جميع الشوائب الموجودة في إشارة الجهد والتيار وحل جميع مشاكل جودة الطاقة في الشبكة الكهربائية.

وتستخدم المرشحات عاكس إلكتروني ذو 27–مستوى مما يتيح لها دقة بالغة وفعالية في العمل بقدرة إجمالية 15 كيلو فولت أمبير يتم من خلالها شحن البطاريات لأوقات الحاجة القصوى وتزويد الشبكة الكهربائية بالزائد عن حاجة الشحن.

يعتمد تزويد الشبكة بالطاقة الكهربائية على قيمة الحمل ومقدار تردد الشبكة ومؤشر الطاقة المتوفرة في البطاريات ومعامل الطاقة عند نقطة ربط المرشح، وتم تصميم النظام والتأكد من عمله بإستخدام برنامج الماتلاب.

ويقوم هذا النظام بحذف جميع الشوائب الموجودة في الشبكة الكهربائية بنسبة تصل الى 99%،بالاضافة الى القدرة المثالية على تحسين معامل القدرة ودعم الشبكة الكهربائية بالطاقة الناتجة من الخلايا الشمسية والمخزنة في البطاريات وقت الحاجة، ويعتبر هذا النظام فريد من نوعه نظرة لدقة عمله وقدرته على تخطي العقبات بسرعة فائقة.